Bromate Removal from Water Using Activated Carbon (AC) and Modified Multi-walled Carbon Nanotubes (MWCNT)

BY

Aasem Mohammed Nour Zeino

A Thesis Presented to the
DEANSHIP OF GRADUATE STUDIES

KING FAHD UNIVERSITY OF PETROLEUM & MINERALS

DHAHRAN, SAUDI ARABIA

In Partial Fulfillment of the
Requirements for the Degree of

MASTER OF SCIENCE

In

CHEMISTRY

May, 2012

KING FAHD UNIVERSITY OF PETROLEUM & MINERALS
DHAHRAN, SAUDI ARABIA

DEANSHIP OF GRADUATE STUDIES

This thesis, written by Aasem Mohammed Nour Zeino under the direction of his thesis advisor and approved by his thesis committee, has been presented to and accepted by the Dean of Graduate Studies, in partial fulfillment of the requirements for the degree of **MASTER OF SCIENCE IN CHEMISTRY**.

Thesis Committee

Dr. Abdalla M. Abulkibash
(Thesis Advisor)

Dr. Muataz Ali Atiah
(Member)

Dr. Mazen M. Khaled
(Member)

Dr. Abdullah J. Al-Hamdan
(Department Chairman)

Dr. Salam A. Zummo
(Dean of Graduate Studies)

13/5/1m

Date

DEDICATION

This Thesis Is Dedicated

To:

My Great Islamic Nation

My Beloved Parents for their Prayers

My Brothers, Sisters & Wife for their Care & Support

ACKNOWLEDGMENT

In the name of Allah, the Most Gracious the Most Merciful,

All praise and glory goes to Almighty Allah who gave me the patience and courage to carry out this research. Then, I pay my sincere appreciation and gratitude to my advisors Dr. Abdullah Abulkibash, Dr. Moataz Atiah and Dr. Mazen Khalid for offering me the opportunity to explore the nanoscale world. Their valuable guidance and constant endeavor were indispensable for me to carry out this work.

My thanks extended to Mr. Izzat Kazi for his cooperation during Ion Chromatography (IC) analyses and thanks for Water Research Center in KFUPM for their continuous support. Kind thanks to Dr. Anwar Ul-Hamid for his kind cooperation during FE-SEM imaging and XRD analysis.

I would like to thank sincerely my great mother for her support, guidance, advices and encouragements during my life. Also, my thanks extended to my all my family for their prayers and support. Sincere thanks & prayers to my uncle Dr. Badr Ghawji for his support, encouragement and valuable advices always.

Sincere thanks to my honest & helpful wife for her support. Also, thanks for all Syrian colleagues in KFUPM who help and support me during the last two years especially Mr. Abdulnaser AlSharaa, Mr. Mohammed Al-Bakri.

Finally, Special thanks for King Fahd University of Petroleum & Minerals (KFUPM) for giving me the chance to do the work with their full support and facilities.

TABLE OF CONTENTS

LIST OF TABLES

LIST OF FIGURES

THESIS ABSTRACT

Full Name: Aasem Mohammed Nour Zeino

Thesis Title: Bromate Removal From Water Using Activated Carbon (AC) and Modified Multi-walled Carbon Nanotubes (MWCNT)

Major Field: Chemistry

Degree: Master

Date of Degree: April 2012

In this work, a comparison study was done between different samples of activated carbon (AC) and multi-walled carbon nanotubes (MWCNT) for bromate (BrO_3^-) removal from water. MWCNT samples were prepared in KFUPM laboratories through specific procedures, and then all these samples were fully characterized by SEM, FTIR, EDS and TGA to ensure the required composition. The results showed that AC and MWCNTs have good capability to remove bromate from water through an adsorption/reduction mechanism on adsorbent surface. AC-Raw and AC-0.2% Ag results showed the highest adsorption capacities 0.4860 mg/g and 1.1930 mg/g, respectively at pH 7.5. CNT-Raw and CNT-1% Fe showed also good adsorption capacities 0.3220 mg/g and 0.3460 mg/g, respectively at pH 7.5. Bromate removal mechanism is considered to be through reduction process when activated carbon is used. However, in case of CNT samples the mechanism is mainly adsorption. The adsorption capacity of AC is better than that of CNT for the tested samples. Adsorption capacity increases if the pH of the solution and the adsorbent dosage decrease. The presence of co-anions also decreases the adsorption capacities of both AC and CNT.

ملخص الدراسة

اسم الطالب:	عاصم محمد نور زينو
عنوان الرسالة:	إزالة أيون البرومات من الماء باستخدام أنواع مختلفة من الفحم المنشط (AC) وأنابيب الكربون النانوية (MWCNT).
التخصص:	كيمياء
الدرجة:	ماجستير
تاريخ الشهادة	أبريل 2012

في هذه الدراسة، تمت دراسة مقارنة بين استخدام الفحم المنشط (AC) وأنابيب الكربون النانوية متعددة الجدران (MWCNT) في إزالة أيون البرومات (BrO_3^-) من الماء. تم تحضير جميع عينات أنابيب الكربون النانوية متعددة الجدران (MWCNT) في مختبرات جامعة الملك فهد للبترول والمعادن ومن ثم تم إجراء الاختبارات المطلوبة بواسطة: المجهر الإلكتروني الماسح (SEM) والأشعة تحت الحمراء (FTIR) ومطيافية الطاقة المتبعثرة (EDS) والتحليل الحراري الوزني (ATG) للتأكد من مطابقة مواصفات المواد المحضرة للمعايير المطلوبة. أظهرت نتائج الاختبارات التي أجريت على الفحم المنشط وأنابيب الكربون النانوية أن كليهما له قدرة على إزالة البرومات من المياه من خلال ميكانيكية امتصاص/اختزال للأيون على سطح المادة الماصة. حققت نتائج الفحم المنشط الخام (AC-Raw) والفحم المنشط المطعم بالفضة (AC-0.2% Ag) أعلى نتائج إزالة للبرومات من الماء حيث بلغت قيمة سعة الامتزاز لكل منهما 0.4860 ملغ/غ و 1.1930 ملغ/غ على الترتيب عند قيمة أس هيدروجيني 7.5. أيضاً، أظهرت نتائج إزالة البرومات باستخدام أنابيب الكربون الخام (CNT-Raw) وأنابيب الكربون المطعمة بالحديد نتائج جيدة حيث بلغت قيمة معاملات امتزازها 0.3220 ملغ/غ و 0.3460 ملغ/غ على الترتيب عند قيمة أس هيدروجيني 7.5. تكون الميكانيكية الرئيسية لإزالة البرومات ميكانيكية اختزال عند استخدام الفحم المنشط، بينما تكون الميكانيكية الرئيسية عند استخدام أنابيب الكربون النانوية ميكانيكية امتزاز. في المجمل، تكون قدرة إزالة البرومات باستخدام الفحم المنشط أعلى من مثيلاتها في نفس الشروط عند استخدام أنابيب الكربون النانوية التي جرت عليها الاختبارات. لوحظ أن قدرة امتزاز

البرومات بواسطة كل العينات تزداد مع انخفاض قيمة الأس الهيدروجيني للمحلول وانخفاض كمية المادة الممتزة المضافة. ولوحظ أيضاً أن وجود أنيونات أخرى في الماء تضعف من قدرة المواد الممتزة على امتزاز البرومات أو اختزاله ضمن الظروف المطبقة في الاختبارات.

CHAPTER 1

INTRODUCTION

1.1 WATER QUALITY

Water is the blue gold of the 21st century and is becoming more valuable due to the increased consumption and demand. It is one of the prime substances responsible for life on earth and essential for human cell activities. Its quality is an important factor for human health and different industrial applications. Nowadays, water pollution is a major global problem which requires ongoing evaluation and revision of water resource policy at all levels. It has been suggested that it is the leading worldwide cause of deaths and diseases which accounts for the deaths of more than 14,000 people daily [1].

Water pollution affects our rivers, lakes, oceans and drinking water and with the increase of population and industrial development, demand for water has also increased. Water becomes polluted when harmful chemical & biological contaminants are present in it. Chemical pollution includes organic & inorganic contaminants such as acids, ammonia, detergents, disinfection by-products, heavy metals, fertilizers and others. Wide range of chemical & industrial means have been employed for water treatments and purification such as Reverse Osmosis (RO), membrane bio-reactors (MBR), Activated Carbon beds (AC) and industrial waste water treatment plants (IWWTP).

However, the international organizations have introduced regulations concerning the water quality that makes it suitable for human consumption. The most popular regulations are of U.S. Environmental Protection Agency (USEPA), World Health Organization (WHO), The European Union standards (EU) and Food & Drug administration (FDA). In this study the removal of the disinfection by-product bromate BrO_3^- by using different carbon based materials such as Activated Carbon (AC) and Carbon Nanotubes (CNT), is considered.

1.2 CARBON NANOTUBES

Carbon nanotubes (CNTs) are allotropes of carbon with a cylindrical nanostructure discovered by Iijima in 1991 [2]. CNTs are members of the fullerene structural family and have novel mechanical, electrical, optical and chemical characteristics which are valuable in nanotechnology. Carbon nanotubes have been constructed with length-to-diameter ratio of up to 132,000,000:1 [3], significantly larger than for any other material. They are potentially useful in a wide variety of applications in nanotechnology, electronics, optics, and other fields of material. The CNTs exhibit extraordinary strength and unique electrical properties enabled them to be used as semiconductors and conductors.

Carbon nanotubes are categorized as single-walled carbon nanotubes (SWCNTs) and multi-walled carbon nanotubes (MWCNTs). Individual CNTs naturally align themselves into "ropes" held together by Van Der Waals forces. Applied quantum chemistry, specifically, orbital hybridization best describes chemical bonding in nanotubes. The chemical bonding of CNTs is entirely due to sp^2 hybridization, similar to those of graphite. The resulting bonds are stronger than those

of sp^3 hybridization found in alkanes. Thus, the unique properties of CNTs are mainly due to the strong bonds. Single-walled carbon nanotubes (SWCNT) have a diameter which is close to 1 nanometer with a considerable length.

The structure of a SWCNT can be conceptualized by wrapping a one-atom-thick layer of graphite called graphene into a seamless cylinder. Multi-walled carbon nanotubes (MWCNT) consist of multiple rolled layers (concentric tubes) of graphite. Different types of carbon nanotubes could be produced by different techniques. The most common techniques used are; arc discharge, laser ablation, chemical vapor deposition (CVD), and flame synthesis. These different methods have their own advantages and disadvantages. However, the chemical vapor deposition is considered to be the most efficient method.

CNTs have attracted special attentions to many researchers and engineers because they possess unique morphologies and have showed excellent properties and great potential applications such as composite reinforcement, nanodevice component, gas adsorption material and catalyst support phases [4]. Moreover, CNTs are also good anion and cation adsorption materials used in water & wastewater treatment, as they exhibit exceptionally large specific surface areas. In addition to the remarkable mechanical properties, their hollow and layered nanosized structures make them a good candidate as adsorbents [4].

1.3 ACTIVATED CARBON

Activated carbon (AC) is a form of carbon that has been processed to make it extremely porous and to have a very large surface area suitable for adsorption as well

as chemical reactions**.** AC is also called activated charcoal, activated coal or carbo activatus. Due to its high degree of microporosity, just 1 gram of activated carbon has a surface area of 500 m^2 as determined typically by nitrogen gas adsorption. Sufficient activation for useful applications may come solely from the high surface area, though further chemical treatment often enhances the adsorbing properties of the material. Activated carbon is usually derived from charcoal.

There are different classes of activated carbon classified based on their physical characteristics and general purposes as follow: Powdered activated carbon (PAC), Granular activated carbon (GAC), Extruded activated carbon (EAC), Bead activated carbon (BAC), Impregnated activated carbon and others. Activated carbon is produced from carbonaceous source materials like nutshells, peat, wood, lignite, coal and petroleum pitch. It can be produced by physical reactivation or chemical activation.

Activated carbon (AC) has a wide range of applications such as gas purification, gold purification, metal extraction, water purification, medicine, sewage treatment, air filters in gas masks and respirators, filters in compressed air and many other applications. Furthermore, it has numerous environmental applications in removing pollutants from air or water streams both in the field and in industrial processes such as groundwater remediation, drinking water filtration, air purification and volatile organic compounds capturing [5].

1.4 BROMATE

Bromate is a disinfection by-product (DBP) produced from the ozonation/oxidation of bromide containing water. Its presence in drinking water is a concern for public health since it is considered a genotoxic carcinogen [6]. The maximum allowed contaminant level (MCL) is 10 μg/L as proposed by the European Union [7] and the U.S. Environmental Protection Agency [8], while the World Health Organization set a provisional guideline value of 25 μg/L [9].

1.5 STATEMENT OF THE PROBLEM

In the drinking water industry, the primary goal is to provide the community with water that is both safe to drink and aesthetically acceptable. In order to provide safe water, disinfection of the drinking water must be carried out to destroy the harmful organisms (pathogens). Chlorine is generally used as a disinfectant for drinking water but it is becoming unpopular due to its dangerous disinfection by-products such as Trihalomethanes (THM). Ozone is a strong oxidant and can replace chlorine that has been used as a disinfectant in drinking water for a period of one hundred years [10].

Similar to chlorination, ozonation process may produce some harmful disinfection by-products (DBP). Bromate (BrO_3^-) formation by the ozonation of bromide containing water is considered as a very critical issue in drinking water because it is carcinogenic. It has been suspected as having potential health effects according to WHO and USEPA regulations [11]. So, bromate removal or minimizing its concentration is a key scientific issue in drinking water or any water source

contaminated by bromate. The maximum contaminant level (MCL) allowable for bromate is 10 μg/L as recommended by USEPA. Therefore, it is very important to study the methods of removing bromate to reach the most efficient and effective solutions of the bromate problems.

Several techniques are being applied in attempts to reduce the levels of bromate in drinking water supplies, including filtration, ultraviolet irradiation, photocatalytic decomposition, arc discharge, coagulation, chemical reduction, biological remediation, membrane bioreactor (MBR), and activated carbon adsorption [12]. Activated carbon is a cost-effective solution for this purpose and could be the most appropriate one. Nanotechnology could also help in bromate removal by using different types of CNTs at different conditions.

1.6 RESEARCH OBJECTIVES

Three main objectives of this project can be summarized as follows:

- To produce high quality & quantity of cheap MWCNTs using the successfully designed chemical vapor deposition technique with the optimized conditions.
- To remove bromate (BrO_3^-) from water using different types of functionalized & modified MWCNTs and AC as adsorbents.
- To study the effects of test conditions such as pH, contact time, initial bromate concentration, adsorbent concentration and agitation speed on bromate removal.
- To compare the results of MWCNTs and Activated carbon (AC) for bromate removal from water.

1.7 IMPORTANCE OF THE STUDY

Since the drinking water of high quality is a primary goal for human being, water should be free from all physical & chemicals contaminants. Bromate (BrO_3^-) is considered as a serious pollutant for drinking water; hence many researchers have investigated on its removal or minimizing its concentration using several methods. These methods include the activated carbon as an adsorbent. In addition, controlled conditions of ozonation process were employed. The results of bromate removal by AC were promising and applicable.

Carbon nanotubes (CNT) can be applied in various fields, one of which is the environmental field especially, water treatment. This work has been done to study the application of CNTs for the removal of BrO_3^- from water. Different conditions such as the contact time, the pH and the adsorbent dosage have been employed. The performances of AC and CNTs as adsorbents have been investigated. The results of the removal of BrO_3^- by applying those adsorbents were compared.

CHAPTER 2

LITERATURE REVIEW

Chemistry of bromate removal from drinking water requires essential information about: (1) Bromate formation and the effective factors during the ozonation process; (2) Water regulations related to bromate and its health risks; (3) Synthesis of carbon nanotubes (CNTs), their structure, functionalization, properties and applications; (4) Activated carbon (AC), its synthesis, structure, properties and applications; (5) Bromate removal techniques. Each of three points is addressed in the following literature review.

2.1 WATER DISINFECTION

2.1.1 Introduction

Drinking water quality is a key issue for the human life. Therefore, different techniques have been used to treat the water to achieve the required standards. Drinking water disinfection is vital for preventing the spread of diseases caused by waterborne harmful pathogens. However, chemical disinfectants can also form by-products with potential health concerns. Chlorine, the most popular disinfectant in the United States, has come under scrutiny because: (a) It reacts with natural organic matters (NOM) to form carcinogenic chlorinated compounds, known as disinfection by-products (DBPs), (b) its ineffectiveness in inactivating protozoa in general, and cryptosporidium parvum oocysts in particular [16]. Trihalomethanes (THMs) and haloacetic acids (HAAs) are the two most prevalent groups among known specific

DBPs formed during chlorination of natural waters [17]. Because of concerns over the effect that these DBPs might have on human health, USEPA has set stringent limits for four THMs and five HAAs [18]. In response to these regulations, a great deal of effort has been made to find alternative disinfectants, such as chloramines, ozone and chlorine dioxide, to lower the concentrations of these two groups of regulated DBPs [19].

2.1.2 Ozonation Process

Ozone is a potent oxidant and disinfectant that decomposes quickly in drinking water. Because of its instability, ozone will not produce a persistent disinfectant residual in the distribution systems [17]. Ozone is used widely due to its control of DBPs and biological stabilization, or minimization of the microbiological growth potential in water. Many studies were conducted by the American Water Works Association Research Foundation (AWWA). The results of those studies indicated that ozone has a higher inactivation capacity of pathogens in comparison with chlorine based disinfectants [20]. The formation reaction of ozone from oxygen and ‘’energy’’ such as ultraviolet (UV) of a wavelength < 200 nm, or high voltage source occurs according to the following equation [21]:

$$3O_2 + \text{energy} \longrightarrow 2O_3 + \text{heat} + \text{light} \qquad \textbf{(2.1)}$$

However, Similar to chlorine, ozone also reacts with inorganic and natural organic matters (NOM) in water to form undesirable and possibly harmful by-products. The most possible DBP could be formed during drinking water disinfections by ozone, ozone/chlorine or ozone/chloramines are mentioned in Table 2. This work

investigates the removal of bromate that results from the ozonation of water containing bromide ion.

Non-halogenated DBPs
Aldehydes: formaldehyde, acetaldehyde, propanal, butanal, 2-methyl propanal, pentanal, 3-methyl butanal, hexanal, heptanal, octanal, nonanal, decanal, undecanal, benzaldehyde, 3-methoxy-4-hydroxybenzaldehyde, cyanoformaldehyde **Ketones:** acetone, 2-butanone, 3-methyl-2-butanone, <separator/>2-pentanone, 3-hexanone, 2-hexanone, 3-methylcyclopentanone, C7-ketone (2 isomers), 6-methyl-5-heptene-2-one, 6-hydroxy-2-hexanone dicarbonyls, glyoxal, methylglyoxal, dimethylglyoxal, isomer of 2,3-butanedione, C5-dicarbonyl,5-ketohexanal **Carboxylic acids:** 2-methylpropanoic acid, butanoic acid, 3-methylbutanoic acid, pentanoic acid, hexanoic acid, heptanoic acid, octanoicacid, nonanoic acid, decanoic acid, undecanoic acid, dodecanoic acid, tridecanoic acid, tetradecanoic acid, pentadecanoic acid, hexadecanoic acid, heptadecanoic acid, octadecanoic acid, phenylacetic acid, benzoic acid, ethandioic acid, heptanedioic acid, octanedioic acid, nonanedioic acid, decanedioic acid, 1,2,4,5-benzenetetracarboxylic acid, 1,2.3,4-benzenetetracarboxylic acid, 1,2,3,5-benzenetetracarboxylic acid **Aldo- and Ketoacids:** 3-ketobutanoic acid, 3-methyl-2-ketobutanoic acid, 9-oxononanoic acid **Nitriles:** benzeneacetonitrile,heptanitrile
Halogenated DBPs
Haloalkanes/haloalkenes: chloroform, bromoform, iodoform, bromochlromethane, chlorodiiodomethane, bromodiiodomethane, dibromochloromethane, dichloroiodomethane, bromochloroiodomethane, dibromoiodomethane, tribromochloromethane, 1,2-dibromo-1-chloroethane, 2,3-dichlorobutane, hexachlorocyclopentadiene Haloaldehydes: chloroacetaldehyde, trichloroacetaldehyde, dichloroacetaldehyde, 2-chloro-2-methylpropanal, 2-bromo-2-methylpropanal **Haloketones:** 1,1-dichloropropanone, 1,3-dichloropropanone, 1-bromo-1-chloropropanone, 1,1,1-trichloropropanone, 1,1,3-trichloropropanone, 1-bromo-1,1-dichloropropanone, 1,1,3-tribromopropanone, 1,1,3,3-tetrachloropropanone, 1,1-dibromo-3,3-dichloropropanone, 1,3-dibromo-1.3-dichloropropanone, **Halodicarbonyls:** 2,2,4-trichloro-1,3-cyclopentenedione **Haloacids:** chloroacetic acid, bromoacetic acid, dichloroacetic acid, trichloroacetic acid, bromochloroacetic acid, dibromoacetic acid, 2-chloropropanoic acid,2,2-dichloropropanoic acid, 2-chloro-3-methyl maleic acid **Haloacetonitriles:** dichloroacetonitrile, bromochloroacetonitrile, dibromoacetonitrile, bromodichloroacetonitrile, dibromochloroacetonitrile **Haloalcohols:** 2-bromoethanol, 3-chloro-2-butanol **Halonitromethanes:** dibromonitromethane, trichloronitromethane, tribromonitromethane **Others:** chloromethyl benzene, bromoxylene, 2-chlorobenzothiozole, 2-benzobromothiazole, 2,2,2-trichloroacetamide, methane sulfonyl chloride, dichloromethyl sulfone

Table 1: Ozone, ozone–chlorine, and ozone–chloramines DBPs [22]

2.2 BROMATE

2.2.1 Bromate Chemistry

Sodium bromate and potassium bromate are white crystalline substances that are readily soluble in water [13]. Additional information about their physical and chemical properties is presented in Table 1. Sodium bromate is produced by the introduction of bromine into a solution of sodium carbonate. Sodium bromate is used in conjunction with sodium bromide to extract gold from gold ores [14]. Potassium bromate is produced by passing bromine into a solution of potassium hydroxide. An industrial electrolytic process is used for large-scale production of potassium bromate [15].

Property	Value	
	Sodium Bromate	Potassium Bromate
CAS No.	7789-38-0	7758-01-2
Synonyms	Bromic acid, sodium salt	Bromic acid, potassium salt
Molecular formula	NaBrO3	KBrO3
Molecular weight	150.89 g/mol	167.01 g/mol
Physical state and appearance	White crystals	White crystals
Melting point	381 °C	350 °C
Boiling point	1390 °C	370 °C (decomposes)
Density (17.5°C)	3.339 g/cm^3	3.27 g/cm^3
Solubility (Water)	275 g/L at 0°C 909 g/L at 100°C	133 g/L at 40°C 497.5 g/L at 100°C
Solubility (Organic)	Insoluble in alcohol	Slightly soluble in alcohol
LD_{50}	NA	321 mg/kg

Table 2: Physical and chemicals properties of sodium bromate, potassium bromate source: adapted from EPA/635/R-1/002

2.2.2 Bromate Formation During Ozonation

Bromate (BrO_3^-) is one of the most important DBP resulting from the ozonation of drinking water containing bromide (Br^-). Bromate formation during ozonation is depends on the water quality and conditions like the pH, the concentration of Br^-, alkalinity, ammonia presence, temperature, NOM characteristics, ozone contact time and concentration [22][23][24]. Bromate formation is considered as a vital issue for the quality of drinking water due its carcinogenicity. Based on the works of Kurokawa et al. (1986) [25] and DeAngelo et al. (1998) [26], it was found that the ingestion of aqueous bromate caused renal cell tumors in rats [24]. Bromate formation is highly dependent on bromide concentration in water. Based on Amy et al. (1993) survey for 100 US drinking water facilities, bromide concentration in average was 100 µg/L. Kurokawa et al. (1993) summarized that the bromate concentrations in drinking water had the average of 0 – 60 µg/L. Butler et al, has mentioned that the concentration of bromate after ozonation is ranging from 0.4 - 100 µg/L. However, bromate levels exceeding 2 mg/L were detected in a United Kingdom aquifer, resulting from a chemical production plant spillage [51].

Bromate formation during the ozonation of bromide containing waters can occure through two possible mechanisms. These mechanisms are known as Direct Molecular Ozone mechanism, and Indirect Hydroxyl radical mechanism.

Molecular Ozonation Mechanism is the direct ozonation pathway uses molecular ozone to oxidize efficiently bromide into hypobromous acid and hypobromite (HOBr, OBr^-) and then to bromate as explained in Figure 1. The direct

ozonation pathway suggests that bromate formation is driven by dissolved ozone. The reaction is pH dependent since hypobromite (OBr^-) is in equilibrium with hypobromous acid (HOBr) (Figure 2). Oxidation of hypobromous acid is very slow in comparison with hypobromite, so it doesn't contribute significantly in bromate formation. Because OBr^- can be oxidized to bromite (BrO_2^-) at an appreciable rate, bromate (BrO_3^-) formation is favored at high pH (range of 7-8) upon continuous ozonation [23].

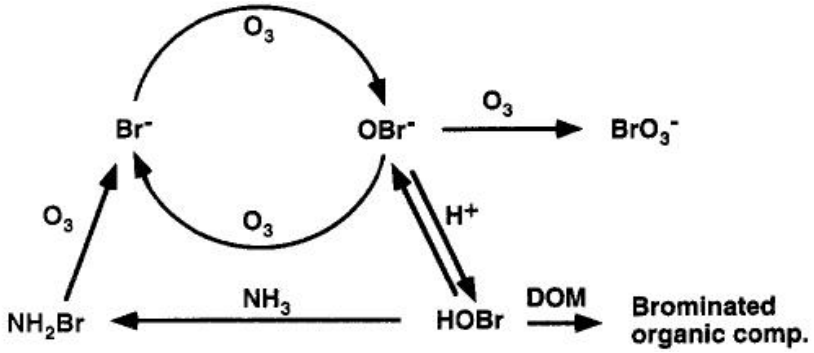

Figure 1: Bromate formation through molecular ozonation mechanism [23]

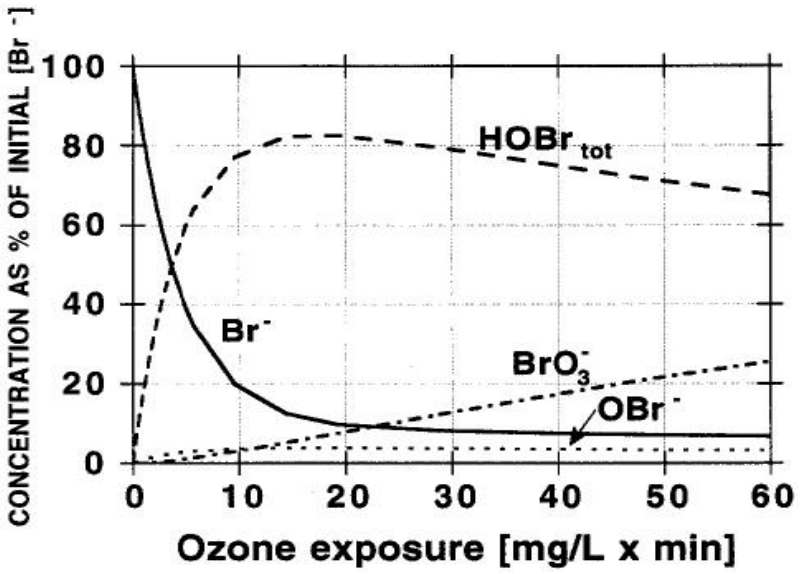

Figure 2: Model calculation for an extended ozonation of a bromide containing water at pH 7.5 .Concentrations of different species are given in percent of initial [Br-] vs the ozone exposure (ct value)[27]

Hydroxyl Radical Ozonation Mechanism is an indirect pathway indicates that $OH^{\cdot}$ Radicals play the significant role in bromate formation. The rapid oxidation of Br- by $HO^{\cdot}$ radical and forming intermediate adduct $HOBr^{-}$ is the key reaction in initiating the formation of BrO_3 as in Figure 3.

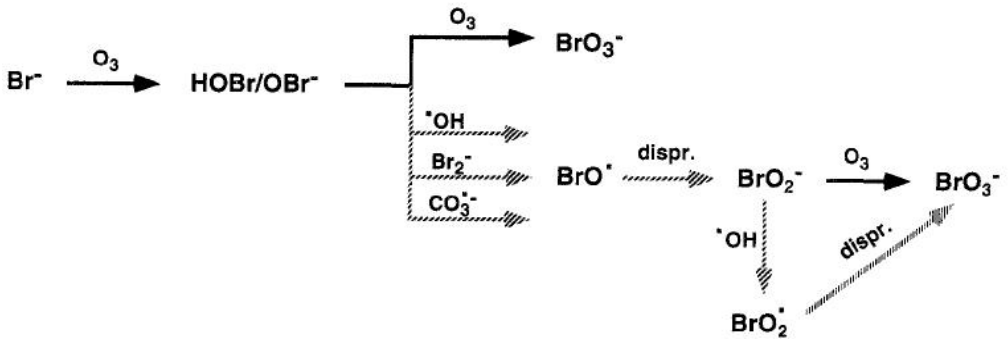

Figure 3: Comparison of the molecular ozone mechanism and the OH radical mechanism. The OH radical mechanism includes reactions of secondary oxidants as $CO_3^{\cdot-}$ and $Br_2^{\cdot-}$.

2.2.3 Parameters Affecting Bromate Formation

- **Bromide Concentration**

Formation of bromate increases with bromide concentration due to the reaction of ozone with bromide to produce OBr^{-}, this ion further reacts with ozone to produce bromate. Bromide and hypobromite have large rate constants with respect to scavenging $OH^{\cdot}$ radicals, and therefore could stabilize the rate of O_3 decay and possibly lead to more direct ozonation of Br^{-} species [28].

- **Temperature**

Temperature affects the solubility of the ozone as well as its chemical reaction rate coefficients. The temperature increases the activation energy and the reaction rates of

ozone decomposition. So, the concentration of hydroxyl radicals increases with increasing temperature and therefore bromate formation will be accelerated at higher temperatures. However, the temperature has a relatively small effect on bromate formation relative to pH and ammonia concentration (von Gunten and Pinkernell, 2000) [29].

- **pH Value**

The pH has great influence on the bromate formation [29]. Decreasing pH can decrease the bromate formation in two ways:

(1) Shifts the HOBr/OBr– equilibrium to HOBr to prevent further oxidation by ozone.

(2) Decreases of the rate of $HO^{\cdot}$ radical formation from ozone decomposition which results in a decrease in the rate of the oxidation of HOBr.

- **Alkalinity**

Alkaline species may reduce the decomposition rate of the dissolved ozone and inhibit the hydroxyl radical pathway of bromate formation or other ozone consumption reactions. This means that water with high alkalinity may have better disinfection performance and lower DBP formation (Fabian, 1995) [30].

- **Ammonia**

Ammonia (NH_3) reacts with ozone very slowly, and does not significantly affect ozone decomposition. However, in the presence of the bromide ion, ammonia can mask the hypobromate ion formed during ozonation and thereby delay the formation of bromate, (Langlais et al., 1991) [31]. As a result, the formation of bromate can be inhibited in ammonia-containing water.

- **Natural Organic Matter (NOM)**

Generally, the presence of the NOM in water lowers the stability of ozone through direct reaction with molecular ozone and consumption of $HO^{\cdot}$ radicals. The presence of NOM inhibits the formation of bromate especially at the initial period of ozonation (Song, 1996) [32].

The effects of the above water quality parameters on ozone decomposition and bromate formation are summarized in Table 3 [33].

Parameter	Disinfection efficiency	Decomposition rate	Bromate Formation rate
Temperature +	+	+	+
pH +	-	+	+
Bromide +	-	+	+
Alkalinity +	+	-	-
NOM +	-	+	-
Ammonia +	Unchanged	Unchanged	-

Table 3: Summary of parameters affecting bromate formation ("+": increasing concentration or value; "_": decreasing concentration or value)

2.2.4 Health Effects of Bromate

The presence of bromate in drinking water is a concern for public health since it is considered a genotoxic carcinogen. Bromate has been classified as a Group 2B or "possible human" carcinogen by the International Agency for Research on Cancer (IARC) although evidence of its carcinogenicity to human is inadequate [34].

Evidence has been noted of tumor induction in rodent studies [35]. Corresponding human toxicity data are limited to acute accidental poisoning cases, where symptoms may include severe gastrointestinal irritation, depression of the central nervous system, and renal failure [36]. The World Health Organization (WHO) recommends recently a provisional guideline value of 0.01 mg/L (10 ppb) for drinking water [37]. A maximum allowed contaminant level (MCL) of 10 μg/L (0.01 mg/L = 10 ppb) was imposed for bromate by the European Union [38] and the U.S. Environmental Protection Agency [36].

2.3 BROMATE REMOVAL

2.3.1 Using Activated Carbon

Many workers have studied the adsorption of activated carbon (granular or powder) to remove BrO_3^- from water and have found that it is effective & viable. Gerz and Schneider have observed in 1993 [39] that bromate was reduced by using granular activated carbon (GAC) columns depending on the GAC characteristics. Miller et al. (1993) [40] have noted that smaller carbon particles provide more effective reduction. Yamada et al. in 1993 [41] conducted preliminary experiments and concluded that BrO_3^- is first adsorbed on AC surface and then get reduced to Br^-. The BrO_3^- that is removed by activated carbon has been postulated to be adsorbed first, then reduced to hypobromite (BrO^-) and finally reduced to bromide (Br^-) on the activated carbon surface according to the equations 2.2 & 2.3 (Siddiqui et al. 1996) [47]. Siddiqui et al. (1994) [42] observed the bromate reduction by UV light (180 - 254 nm), but he concluded that the application of UV light for BrO_3^- reduction is not

an economical solution. Mills et al. (1996) [43] found that the use of platinised titanium dioxide catalyst enhanced the rate of bromate reduction by UV radiation for the wavelength 254 nm.

$$\equiv C + BrO_3^- \longrightarrow BrO^- + \equiv CO_2 \quad \textbf{(2.2)}$$

$$\equiv C + 2\ BrO^- \longrightarrow 2Br^- + \equiv CO_2 \quad \textbf{(2.3)}$$

Where **(≡C)** represents the surface of activated carbon and **($\equiv CO_2$)** represents the oxidized surface.

Since activated carbon has proven capability of transferring electrons for reduction reactions, the reduction of BrO_3^- to Br^- by GAC has also been investigated by Asami et al. (1999) [44], Bao et al. (1999) [45], Miller et al. (1996) [46] and Siddiqui et al. (1996) [47]. There are some factors that affect the efficiency of bromate reduction by GAC including carbon surface chemistry, solution pH, and the presence of natural organic matter (NOM) and other anions such as chloride, nitrate and sulfate. Miller et al. (1996) have examined the metals on the surface of AC by using energy dispersive X-ray (EDX) and found that the presence/absence of surface metals has no effect on BrO_3^- reduction. Doing acid-washing for the sample followed by outgassing (AWOG) at 900 ^oC under nitrogen atmosphere resulted in a 43% decrease in the carbon's surface oxygen content and an increase in the surface pH from 5.8 to 7.1 (Miller, 1996). The AWOG carbon showed a marked improvement in bromate reduction which could be due to more favorable electrostatic interactions between bromate and the carbon and the presence of accessible reduction sites since AWOG carbon has a lower surface oxygen content and higher pH than virgin carbon (Miller, 1996) Fig 4.

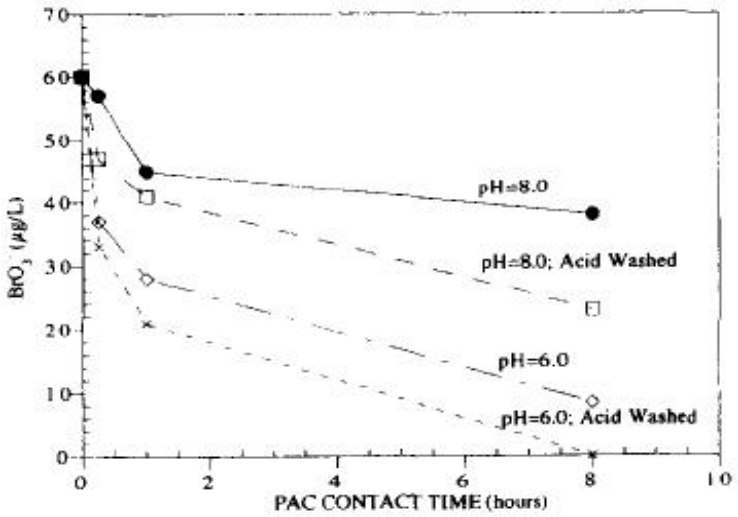

Figure 4: Effect of Acid washing PAC on BrO_3^- removal at different contact time and pH value (Siddiqui et al. 1996)

Studebaker and coworkers (1957) also found that carbons with lower surface oxygen contents tend to be basic and have anion exchange capability due to their positive charge. Basic carbons adsorb acid (H^+) in aqueous dispersion, leaving excess OH^- in the dispersion which yields a basic pH, and a basic carbon has a positive surface potential (Huang, 1978) [48]. Graham et al. in 1955) [49] found that the adsorption of an anion decreased as the acidity of the carbon increased (low pH_{zpc}), which could be attributed to unfavorable electrostatic interactions between the anions and the acid groups. Razvigorova et al. (1998) [50] found that the nitrate reduction capability of the apricot stone based carbon was greatly decreased by oxidizing the carbon with potassium permanganate; the authors concluded that the oxidation of the carbon created acidic oxygen groups which block the reduction sites on the carbon.

The pH of the solution is affecting bromate reduction where the reduction by GAC is increasing as pH decreasing which decreasing bromate. Siddiqui et al. (1996)

attributed this result to the reduction in surface charge of the carbon and to the higher reactivity of bromate at low pH. As protons (H+) are added to the carbon, the number of negatively charged groups on the carbon decreases, and a more favorable electrostatic interaction between the carbon and bromate is possible as in Figure 5. The charge on the surface is related to solution pH and pH_{zpc} (pH at point of zero charge) of the material. For example, the charge will be positive if the pH is less than pH_{zpc} of the carbon. The pH_{zpc} varies among carbons, and the literature describes carbons with pH_{zpc} ranging from approximately 3 to 9 (Siddiqui et al., 1994). Therefore, the electrostatic attraction between bromate and the carbon will depend not only on the solution pH but also on the type of carbon. Decreasing the pH also increases bromate reactivity as in Figure 6 and Figure 7.

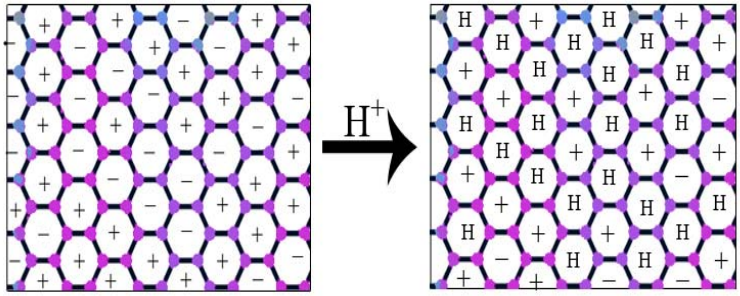

Figure 5: It shows that the addition of H^+ will decrease the negative charge on the surface and increase bromate – AC interaction

Carbon	Capacity[a]	pH_{ZPC} (Fig. 4)	Rating[b]
D-10	0.43	8.0	1
D-10[c]	0.45	8.2	1
F-300	0.41	7.1	2
F-400	0.13	6.3	3
F-400[d]	0.12	5.6	3
HDB	<0.1	3.5	4

[a] Removal capacity = mg BrO_3^-/g PAC.
[b] 1-Best and 4-Worst with respect to BrO_3^- removal.
[c] Acid washed PAC.
[d] Thermally regenerated GAC.

Figure 6: Rating of different AC types and its relation with pH_{zpc} value (Siddiqui et al. 1996)

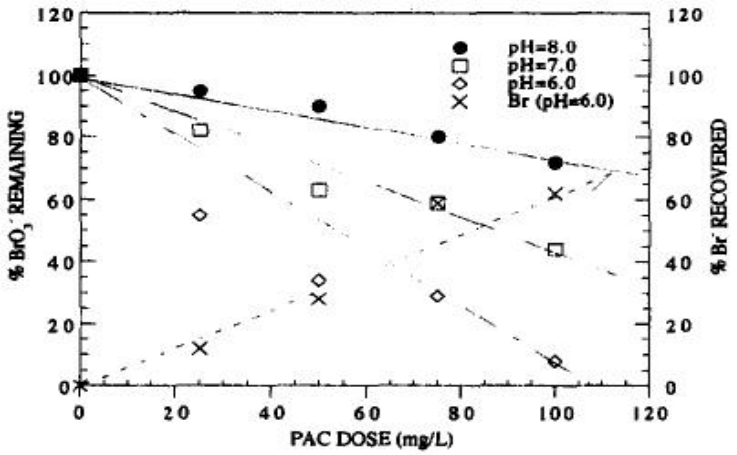

Figure 7: Effect of pH on BrO_3^- removal and PAC dose (Siddiqui et al. 1996)

The existence of NOM in water will decrease the bromate reduction capability of carbons presumably by blocking the active reduction sites according to studies done by Siddiqui et al. for comparing bromate reduction in organic-free water and natural waters. On the other hand, the presence of some anions such as: Cl^-, SO_4^{-2} and NO_3^- in water could decrease the reduction rate of bromate. Mills et al. (1996) performed kinetic studies on two natural waters to investigate the effect of other anions on bromate reduction. The first sample of water had 4.6 mg/l DOC, 76 mg/l Cl^- and 147 mg/l SO_4^{-2}. The other sample had 1.6 mg/l DOC, 9 mg/l Cl^- and 26 mg/l SO_4^{-2}. For a 10-min contact time, more bromate was reduced in the water with lower DOC and anion concentrations. In the short duration of the kinetic test, it is probable that chloride and sulfate were ion exchanging to the sites required for bromate reduction, but the separate effects of organic and inorganic constituents were not determined. Bao et al. (1999) investigated the individual effects of NOM, bromide, nitrate, and sulfate on bromate reduction efficiency, by spiking organic-free water

with one of the aforementioned constituents at a time; both NOM and the inorganic anions hastened bromate breakthrough from a GAC filter. However, they have made a comparison of four different types of ACs for BrO_3^- removal and found the results as in table 4.

Activated Carbon	Removal Capacity (mg BrO_3^-/g C)	
	GAC mode[a]	PAC mode[b]
A (pH_{zpc} = 8.1)	> 8.0	0.90
B (pH_{zpc} = 7.1)	2.1	0.41
C (pH_{zpc} = 4.1)	0.42	0.19
D (pH_{zpc} = 7.2)	< 0.05	< 0.05

[a]Capacity was calculated when 50% breakthrough occurred

[b]MQW; pH 7.2, initial BrO_3^- = 100 μg/l; PAC dose = 50 mg/l, contact tiem = 24 h

Table 4: Comparison of BrO_3^- removal efficiency on activated carbons in GAC and PAC application modes (Bao et al. 1999)

Bao and coworkers had done the research on a pilot plant. So, they studied the effect of bed depth, operation hours, bed filtered volume and bromate concentration in the influent. Measuring the concentrations of BrO_3^- and Br^- in the influent and effluents collected at different bed depths showed that BrO_3^- concentrations have decreased with depth, while Br^- concentration has increased with depth, and that the reduction rate of BrO_3^- is nearly equaled to the increase of Br^- as in Figure 8. This result confirms that the mechanism is a reduction of BrO_3^- to Br^- by GAC which was proposed before by other researches (Siddique et al. 1994, Yamada et al. 1993).

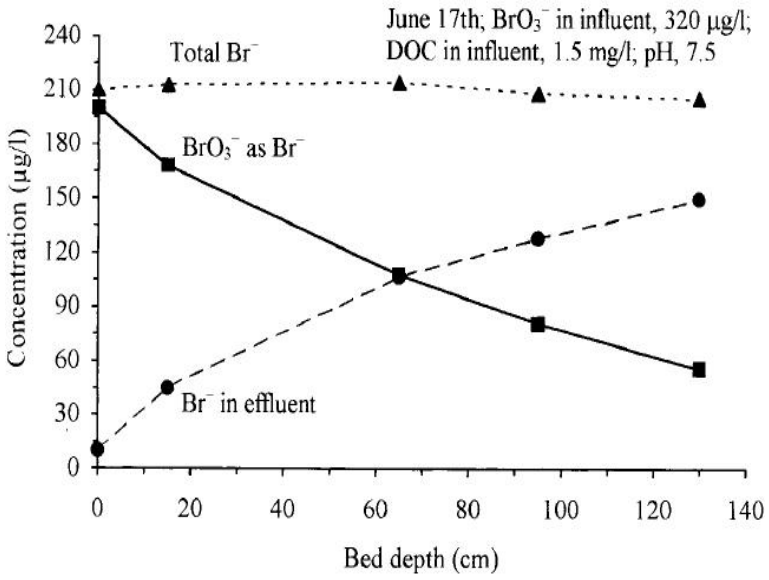

Figure 8: BrO_3^- reduction and Br^- formation as a function of bed depth of GAC A filter (loading rate 3.9 m/h, depth 0 cm corresponds to the top of the filter)

Kirisits et al. (2000) [54] has investigated the removal of BrO_3^- in the presence of virgin and acid-washed outgassed (AWOG) GAC by using GAC filters. Batch kinetic studies were performed to determine the relative amount of interference with BrO_3^- reduction caused by several constituents of natural water such as chloride, sulfate and nitrate. The results of the kinetic studies were compared by tabulating the mass of bromate removed per gram of carbon after 300 minutes (M_{300}). Figure 9 shows the kinetic results for virgin GAC in DDW (distilled-deionized water) and DFE (natural water). As expected, bromate reduction in DDW was faster than that in DFE due to the absence of NOM and inorganic anions. The M_{300} values for these and other kinetic studies have been tabulated in Table 5. The highest value was 0.0262 g of BrO_3^-/g of AC.

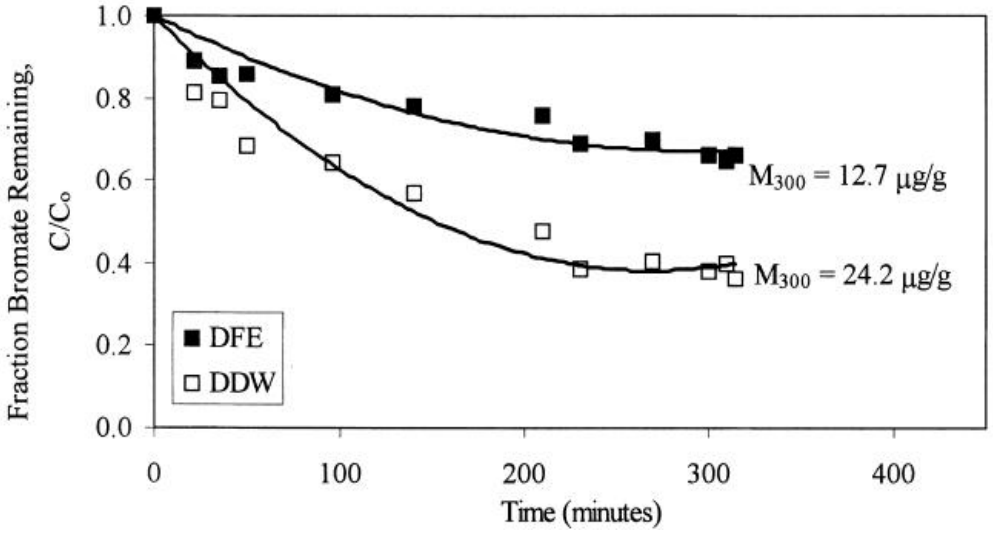

Figure 9: Kinetic studies of bromate reduction in DDW and DFE (initial conditions: 1000 mg/l virgin carbon, 5 mM phosphate bu€er, pH 6.5, 37±39 mg/l BrO_3^-. (Kirisits et al. 2000)

Kinetic Study	M_{300} (mg/g)
DDW	0.0242
DFE	0.0127
DDW; 0.14 mM chloride	0.0172
DDW; 0.11 mM sulfate	0.0172
DDW; 0.13 mM bromide	0.0140
DDW; 0.16 mM nitrate	0.0186
DDW with DFE anions (20 mg/l chloride, 41 mg/l nitrate, 18 mg/l sulfate)	0.0120
DDW; 2 mM phosphate buffer	0.0241
DDW; 3 mM phosphate buffer	0.0262

Table 5: M_{300} values demonstrating the effect of anion presence on bromate reduction (initial conditions: 1000 mg/l carbon, pH 6.5, 5 mM phosphate buffed unless otherwise noted, 36±44 mg/l BrO_3^- (Kirisits et al. 2000)

Four kinetic studies were conducted by Kirisits et al. in DDW spiked with chloride, sulfate, bromide, or nitrate (0.11±0.16 mM). As demonstrated by the M_{300} values in Table 5, despite differences in charge and size, similar molar concentrations of Cl^-, SO_4^{-2}, Br^- and NO_3^- have similar impacts on BrO_3^- removal. The presence of

bromide has a greater impact than the other anions. This is consistent with the findings of Bao et al. (1999) who showed faster bromate breakthrough from a GAC filter in NOM free water that had been spiked with 300 mg/L bromide as compared to breakthrough in NOM free water without the bromide spike. A possible explanation for the observed reduction in the rate in the kinetic studies is that the inorganic anions compete with bromate for ion exchange sites where bromate reduction occurs. The mass of each anion that was either taken up or released by the carbon is shown in table 6 below.

Anion	Anion Uptake (mg anion/g carbon)
0.14 mM chloride	- 0.1
0.11 mM sulfate	- 2.0
0.13 mM bromide	0.8
0.16 mM nitrate	2.0

Table 6: Anion uptake by virgin carbon during bromate reduction kinetic studies (initial conditions: 1000 mg/l carbon, DDW, pH 6.5, 5 mM phosphate buffer, 36±44 mg/l BrO_3^- (Kirisits et al. 2000)

The data shows that the activated carbon released approximately 0.1 mg chloride/g carbon and 2.0 mg sulfate/g carbon. It should be noted that similar amounts of chloride and sulfate were released by the carbon in DDW without anion spikes; in a kinetic study in DDW, approximately 0.2 mg/g chloride and 2.7 mg/g sulfate were released by the carbon. Since calcium chloride, zinc chloride, magnesium chloride and sulfuric acid are common additives in the carbon activation process (Cookson, 1978) [55], chloride and sulfate can be impurities of the GAC product. It is possible that two mechanisms are at work in determining the amount of chloride and sulfate in solution. First, salts of chloride and sulfate may be deposited

on the carbon as a result of the activation process and may not be attached to the carbon at functional groups which are active for bromate reduction. These deposits dissolve when the carbon is placed into water, resulting in an increase in the aqueous concentrations of sulfate and chloride. Second, sulfate and chloride (from the dissolution and from an external spike) may be able to compete for bromate reduction sites, and this would result in a decrease in the aqueous concentrations of sulfate and chloride. This is in consistence with the findings of Bautista-Toledo et al. (1994) [56] who determined that chromate and chloride compete for chromate reduction sites in a virgin carbon. It seems that the dominant mechanism for chloride and sulfate is the dissolution of their salts because a similar increase in their concentrations was observed when the carbon was added to DDW without external anion spikes.

However, chloride and sulfate may still be taken up by ion exchange, and thus, they may be competing with bromate for ion exchange sites. When the concentrations of chloride and sulfate are increased by an external spike, there is even more competition for bromate reduction sites. In order to be reduced, bromate could first have to find an available reduction site or displace the sulfate or chloride. This would result in slower bromate removal in the presence of these anions, as shown in Table 5. Table 6 shows that 0.8 mg/g bromide was taken up by the carbon. Bromide adsorption by GAC was also observed by Asami et al. (1999) [44]. Bromide, from solution and from bromate reduction, appears to occupy reduction sites; this slows the rate at which bromate is reduced and decreases the M_{300} value (Table 5). Bromide concentration was measured for all kinetic studies. Bromate reduction to bromide was

confirmed, as shown by other researchers (Miller et al., 1996; Asami et al., 1999; Bao et al., 1999; Siddiqui et al., 1994, 1996).

Since a substantial mass of nitrate was adsorbed by the carbon (2.0 mg/g, as shown in Table 5), additional experiments were performed in order to further examine the relationship between nitrate uptake and bromate reduction. Kinetic studies were performed using four different initial nitrate concentrations (9.9, 19.3, 27.4, 39.2 mg/l). The M_{300} values for these tests are compared to those of DDW and DFE in Table 7. Bromate removal did not decline substantially as the initial nitrate concentration was increased from 9.9 to 39.2 mg/l even though the nitrate uptake by the carbon increased. This indicates that not all of the sites occupied by nitrate are bromate reduction sites. In the presence of a nitrate spike, bromate removal was lower than that in DDW presumably due to the occupation of bromate reduction sites by nitrate. Bromate removal in DFE was lower than that in DDW with a nitrate spike, most likely because of the presence of other anions (sulfate and chloride) and NOM. Table 7 shows that the nitrate uptake in DFE was lower than expected based on the trend of nitrate uptake in DDW; however, this was likely due to the fact that the nitrate in DFE had competition for ion exchange sites from chloride and sulfate.

Initial nitrate concentration (mg/l)	Nitrate uptake by the carbon (mg/g)	M_{300} (mg/g)
DDW; 0.0	-	0.0242
DDW; 9.9	2.0	0.0186
DDW; 19.3	3.3	0.0183
DDW; 27.4	3.6	0.0166
DDW; 39.2	4.4	0.0160
DFE; 43.5	3.6	0.0126

Table 7: Nitrate uptake by virgin carbon during bromate reduction kinetic studies (initial conditions: 1000 mg/l carbon, pH 6.5, 5 mM phosphate buffer, 37±44 mg/l BrO_3^- (Kirisits et al. 2000)

Other kinetic experiments were extended for a month to compare the mass of BrO_3^- removed by carbon in DDW to that in DDW with various anion spikes. The initial bromate concentration was between 1.8±2.0 mg/l. The results of these experiments are given in Table 8, as well as the uptake or release of the other anions. The control experiment, run with no carbon, showed little decrease in bromate. In each of the other experiments, the bromate concentration was reduced approximately to the detection limit. The data also show the uptake of chloride and nitrate and the net release of sulfate. Table 4 shows no difference in BrO_3^- removal in the presence of inorganic anion spikes after a one-month contact time. Therefore, Kirisits et al. suggested that the presence of the inorganic anions decreases the rate of bromate reduction, but does not necessarily decrease the total mass of bromate that can be reduced given sufficient time (i.e. one month). Quite a large mass of bromate was reduced in these experiments (2.0 mg BrO_3^-/g carbon). Since this is a reduction process not just a physical adsorption process, it may not be possible to calculate a

carbon's "capacity" for bromate removal. It is not yet known if the bromate reduction sites are capable of being regenerated or if the sites are destroyed after bromate reduction. Site regeneration may be possible, as Kim and Snoeyink (1980) [57] demonstrated the regeneration of monochloramine reduction sites.

Experiment	Mass concentration removed (mg anion/g carbon)			
	Bromate	***Chloride***	***Nitrate***	***Sulfate***
Control (no carbon) in DDW; (mg/l)	0.2	0.1	0.0	0.0
DDW	1.9	0.0	0.0	- 3.4
DDW; 24.1 mg/l chloride	1.9	1.5	0.0	- 3.1
DDW; 25.1 mg/l nitrate	1.9	0.0	5.1	- 3.1
DDW; 49.0 mg/l sulfate	2.0	0.0	0.0	- 3.8
DDW; 23.7 mg/l chloride, 25.2 mg/l nitrate, 49.2 mg/l sulfate	1.8	1.3	3.8	- 4.6

Table 8: One-month bromate reduction studies (initial conditions: 1000 mg/l carbon, DDW, pH 6.5, 5 mM phosphate buffer, 1.84± 1.97 mg/l BrO_3^-)

Huang et al. 2007 [52] has done a research on the effects of the characteristics of activated carbon on the removal of bromate. They used three commercial forms of activated carbon (AC), Norit (AC_N), Calgon (AC_C) and YUB (AC_Y), from various sources and were evaluated in kinetic and isotherm experiments. The specifications of each form are summarized in Table 9. The kinetic adsorption of BrO_3^- was performed in a rotary tumbler at a rate of rotation of 120 rpm. A suitable dose of carbon was introduced into 100 mL amber glass bottles. The carbon that was used in the kinetic tests was soaked overnight in Milli-Q water (buffered with 10mM Na_2HPO_4/H_3PO_4, adjusted to pH 7.5 by adding HCl) to enhance the wetting of the carbon surface and

the internal pore structure. Then, 200 μL of a 100 mg/L solution of BrO_3^- was injected until the BrO_3^- concentration in the bottle was 200 μg/L. The bottles were filled with BrO_3^- solution to eliminate headspace and capped with Teflon septum caps. Then, they were placed on a rotary tumbler with samples that were obtained at predetermined intervals over a period of 24 h. Samples were filtered through pre-washed 0.45 μm filters to remove activated carbon and the residual BrO_3^- concentration was determined.

Specifications	Norit (AC_N)	Calgon F-400 (AC_C)	YUB (AC_Y)
Material	Coconut Shell	Bituminous coal	Wood
Mean Particle size (mm)	1.4	1.2	1.2
Surface Area (m^2/g)	950	950	980
Iodine Number (mg/g)	1020	1000	1000
V_{meso} (cm^3/g)	0.089	0.175	0.760
Oxygen Content (%)	3.5	4.3	11.5
Basic groups (meq/g)	0.23	0.57	0.71
pH_{zpc}	5.2	5.8	4.1

Table 9: Manufacturer's specifications and surface e proterpties for activated carbons (modified from Huang et al. 2007)

(Note: It seems that pH_{zpc} values are mixed and not accurate for other above values of basic groups concentration and below BrO_3^-).

Huang et al. presented the batch kinetic removal curves of amounts adsorbed (q_e) versus contact time (t) for the three carbons of interest with a BrO_3^- single component as in Fig 10. Clearly, 20 hours is enough for all of the adsorption systems to reach equilibrium. The kinetics of adsorption of BrO_3^- on the three carbons is currently described using three kinetic models: pseudo-first order, pseudo-second order and intraparticle diffusion models to identify the potential rate-controlling steps

in this work. Furthermore, They found that the surface chemistry will affect on the adsorption, by comparing the adsorbed amounts of BrO_3^- on AC_y which has oxygen content of 11.5%, and two other heat-treated carbons (oxygen contents = 6.9 and 4.2% respectively). The adsorbed amount is higher on carbons of lower oxygen contents. The surface chemical groups are classified according to their acid–base character [53]. At a fixed pH (7.5), the properties of these groups were strongly correlated with the adsorption of BrO_3^-. The virgin carbon, which was more effective than the acid-washed carbons in removing BrO_3^-, has many more basic groups. The infrared spectra (IR) of these carbons reveal that the raw carbons contain more hydroxyl groups than the acid-washed carbons [52]. Weak ionic interactions typically participate in the adsorption of BrO_3^- by activated carbon surfaces by bonding between the negatively charged side of the anion and the positively charged carbon surface. Based on the discussion of the effects of carbon surface chemistry on BrO_3^- adsorption, both the physical and the chemical effects are suggested simultaneously to influence adsorption.

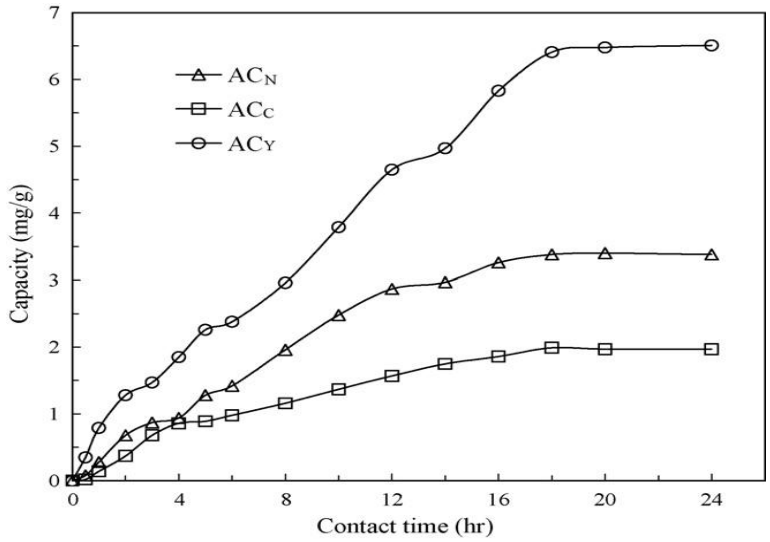

Figure 10: Kinetics plots of BrO_3^- Removal by three selected ACs (Huang et al. 2007)

As a conclusion from Huang et al. research, the adsorption kinetics and isotherms of BrO_3^- on activated carbon reveal that the characteristics of activated carbon influence the capacity for the adsorption–reduction of BrO_3^- .These properties were found to affect the amount of BrO_3^- reduced. First, carbons with the largest mesopores (V_{meso}) have adsorbed most of the BrO_3^-. Second, the intraparticle diffusion played a significant role. Therefore, it is of prime importance to select the carbon porosity and pore size to accelerate the BrO_3^- adsorption. Third, the functional groups on the carbon surface importantly determine its capacity to adsorb BrO_3^-. The carbons with more basic surface groups and higher pH_{zpc} had a higher BrO_3^- adsorption capacity, suggesting that protons are adsorbed on the available surface hydroxyl groups or phenolic groups under typical pH conditions. Finally, to achieve effective BrO_3^- removal from an aqueous solution, the combination of mesopore volumes and surface chemistry should be considered as the principal criterion for adsorbent selection.

Win-yi DONG et al. (2009) [58] have made a comparison between virgin GAC and Silver supported AC. They have studied the effects of solution pH, initial BrO_3^- concentration, co-existing ions on the BrO_3^- removal mechanism. The general physical properties for these two samples were close to each other, and the silver content in the silver-supported AC was between 0.06 - 0.15%. The textural structure examination for both samples can be observed from SEM photographs in figure 11. These photomicrographs show surface structure of silver-AC and virgin GAC. It is obvious that silver was distributed well proportioned on the surface and pores of the carbon.

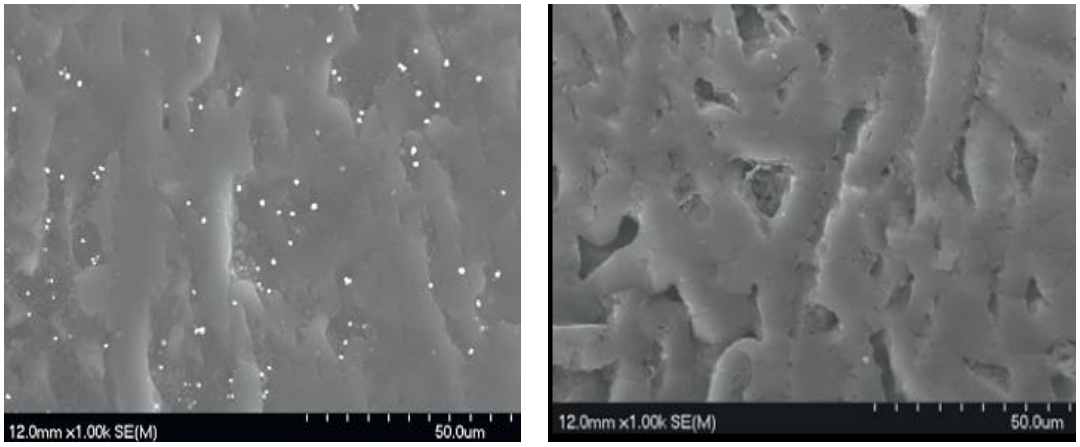

(a) Silver-AC (b) GAC

Figure 11: SEM photographs of two GACs (DONG et al. 2009)

They made a comparison between GAC and Silver-AC for bromate removal presented as fraction BrO_3^- remaining (C/C_0) vs. contact time as in figure 12. It is clear that a period of eight hours is sufficient for attaining the equilibrium for both Silver-AC and GAC removal system. However, a much better removal of BrO_3^- was achieved by silver-AC, as compared to using the virgin GAC. After 20h treatment, the residual BrO_3^- was 19.8µg/L with silver-AC and 38.8µg/L with the virgin GAC when the initial BrO_3^- concentration was 102µg/L. And the removal efficiency of bromate increased about **25%** by using silver-AC. The proposed mechanism was that BrO_3^- is firstly adsorbed on GAC and then reduced. Dong has also concluded that the pH value has an important influence on BrO_3^- reduction. The BrO_3^- reduction increases as the solution pH decreases. He has adapted the explanation of Siddiqui et al. in 1996. The initial concentration of BrO_3^- has a great impact on the removal capacity. The higher the initial concentration of BrO_3^- has the higher BrO_3^- removal according to figure 13.

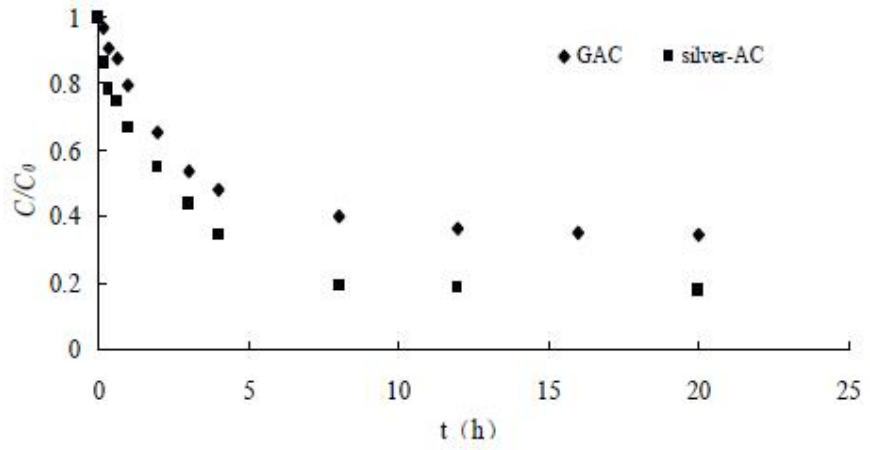

Figure 12: BrO_3^- uptake by Silver-AC and virgin GAC (initial BrO3 =102 µg/L, T=298K, pH=7.58) (DONG et al. 2009)

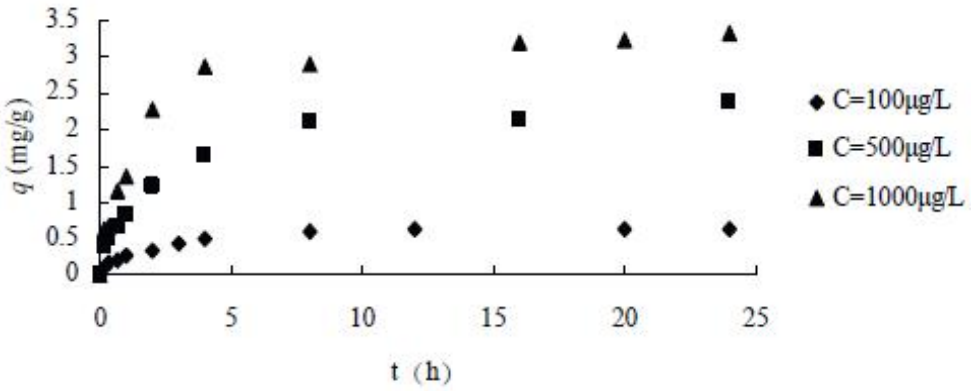

Figure 13: Effect of initial BrO_3^- concentration (T=298K, pH=7.58) (DONG et al. 2009)

The effects of some inorganic anions such as F^-, Cl^-, SO_4^{-2}, Br^- and PO_4^{-3} on BrO_3^- removal were studied also. Every anion was prepared in three different concentrations (0.1, 1.0, 10 mg/L) while the initial BrO_3^- concentration was 0.1 mg/L. The effect of the co-existing anion in reducing silver-AC ability to remove BrO_3^- is shown in Figure 14. The effect of anions in reducing BrO_3^- removal may be attributed

to the fact that these anions are competing with BrO_3^- for the active sites on the carbon surface. It should be noted that Cl^-, F^- and Br^- had a slight effect on the removal of BrO_3^- ,while SO_4^{-2}, CO_3^{-2}, NO_3^- and PO_4^{-3} showed a stronger influence. The reason may be due to large molecular weights of these four anions, hence, they may occupy more sites required for bromate removal. The affinity of the anions for silver-AC sites decreased in the following order $CO_3^{-2} > PO_4^{-3} > SO_4^{-2} > NO_3^- > Br^- > Cl^- > F^-$ when the co-existing anion concentration was 10 mg/L.

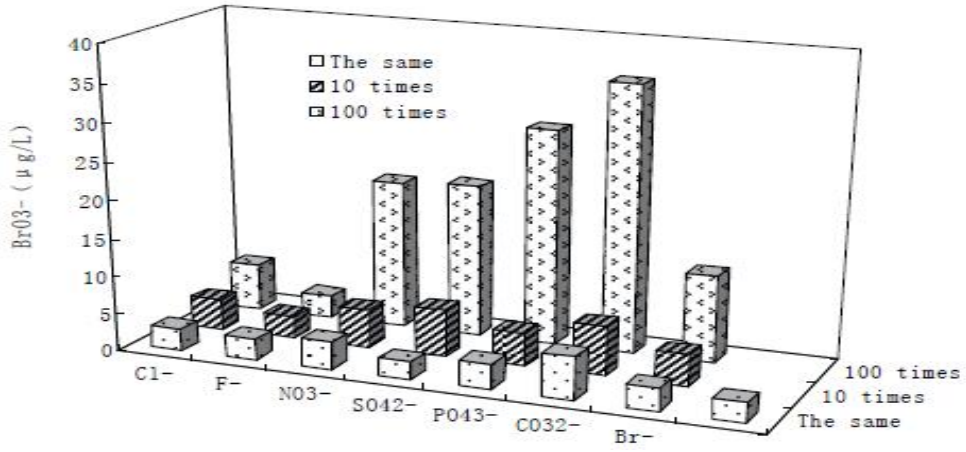

Figure 14: Effect of co-anions (DONG et al. 2009)

2.3.2 Using Other Techniques

Other techniques have been applied for bromate removal. Naoyuki et al. (2009) [59] used Activated carbon Felt Electrode for electrochemical reduction of BrO_3^- ion. Cristina T. Matos et al. (2008) [60] also found that ion exchange membrane bioreactor (IEMB) is effective solution for bromate ion removal. The work evaluated the applicability of the IEMB concept for the removal of bromate from drinking water

in situations where nitrate is also present in concentrations up to 3 orders of magnitude higher than bromate concentration. The batch results obtained showed that the biological reduction of BrO_3^- was slow and only occurring after the complete reduction of NO_3^-. The specific bromate reduction rates varied from 0.027 ± 0.01 mg $BrO_3^-/g_{cell\ dry\ weight}$·h to 0.090 mg $BrO_3^-/g_{cell\ dry\ weight}$·h for the studied concentrations. Finally, IEMB has proven to be a technology able to solve specific problems associated with the removal of BrO_3^- from water, since it efficiently removes BrO_3^- from drinking water even in the presence of NO_3^-, without secondary contamination of the treated water by cells or excess of carbon source. Leon S. Downing et al. (2006) [61] used hydrogen-based membrane biofilm reactor (MBFR) for bromate reduction and he got good results also.

2.4 CARBON NANOTUBES (CNTs)

2.4.1 History of Carbon Nanotubes

The current huge interest in carbon nanotubes is a direct consequence of the synthesis of buckminsterfullerene, C_{60}, and other fullerenes, in 1985. Fullerenes were accidentally discovered by Kroto and Smalley where they had found strange results in mass spectra of evaporated carbon samples and their stability in the gas phase was proven (Daenen, et al., 2003)[62]. Figure 15 shows the structure of C60 of buckminsterfullerene. The discovery of fullerenes has prepared to the discovery of carbon nanotubes by Sumio Iijama in 1991. He managed to prepare a new type of finite carbon structure consisting of needle-like tubes grown on the negative end of the carbon electrode used in the arc-discharge evaporation of carbon in an argon-

filled vessel. Figure 16 shows electron microscope images of multi-walled carbon nanotubes which were initially discovered by Iijama.

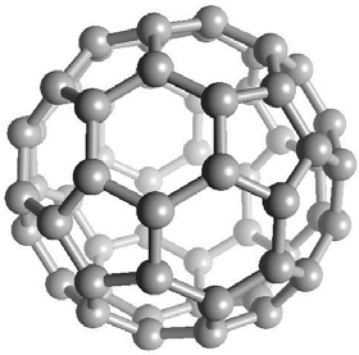

Figure 15: The structure of C60, buckminsterfullerene.

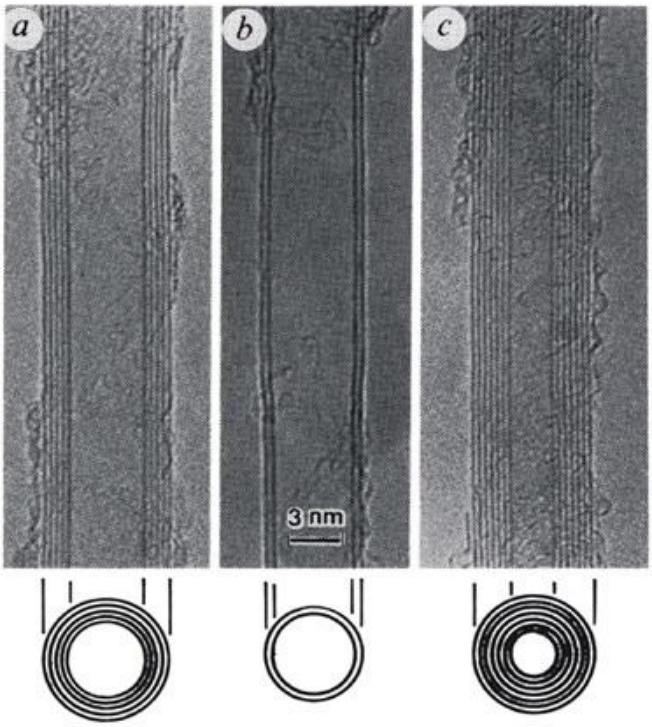

Figure 16: Electron micrographs of microtubules of graphitic carbon. Parallel dark lines correspond to the (002) lattice images of graphite. A cross-section of each tubule is illustrated. (a) Tube consisting of five graphitic sheets, diameter 6.7 nm. (b) Two-sheet tube, diameter 5.5 nm. (c) seven-sheet tube, diameter 6.5 nm, which has smallest hollow diameter (2.2 nm) [2].

In 1993, Iijima and Ichihashi reported the synthesis of abundant single-shell tubes with diameters of about 1 nm [63]. Figure 17 illustrates an image of single-walled nanotubes (SWNT). During this period, Bethune and his IBM Almaden colleagues discovered that transition metals such as cobalt can catalyze the formation of single-wall carbon nanotubes [64]. In 1996 Thess *et al.* synthesized bundles of single wall carbon nanotubes for the first time [65]. Since then, a new era of intensive research has begun, along with the improvement of the production and characterization techniques, to assess potential CNTs applications.

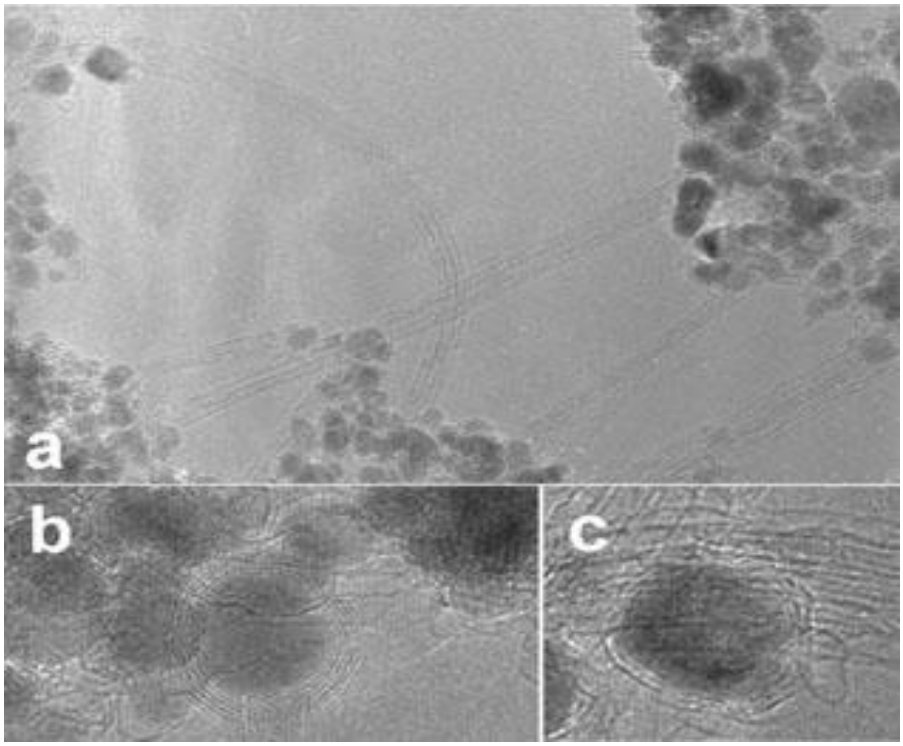

Figure 17: TEM images of SWCNT [64]

2.4.2 The Structure of Carbon Nanotubes

CNTs are sheets of graphenes folded up into seamless cylinders as in Figure 18 (Meyappan et. al., 2005) [66]. CNTs are divided into either single-walled carbon nanotubes (SWCNTs) or multi-walled carbon nanotubes (MWCNTs) based on the number of rolled sheets, which can be in the range of 2-50 sheets [2], in the wall of the nanotubes (Figure 19).

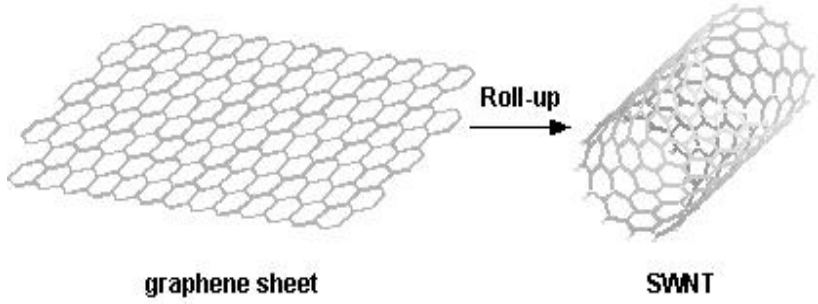

Figure 18: A schematic showing a graphene sheet rolled-up into a single walled carbon nanotube [66]

Figure 19: Schematic theoretical model for multi-walled carbon nanotubes. [62]

The diameter of MWCNTs ranges from 2 to 30 nm whereas that of SWCNTs is 1–2 nm. The spacing between the sheets of graphene in MWCNTs is 0.34 nm. Zheng *et al.* has synthesized a SWNT of a length of 4.8 cm and indicated the possibility of synthesizing a continuous tube without any length limitation [67]. Tang *et al.* have reported the fabrication of mono-dispersed SWNTs of diameter as small as 0.4 nm [68]. A perfect tube is capped at both ends by hemi-fullerenes, leaving no dangling bonds. The perfect tube is capped at both ends by hemi-fullerenes, leaving no dangling bonds. Carbon nanotubes are described by the chiral vector $\overrightarrow{\boldsymbol{C_h}}$, often known as the roll-up vector, which is refers to integer indices graphene unit lattice vectors, where:

$$\overrightarrow{C_h} = n\overrightarrow{a_1} + m\overrightarrow{a_2}$$

The integers (*n*, *m*) are the number of steps along the ziz-zag carbon bonds of the hexagonal lattice and $\overrightarrow{a_1}$ and $\overrightarrow{a_2}$ are unit vectors, shown in Figure 20. The chiral angle (θ) determines the amount of "twist" in the tube where it can be 0° and 30°; giving rise to as ziz-zag (0°) and armchair (30°) geometries. The ziz-zag nanotube is (*n,* 0) and the armchair nanotube is (*n, m*). In MWCNTs, each individual tube can have different chirality.

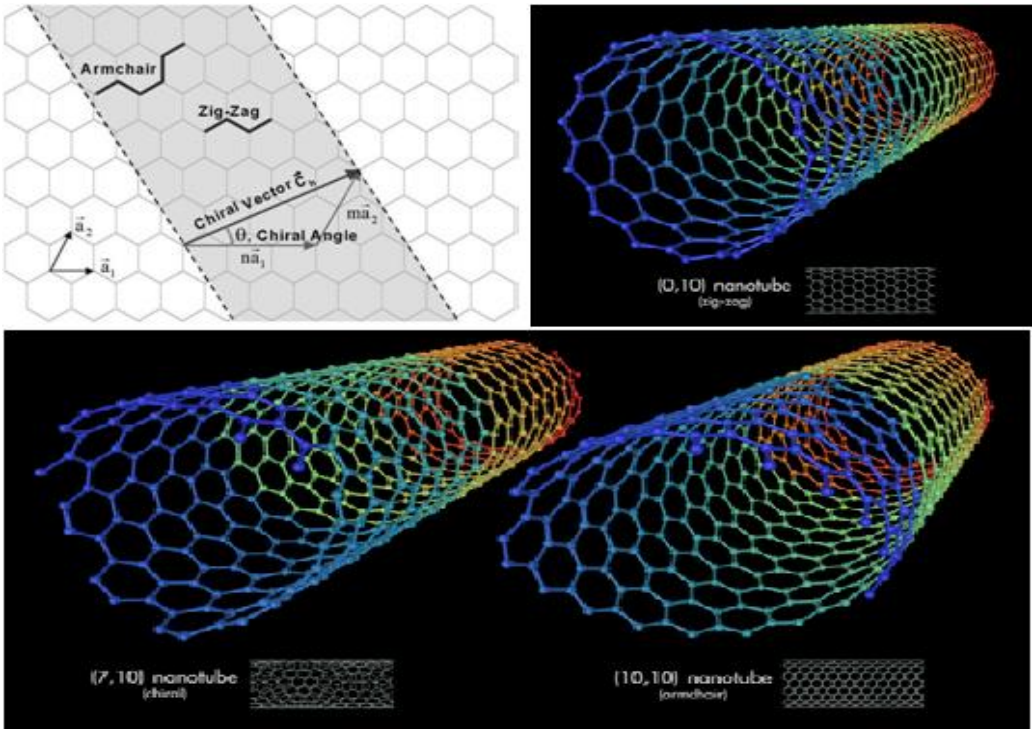

Figure 20: Schematic of the honeycomb structure of a graphene sheet (A). SWCNTs can be formed by folding the sheet along the shown lattice vectors leading to armchair (B), zigzag (C), and chiral (D) tubes, respectively.

The chirality and diameter of the carbon nanotube influence its electronic properties. CNTs can be either metallic or semiconducting by merely changing the tube's diameter. Furthermore, the energy caps for the semiconducting tubes decrease as the tubes diameter increases. All armchair nanotubes are metallic and zig-zag nanotubes are metallic when *n* is a multiple of three as shown in figure 21 [69]. The C-C bonding in CNTs is composed entirely of sp^2 bonds, similar to those of graphite. This bonding structure, which is stronger than the sp^3 bonds found in diamonds, provides the nanotubes with their unique strength. Concentric sheets of MWCNTs are held together by Van Dar Waals bonds [70]. Under high pressure, nanotubes can

merge together, trading some sp^2 bonds for sp^3 bonds, giving the possibility of producing strong, unlimited-length wires.

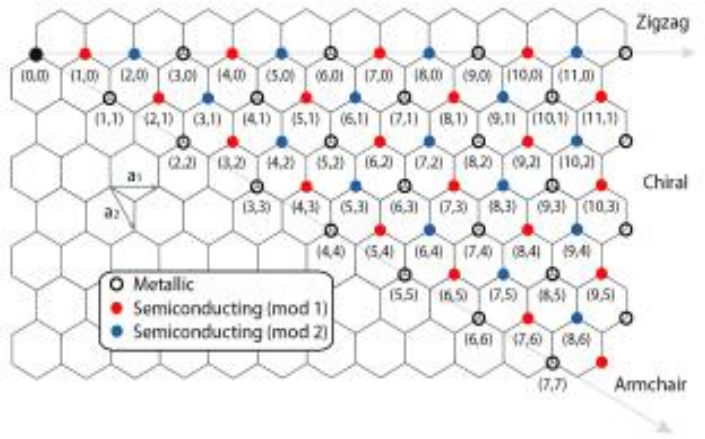

Figure 21: Chirality chart depicting the multitude of (n,m) SWCNT structures possible based on the role-up vectors.

2.4.3 Synthesis of Carbon Nanotubes

There are three methods of producing carbon nanotubes which are arc-discharge, laser-vaporization or laser-ablation technique and chemical vapor deposition. The principle of CNT production is that all known techniques involve a carbon feedstock, a metal catalyst and heat. All the production methods of SWNTs require a metal catalyst, except for carbon arc discharge for MWNTs production; it does not require any metal catalyst [71].

- **Arc Discharge Technique**

This is the first technique used for MWCNTs production by Iijama in 1991. Using this method also, Iijima and Ichihashi in 1993 synthesized SWCNTs in the gas phase [63]. Simultaneously, Bethune et al. enhanced the production SWCNTs by cobalt

catalysis [64]. Lambert *at al.* significantly enhanced the synthesis of SWCNTs through the use of binary metal mixtures i.e. Co and Pt [72]. This method creates CNTs through arc-vaporization of two carbon rods placed opposite to each other, separated by approximately 1 mm, in an inert gas-filled chamber at low pressure. A direct current of 50 to 100A, driven by a potential difference of approximately 20 V, creates a high temperature discharge between the two electrodes.

The discharge vaporizes small part of the anode graphite rod and deposited on the cathode graphite rod, which includes CNTs [2]. Producing CNTs in high yield depends on the uniformity of the plasma arc, and the temperature of the deposit forming on the graphite rod. Generally, it is hard to grow aligned CNTs (SWNTs, DWNTs, or MWNTs) by arc discharge, although partial alignment of SWNTs can be achieved by convection or directed arc plasma. On the other hand, the growth temperature of the arc-discharge method is higher than that of other CNT production methods. As a result, the crystalline structure and perfection of arc-produced CNTs are generally high, and the yield per time units is also higher than other methods [73]. Figure 22 illustrates the technique schematic diagram.

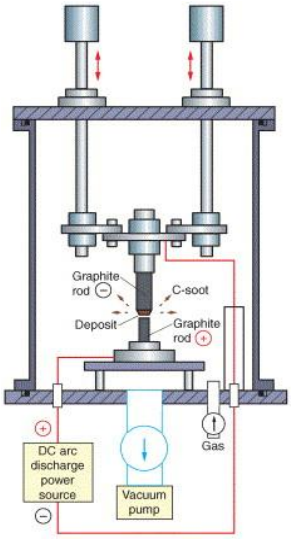

Figure 22: Schematic diagram of an arc-discharge apparatus.

Laser Ablation Technique

In 1995, Guo *et al.* presented a new method for synthesizing SWNTs in which a mixture of carbon and transition metals are vaporized by laser ablation [74]. The following year, Thess *et al.* produced SWNTs in yields of more than 70 % by condensation of a laser-vaporized carbon-nickel-cobalt mixture at 1200°C. The formed nanotubes bundled together into crystalline ropes of metallic character [65]. In this method, samples were prepared by laser vaporization of graphite rods with a 50:50 catalyst mixture of Cobalt and Nickel at 1200°C in flowing argon, followed by heat treatment in a vacuum at 1000°C to remove the C60 and other fullerenes. The initial laser vaporization pulse was followed by a second pulse, to vaporize the target more uniformly.

The use of two successive laser pulses minimizes the amount of carbon deposited as soot. The second laser pulse breaks up the larger particles ablated by the first one, and feeds them into the growing nanotube structure. By varying the growth

temperature, the catalyst composition, and other process parameters, the average nanotube diameter and size distribution can be varied. In contrast to the arc method, direct vaporization allows far greater control over growth conditions, permits continuous operation, and produces a higher yield with a nanotubes better quality [74]. Figure 23 shows a schematic diagram of laser ablation technique.

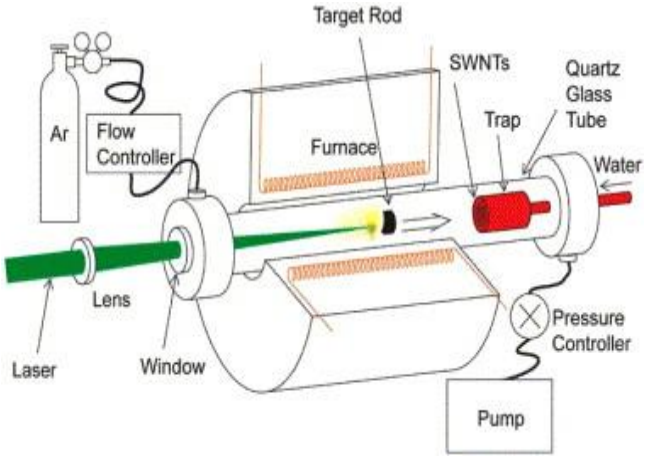

Figure 23: Schematic diagram of laser ablation apparatus.

Chemical Vapor Deposition (CVD)

CVD has been used for producing carbon filaments and fibers since 1959 [75]. Using CVD, Endo *et al.* grew CNT from pyrolysis of benzene at 1100°C [76], while José-Yacamán *et al.* synthesized MWCNTs using catalytic decomposition of acetylene over iron particles at 700 °C [77]. Later, MWCNTs were also grown from ethylene, methane and many other hydrocarbons. Dai *et al.* isolated SWCNT grown by disproportionation of carbon monoxide at 1200°C catalyzed by molybdenum particles [78].

Figure 24 shows a diagram of the setup used for CNT growth by CVD in its simplest form. The process involves passing a hydrocarbon vapor (typically for 15-60 minutes) through a tube furnace in which a catalyst material is present at sufficiently high temperature (600-1200°C) to decompose the hydrocarbon. CNTs grow over the catalyst and are collected upon cooling the system to room temperature [73]. The type of CNTs produced depends on the metal catalyst used during the gas phase delivery and the temperature. In the CVD process SWCNTs are found to be produced at higher temperatures with a well-dispersed and supported metal catalyst while MWCNTs are formed at lower temperatures and even with the absence of a metal catalyst. Table 10 displays a summary of the major production methods, their efficiency and limitations [62].

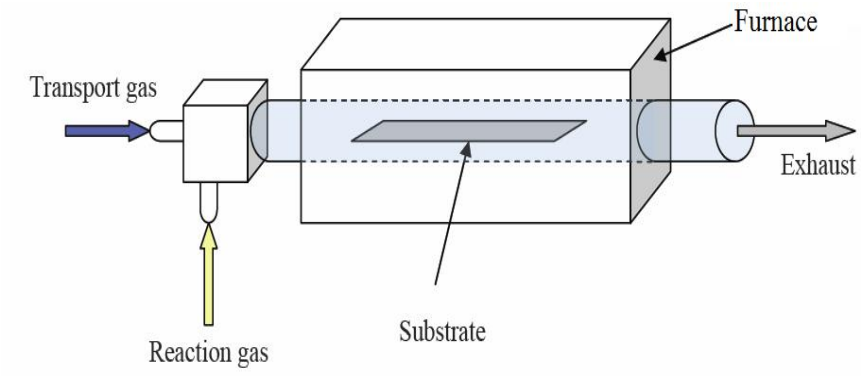

Figure 24: A diagram showing the simplest CVD setup used for CNT growth.

Method	Arc discharge method	Chemical vapor deposition	Laser ablation (vaporization)
Founder	Ebessen and Ajayan, NEC, Japan 1992	Endo, Shinshu University, Nagano, Japan	Smalley, Rice, 1995
Typical yield	30 to 90%	20 to 100%	Up to 70%
SWNT	Short tubes with diameters of 0.6 to 1.4 nm	Long tubes with diameters ranging from 0.6 to 4 nm	Long bundles of tubes (5-20 microns) with individual diameter from 1 to 2 nm
MWNT	Short tubes with inner diameter of 1 to 3 nm and outer diameter of approximately 10 nm	Long tubes with diameter ranging from 10 to 240 nm	Not very much interest in this technique, as it is too expensive, but MWNT synthesis is possible
Advantages	Can easily produce SWNT and MWNTs. SWNTs have few structural defects MWNTs without catalyst, not too expensive, open air synthesis possible.	Easiest to scale up to industrial production, long length, simple process, SWCNT diameter controllable, quite pure.	Primarily SWNTs with good diameter control and few defects. The reaction product is quite pure.
Disadvantages	Tubes tend to be short with random sizes and directions Often needs a lot of purification.	NTs are usually MWNTs and often riddled with defects.	Costly technique because it requires expensive lasers and high power requirement, but is improving.

Table 10: Summary of CNT production methods and properties.

2.4.4 Applications of Carbon Nanotubes

As a new emerging material, CNTs have wide range of applications which will open the future horizons for it to be implemented in industries. The nanosized dimensions, strength and the extraordinary physical properties of these structures make them a very exceptional material with a wide range of potential applications.

Since CNTs discovery, many practical applications have been reported such as chemical sensors, field emission devices (displays, scanning and electron probes/microscopes), catalyst support, electronic devices, high sensitivity nanobalance for nanoscopic particles, nanotweezers, reinforcements in high performance composites, and as nanoprobes in meteorology and biomedical and chemical investigations, medicine/biology (fluorescent markers for cancer treatment, biological labels, drug delivery carriers), anode for lithium ion in batteries, nanoelectronics devices, supercapacitors and hydrogen storage. These are just a few possibilities that are currently being explored. As research continues, new applications will also be developed [79].

2.4.5 Bromate Removal by CNTs

Bromate, as explained above, was removed through using different techniques. CNT's have not been utilized yet for the removal of BrO_3^-. Therefore, this work was initiated for the application of CNTs in BrO_3^- removal. CNTs, were tested for heavy metals removal (as chromium, cadmium, arsenic, etc.) and the results are generally better than that obtained using AC under the same conditions [80]. The proposed mechanisms could be adsorption or reduction of the BrO_3^- existing in water samples. The factors affecting the removal of BrO_3^- are similar to those applied in case of activated carbons. Each of these factors, will be summarized below.

2.4.5.1 Synthesis, purification and modification processes of the CNTs

The technique used to produce CNTs dictates the morphologies of the formed CNTs. Consequently, morphologically different CNTs exhibit different adsorption

capacities. Li *et al.* (2006) [81] have ascertained that the method of producing CNTs influences the adsorption capacity, where they have produced four different kinds of CNTs and treated them with nitric acid. The four kinds behaved differently toward the removal of Pb^{+2} from water. Characterization of the four kinds of CNTs showed that each possesses different porosity, specific surface area, particle size and certain amount of functional groups available on the surface. The kind that has a more functional groups and of larger surface area was more efficient in the removal of BrO_3^- [81].

Furthermore, the treatment/purification process of CNTs has been shown to have an impact on the adsorption efficiency of CNTs which in turn affects the removal of the metal ions. The acid treatment process usually introduce a certain functional groups on the surface of CNTs. Li *et al.* observed that the adsorption capacity increases remarkably when the CNTs were refluxed with concentrated nitric acid at 140 °C for 1 h [81]. It is known that oxidation of carbon surface can offer not only a more hydrophilic surface structure, but also a larger number of oxygen-containing functional groups, which increase the ion-exchange capability of carbon material toward cations [82]. It has been shown that supporting CNTs with certain complexes enhances their adsorption capacity. Li *et al.* (2001) confirmed that the adsorption capacity for Al_2O_3 supported on CNTs is about 4 times higher than that of the grown CNTs in the removal of fluoride from water [83]. Peng et al. (2005) attested that CNTs-iron oxide magnetic composites (Fe_3O_4) can be used to adsorb contaminants from aqueous effluents and after the adsorption is carried out, the adsorbent can be separated from the medium by a magnetic process [84].

2.4.5.2 Effect of pH

The pH of the mediam is one of the most important factors that influence the site dissociation of CNTs and the hydrolysis, complexation and precipitation of ions. The pH at which the net surface charge is zero is called "point of zero charge", pH_{PZC}. When the pH of the solution is higher than pH_{PZC} of the carbon material, a negative charge on the surface will be dominant and the surface has better interactions with cations. But, when the pH decreases less than the pH_{pzc}, the surface charge will be positive and metals adsorption decreases while anions adsorption increases.

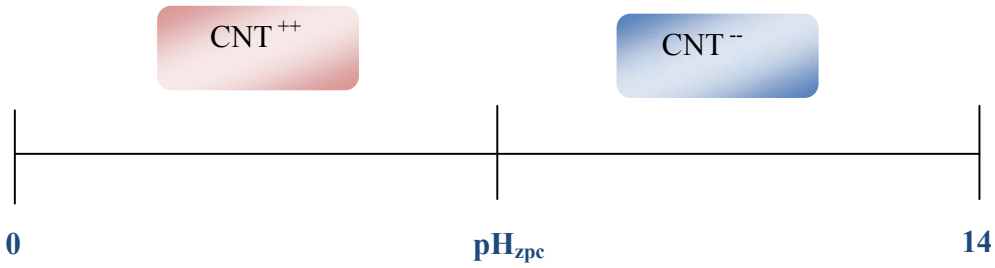

2.4.5.3 Effect of Contact Time

Theoretically, as the time increases, the adsorption capacity is expected to increase until equilibrium is reached. The metal binding sites become saturated as contact time increases. Wang *et al.* (2007) stated that the adsorption of Pb(II) onto acidified MWCNTs increases quickly with contact time at the first 20 min and then reaches equilibrium [85]. Lu *et al.* demonstrated that the adsorption efficiency for dissolved organic carbon, assimilable organic carbon and trihalomethanes increased steeply with time and then slowly reached equilibrium.

2.4.5.4 Effect of CNT Dose

The dosage of CNTs can be associated to the availability of the adsorption sites. Based on the studies made, the adsorption of metal ions can be enhanced by increasing the adsorbent (CNTs) dosage which provides more adsorption sites for binding. Li *et al.* highlighted that the adsorption capacities for Pb^{2+}, Cu^{2+}, and Cd^{2+} increase with increasing of the CNT dosage [82]. The removal ratio of Pb^{2+}, Cu^{2+}, and Cd^{2+} generally increases with an increase in the amount of adsorbent as was confirmed by Hsieh and Horng [86].

2.4.5.5 Effect of Shaking Speed

The adsorption capacity increases with the increase of agitation speed. This is because the increase of speed causes the adsorbent to be well dispersed in solution hence increasing the metal ion adsorption probabilities. Hsieh et al. has implied the effect of dispersion on adsorption efficiency [86].

CHAPTER 3

METHODOLOGY

3.1 PREPARATION OF CNTs

Multi-walled Carbon nanotubes (MWCNTs) used in this study were produced and optimized of King Fahd University of Petroleum and Minerals. The CNTs were kept dry in a glass bottle at a room temperature of 25ºC.

The experiments were done using different types of CNTs whose surfaces were functionalized or impregnated with metal oxides. The types of samples employed are listed below in Table 11. The preparation procedure for each adsorbent is listed in **Appendix (A).** All samples were characterized by using FE-SEM, EDS, TGA-DSC and FTIR, XRD if required as shown in Chapter four.

CNT Type
CNT Raw
CNT Oxidized
CNT-Fe 1%

Table 11: Used types of CNTs in this research

3.2 PREPARATION OF AC

Activated Carbon (AC) samples were collected from commercial sources available in Saudi Arabia. Characterizations of the samples used were made and are discussed in chapter four. The types of AC used in this project are listed in table 12:

AC Type
AC Raw
AC Oxidized
AC-Ag 0.2%

Table 12: Used types of AC in this research

3.3 PREPARATION OF BROMATE STOCK SOLUTION

The standard stock solution of 100 mg/L of BrO_3^- was prepared by using ACS grade of potassium bromate (SIGMA-ALDRICH) dissolved in distilled-deionized water (DDW). The required solutions of specific concentrations were prepared from the stock solution dilution. The glassware utilized was rinsed many times by DDW before each set of samples to prevent any external contamination.

The standard solution 100 mg/l as BrO_3^- was prepared by dissolving 0.2611 g of $KBrO_3$ (MW: 167.00 g/mol) in a 2L grade A volumetric flask and mixed thoroughly. Then the standard solution was tested by IC (Ion Chromatography) to insure the exact concentration and the correction factor if required. Finally, the calculations used for determining the volume of standard solution to be taken for batch experiments are as follow:

$$V_1M_1 = V_2M_2 \tag{3.1}$$

Where:

V_1 = *Volume of standard solution (L)*

V_2 = *Final desired volume*

M_1 = *Concentration of the standard solution (100 mg/L)*

M_2 = *Concentration of the stock solution that we need (mg/L)*

After preparing the standard solutions, the pH of the solutions was adjusted using 0.1M HCl and 0.1M NaOH to the required pH (i.e. 3, 4, 5, 7, 8, 9, 10 and 11). The concentration of BrO_3^- was determined before adsorption and after pH adjustment. All solutions were capped to avoid any contamination.

3.4 BATCH MODE ADSORPTION EXPERIMENTS

Batch mode adsorption experiments were performed in glass flasks at room temperatures 23-25^oC. Weighed amounts of the adsorbents, in this case, different AC & MWCNTs samples, were added to 50 mL Erlenmeyer flasks containing the fixed concentration of bromate, 0.5 mg/l as BrO_3^-. The Erlenmeyer flasks were covered and mounted on the mechanical shaker (*MPI Lab Shaker*) and shaken at different times starting from 1 h to 48 h. The agitation speed was fixed during all experiments. BrO_3^- was tested twice, first after pH adjustment (C_i) and second after shaking, adsorption and filtration (C_f).

After the desired equilibration time, the suspension was filtered through 0.45µm Millipore filter papers. Afterwards, the filtrates were analyzed for BrO_3^-, Br^- using Ion Chromatography (IC) manufactured by Dionex and using the prober column, see Figure 25. The effects of MWCNTs, AC dosage and type, pH and contact time were studied. The amount of BrO_3^- adsorbed/reduced on the MWCNTs or AC was determined by the difference of the initial concentration (C_i) and the equilibrium concentration (C_e). The percentage removed of BrO_3^- ions from the solution was calculated using the following relationship:

$$\%removal = \frac{C_i - C_e}{C_i} \times 100 \quad (3.2)$$

The bromate adsorption capacity (q_e) was calculated by the following equation:

$$\text{Adsorption Capacity } q_e \text{ (mg/g)} = \frac{C_i - C_e}{M_s} \times V \quad (3.3)$$

Where:

V = volume of the solution (L)

M_s = weight of adsorbent (g)

Figure 25: DIONEX Ion Chromatography

Table 13 illustrates the experimental parameters and their variations which were used in the batch mode adsorption experiments. The initial concentration of BrO_3^- was 0.5 ppm (500 ppb).

Carbon Material	Adsorbent Dose (mg)	pH	Initial BrO_3^- conc. (ppm)	Contact Time (H)
CNT Raw CNT-Oxidized CNT-Fe 1% AC Raw AC-Oxidized AC-Ag 0.2%	10 25 50 75 100 125	3 4 5 6 7 8 9 10 11	0.1 0.2 0.5 1.0 2.0	0.5 1 2 4 6 8 12 16 20 24 48

Table 13: Experimental Parameters

3.5 ADSORPTION ISOTHERMS MODELS

Adsorption isotherms are mathematical models that describe the distribution of the adsorbate species among liquid and adsorbent based on a set of assumptions that are mainly related to the heterogeneity/homogeneity of adsorbents, the type of coverage, and possibility of interaction between the adsorbate species. The Langmuir model assumes that there is no interaction between the adsorbate molecules and the adsorption is localized in a monolayer. Freundlich isotherm model is an empirical relationship describing the adsorption of solutes from a liquid to a solid surface, and assumes that different sites with several adsorption energies are involved. In order to model the adsorption behavior and calculate the adsorption capacity for the adsorbent,

the adsorption isotherms will be studied. The Langmuir adsorption isotherm is perhaps the best known of all isotherms describing adsorption and it is often expressed as:

$$Q_e = \frac{X_m K C_e}{(1 + K C_e)} \tag{3.4}$$

Where;

Q_e *= the adsorption density at the equilibrium solute concentration C_e (mg of adsorbate per g of adsorbent)*

C_e *= the equilibrium adsorbate concentration in solution (mg/l)*

X_m *= the maximum adsorption capacity corresponding to complete monolayer coverage (mg of solute adsorbed per g of adsorbent)*

K *= the Langmuir constant related to energy of adsorption (l of adsorbent per mg of adsorbate)*

The above equation can be rearranged to the following linear form:

$$\frac{C_e}{Q_e} = \frac{1}{X_m K} + \frac{C_e}{X_m} \tag{3.5}$$

The linear form can be used for linearization of experimental data by plotting C_e/Q_e against C_e. The Langmuir constants $\mathbf{X_m}$ and **K** can be evaluated from the slope and intercept of linear equation.

In addition, we can describe adsorption with Langmuir if there is a good linear fit. If not then may be some other model will work. Therefore, we can use Freundlich Isotherm.

$$Q_e = K_F C_e^{1/n} \tag{3.6}$$

Where;

Q_e *is the adsorption density (mg of adsorbate per g of adsorbent)*

C_e *is the concentration of adsorbate in solution (mg/l)*

K_f *and* ***n*** *are the empirical constants dependent on several environmental factors and* ***n*** *is greater than one.*

This equation is conveniently used in the linear form by taking the logarithm of both sides as:

$$\ln Q_e = \ln K_f + 1/n \ln C_e \tag{3.7}$$

A plot of ln C_e against ln Q_e yielding a straight line indicates the confirmation of the Freundlich isotherm for adsorption. The constants can be determined from the slope and the intercept.

3.6 KINETIC MODELING

The study of sorption kinetics is applied to describe the adsorbate uptake rate and this rate evidently controls the residence time of adsorbate at solid liquid interface. In order to evaluate the mechanism of sorption of BrO_3^- by the CNTs, the first-order equation, the pseudo-second-order rate equation and the second-order rate equation are calculated by the following equations respectively:

$$\log \frac{q_e - q_t}{q_e} = -\frac{K_L t}{2.303} \tag{3.8}$$

$$\frac{t}{q_t} = \frac{1}{2K_s q_e^2} + \frac{t}{q_e} \tag{3.9}$$

$$\frac{1}{q_e - q_t} = \frac{1}{q_e} + kt \tag{3.10}$$

Where:

q_e = *sorption capacity at equilibrium*

q_t = *sorption capacity at time (mg/g)*

K_L = *the Lagergren rate constant of adsorption (1/min)*

k = *rate constant of the pseudo second-order sorption* ($g.mg^{-1}.min^{-1}$)

t = *time (min)*

The linear plots of log ($q_e - q_t$) versus t; t/q_t versus t and $1/(q_e - q_t)$ versus t of the above equations, q_e, , K_L and k can be determined from the slopes and intercepts.

CHAPTER 4

RESULTS & DISCUSSION

4.1 BROMATE REMOVAL BY CARBONIC ADSORBENTS

To find out the practical optimum conditions for the removal of BrO_3^- from water, the effects of pH, contact time, adsorbent dose, initial BrO_3^- and adsorbent type were investigated. The adsorption capacity (q_e) was calculated for all of the conditions and employed the. Wide range of adsorbents was applied in this work and the results obtained are promising. Two different acids used were to adjust the pH, the hydrochloric acid of 0.1 N and nitric acid of 0.1 N and a comparison was made between the adsorption capacities obtained.

4.1.1 Bromate Removal by AC

Three types of ACs were used in this study: Raw AC, Oxidized AC and AC impregnated with 0.2% Ag. The effects of pH, AC dosage and contact time were studied and a comparison was made between the results obtained. AC processes moderate reduction properties which could be a key factor to understand the reduction of bromate to bromide.

4.1.1.1 Effect of pH

Bromate reduction by AC increases as the solution pH decreases based on Siddiqui findings [47]. This is attributed to the reduction in the charge on the surface

of the carbon and to the higher reactivity of bromate at low pH. As protons (H+) are added to carbon, the number of negatively charged groups decrease on the surface, and more favorable electrostatic interactions occur between carbon and bromate. If the pH is below the point of zero charge (pH_{pzc}) of the used AC sample, the charge on the surface will be positive. The pH_{pzc} varies among carbons and ranging from approximately 3 to 9 [42]. Therefore, the electrostatic attraction between bromate and the carbon depends not only on the pH of the solution, but also on the type of carbon. Decreasing the pH also increases bromate reactivity; for example, Meijers et al. (1996) [87] found that at pH 1, bromate and bromide instantaneously react to form free bromine in the absence of activated carbon.

Figure 26 shows the results of bromate removal by AC at different pH. Bromate removal capacity (q) when HCl is used to adjust the pH has better results than that of HNO_3. This is attributed to the reduction of nitrate (NO_3^-) to nitrite (NO_2^-) at the reduction sites on AC surface which competes with the reduction of BrO_3^-. Nitrite ion was detected by IC with considerable concentrations in many samples after AC addition; which in turn did not exist in the DDI water or in HNO_3 acid. The nitrate reduction reaction on AC surface is written down where (≡C) refers to carbon. The adsorption capacity (q) for AC-0.2% Ag and AC Raw were similar and close in values. AC raw sample was brought from a commercial supplier and manufactured by Calgon Company and the type is FILTRASORB 400. AC-0.2% Ag is a commercial sample brought from Tangshan Tianhe Company (China).

$$\equiv C + 2\ NO_3^- \longrightarrow 2\ NO_2^- + \equiv CO_2 \qquad (4.1)$$

Also, BrO_3^- reduction by AC-raw is better than that by AC-Oxidized. This result could be attributed to: **1-** the pH_{pzc} of AC raw which is 7.9 in comparison with AC-oxidized which is ~ 4.0 and based on the previous studies, as pH_{pzc} increases the reduction & adsorption of bromate increases. **2-** The carboxylic & hydroxyl groups on the surface of the oxidized AC are repelling bromate anion and reduce the adsorption/reduction capacity.

The highest adsorption capacities (q) for all activated carbon samples were obtained by using raw AC and AC-0.2% Ag when HCl was used to adjust the pH with values higher than 0.5 mg BrO_3^-/g AC under experimental conditions of pH = 3.0, shaking speed 150 rpm, contact time 24h, initial BrO_3^- concentration 0.5 ppm and 50 mg AC dosage. Also, the highest removal at pH 7.0 was for the above two samples and the adsorption capacity was around 0.4177 mg/g.

Oxidized activated carbon sample has much lower adsorption capacity than the raw and silver impregnated ones. Adjusting pH by nitric acid (HNO_3) has clearly negative effect on bromate removal by AC since it reacts with the reduction sites on the surface of the activated carbon.

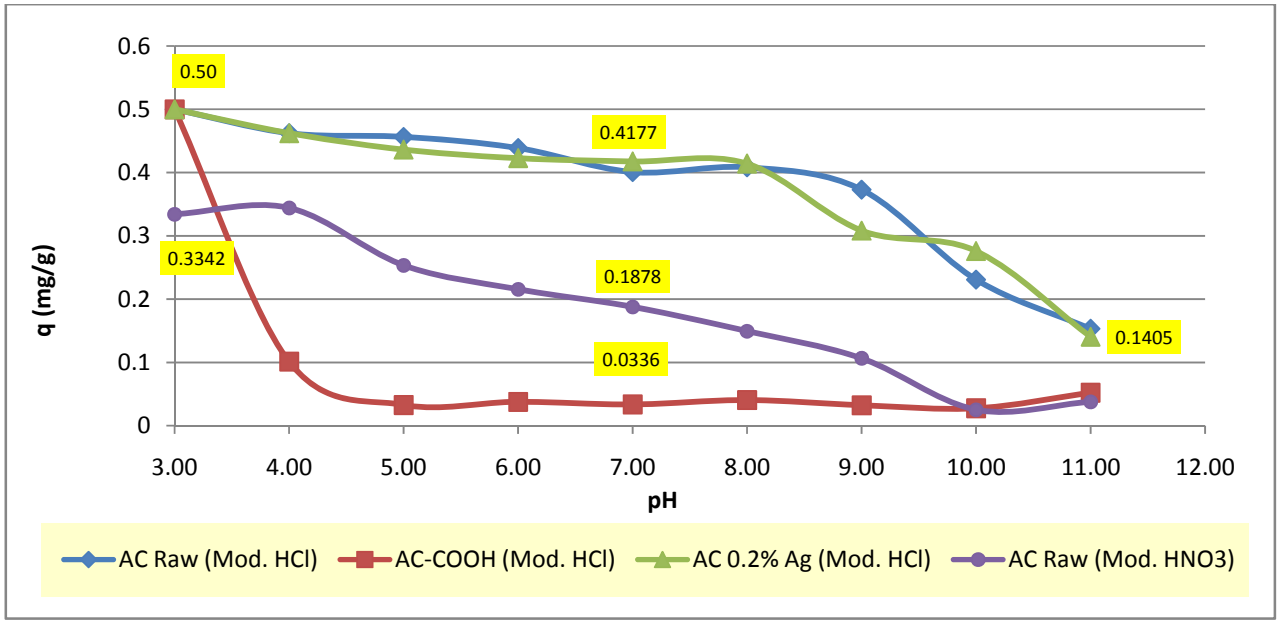

Figure 26: The effect of pH and AC type on Bromate Removal, Contact time 24h, Speed, 150 rpm, Dose 50 mg.

4.1.1.2 Effect of Contact Time

By keeping the values of AC dosage, agitation speed, pH and initial bromate concentration constant, it was observed that bromate adsorption/reduction has positive results in terms of time. The amount of bromate adsorbed for both raw AC and AC 0.2% Ag increased during the reaction time until equilibrium state reached.

Figure 27 shows the bromate removal capacity plot versus contact time. It is clear that the adsorption capacity increases in the first hour and then reaches the equilibrium state with adsorption capacity of 0.3900 mg/g after approximately 2 hours. So, the equilibrium state of BrO_3^- adsorption/reduction was reached after 2 hours contact time when the conditions are: pH 7.5, speed 150 rpm, AC dosage 50 mg and BrO_3^- concentration 0.5 ppm.

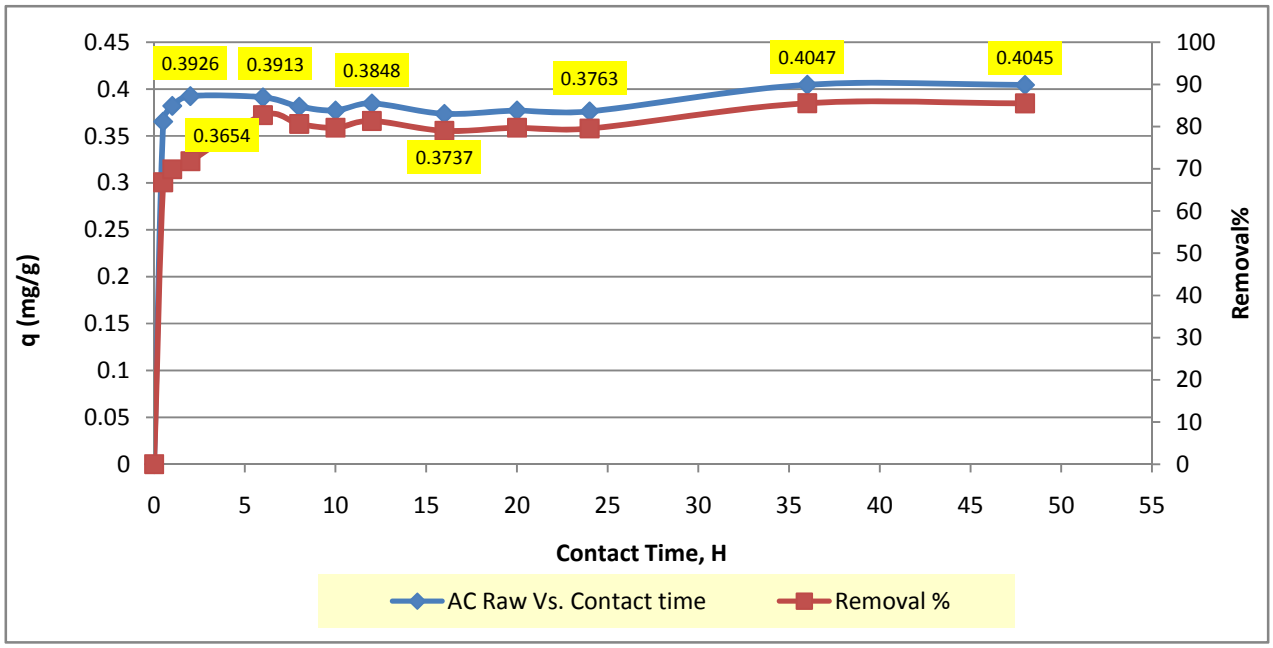

Figure 27: The effect of contact time for AC raw on Bromate Removal, Speed 150 rpm, Dose 50 mg, pH 7.5

The proposed mechanism of BrO_3^- removal is via reduction mechanism because bromide (Br^-) ion formation was detected and was found to increase with time as is shown in Figure 28. It is clear that when the contact time increases, Br^- formation increases due to continuous reduction of BrO_3^- to BrO^- and then to Br^- as Yamada proposed in 1999. Equations 4.2 & 4.3 show the reduction reactions. The mechanism is that first, Br^- will be formed through a reduction reaction, and then it will be adsorbed on AC surface thus competes with BrO_3^-. Accordingly the concentration of Br^- increases.

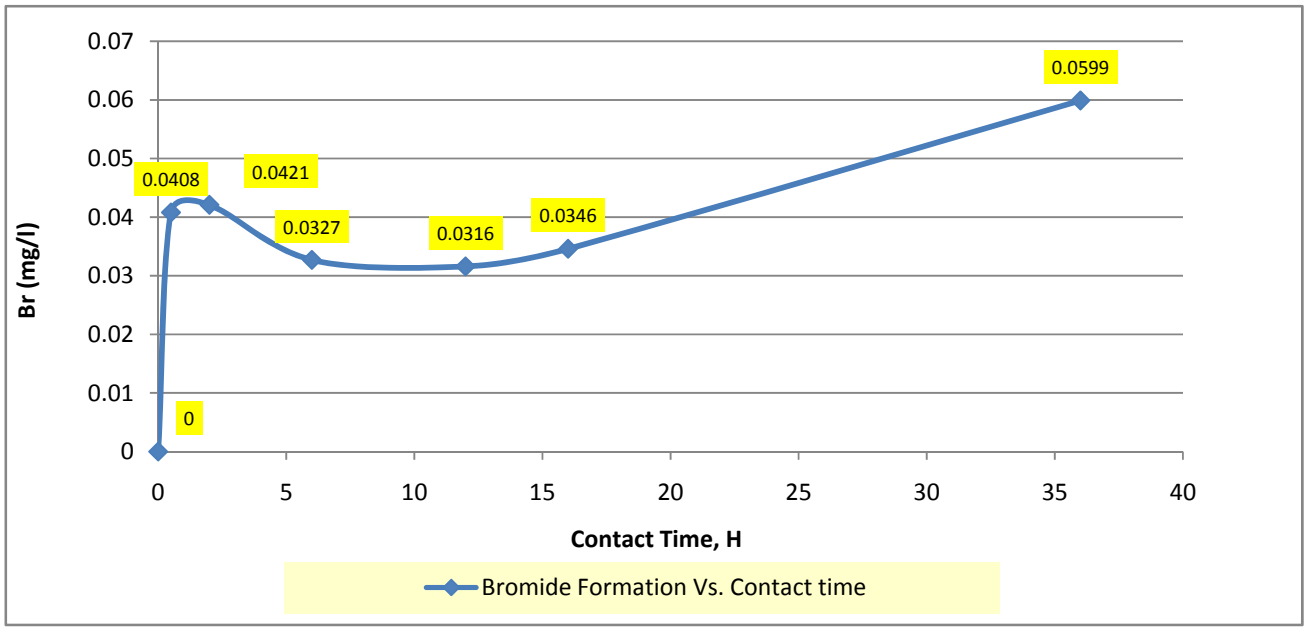

Figure 28: The effect of contact time on Bromide Formation on raw AC, Speed 150 rpm, 50 mg dosage and pH of 7.5

$$\equiv C + BrO_3^- \qquad BrO^- + \equiv CO_2 \qquad (4.2)$$

$$\equiv C + 2\ BrO^- \qquad 2Br^- + \equiv CO_2 \qquad (4.3)$$

Activated carbon impregnated with 0.2% Ag was also investigated at different contact times. Figure 29 shows BrO_3^- adsorption capacity versus contact time when all other variables are constant. The adsorption capacity increases with the contact time until an equilibrium state was reached after 2 hours. The trend is similar to that noticed for raw AC and the mechanism also the same. The equilibrium adsorption capacity is around 0.3900 which is very close to that found for raw AC.

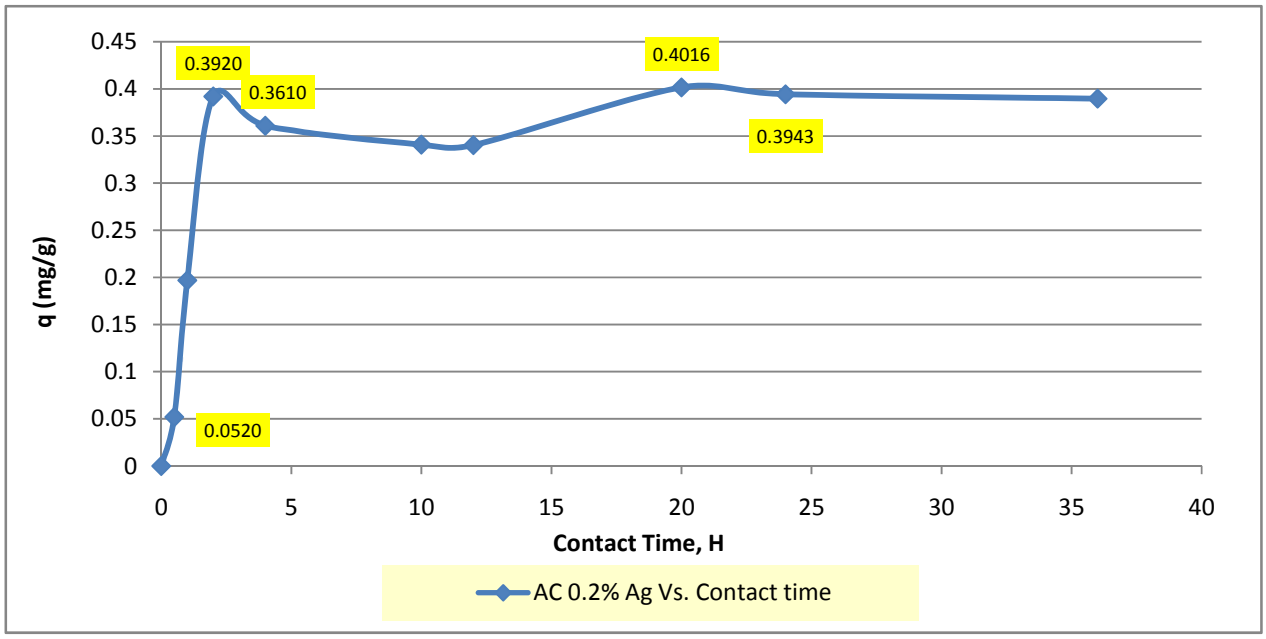

Figure 29: The effect of contact time on Bromate Removal of AC-0.2% Ag, Speed 150 rpm, 50 mg dosage, and pH 7.5

4.1.1.3 Effect of AC Dosage

The batch adsorption experiments were carried out by using various amounts of raw AC, oxidized AC and AC 0.2% Ag ranging from 5 to 125 mg while other factors were kept constant; pH 7.5, agitation speed 150 rpm, contact time 24h and BrO_3^- concentration is around 0.5 mg/l. It has been noted that by increasing the amount of ACs added into the solution; the removal of bromate increases but the overall adsorption capacity (q) decreases. This is due to collection effects of all factors such as initial bromate concentration, removed amount, AC dosage and solution volume when bromate concentration is constant. By using raw AC the removal reached 100 % by adding 125 mg when initial bromate concentration was

0.4152 ppm. The maximum adsorption capacity achieved is 0.486 mg BrO_3^-/g raw AC when AC dosage is 5 mg. Figure 30 shows the percentage of removal and the adsorption capacity versus AC-raw dosage. The maximum adsorption capacity achieved by AC-Oxi is 0.252 mg BrO_3^-/g AC-Oxi. Figure 31 shows the adsorption capacity of BrO_3^- versus AC dosage. Trend line is suggested to exploit the adsorption capacity.

The commercial sample of AC impregnated with 0.2% silver had been studied also. Figure 32 shows the adsorption capacity of AC-0.2% Ag versus dosage when all other factors are constant as stated before. The maximum adsorption capacity is 1.19 mg/g when AC dosage was 5 mg. Finally, the best results were achieved by using AC-0.2% Ag at the lower dosages, then by raw AC. Figure 33 shows the overall results of adsorption capacity versus AC dosages by using the above three AC types.

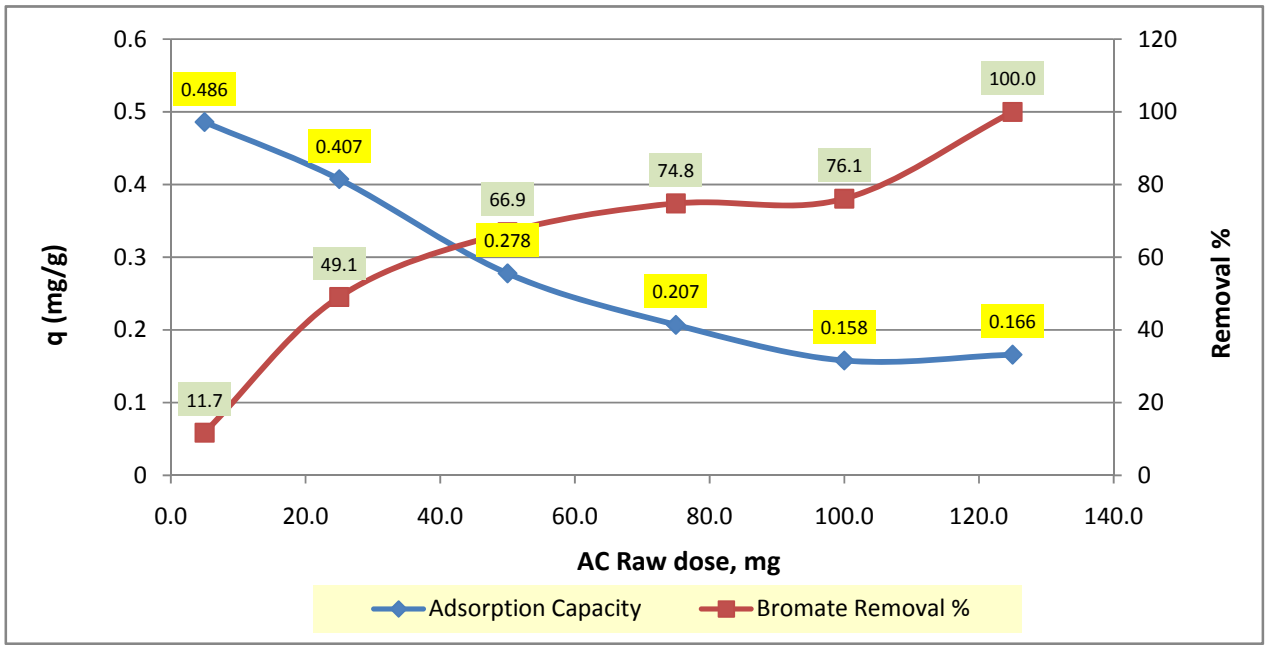

Figure 30: The effect of AC raw dose dosage on Bromate Removal, Contact time 24h, Speed, 150 rpm, pH 7.5.

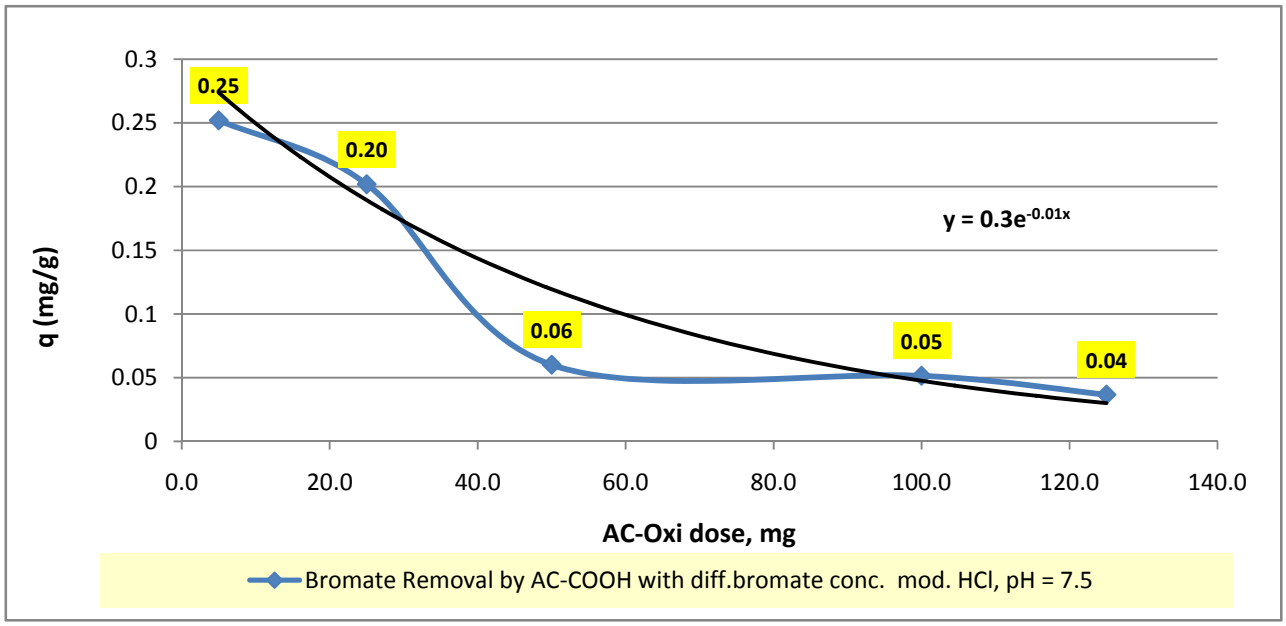

Figure 31: The effect of AC-Oxidized dosage on Bromate Removal, Contact time 24h, Speed, 150 rpm, pH 7.5.

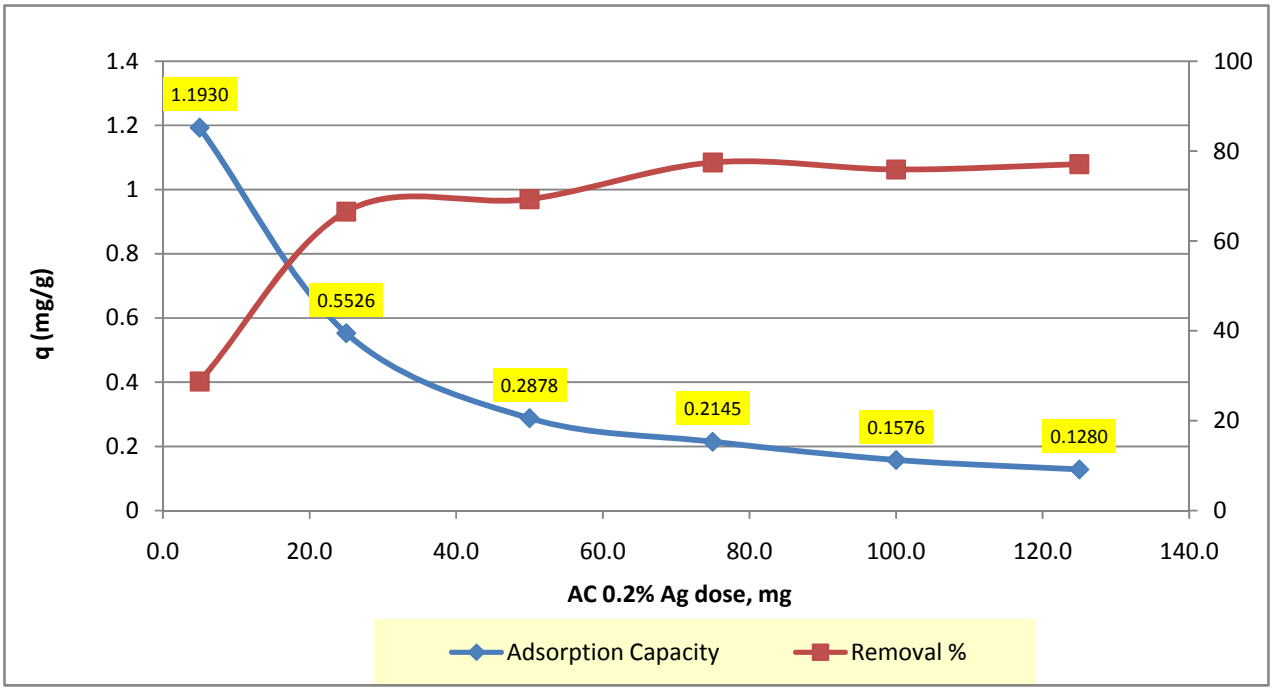

Figure 32: The effect of AC-0.2% Ag dosage on Bromate Removal, Contact time 24h, Speed, 150 rpm, pH 7.5.

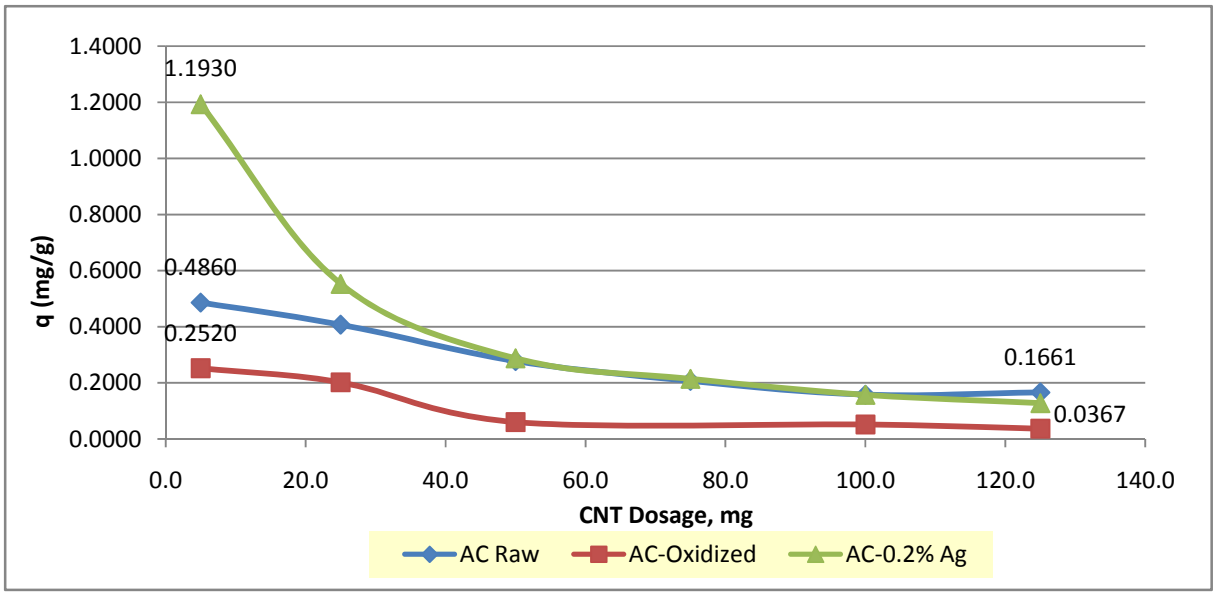

Figure 33: The effect of AC type and dosage on Bromate Removal, Contact time 24h, Speed, 150 rpm, pH 7.5, BrO_3^- concentration ~ 0.5 mg/l.

4.1.2 Bromate Removal by CNT

Three types of CNTs were used in this study: raw CNT, oxidized CNT and CNT impregnated with 1% Fe. The effect of pH, CNT dosage, initial Bromate concentration and contact time were studied as classified below. Also, a comparison was made between using HCl and HNO_3 for pH adjustment in BrO_3^- adsorption by CNT.

4.1.2.1 Effect of pH

The effect of pH on bromate removal is related to the pH_{pzc} of the used CNT in the experiments. The pH_{pzc} of raw CNT and the CNT-Oxidized have been invistigated by Muataz et al. (2010) [88] for the types of CNTs used in this work. Figure 34 shows the pH_{pzc} values for both samples.

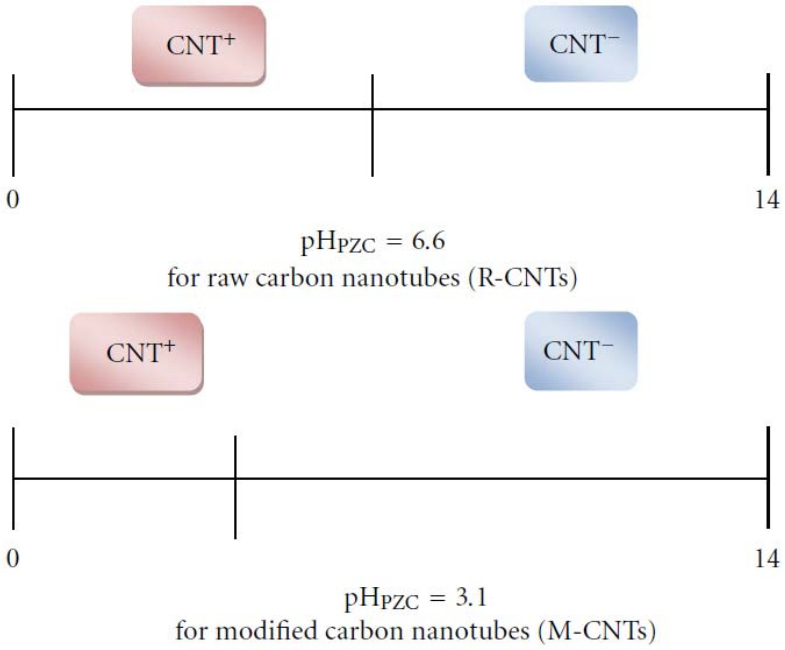

Figure 34: pH_{pzc} of CNT raw and CNT-Oxidized (Muataz et al.)

The pH of aqueous solution is an important variable, which controls the adsorption of ions at the solid-water interfaces. The pH is important parameter for aqueous solutions because it affects the solubility of ions, the concentration of the counter ions on the functional groups of the adsorbent and the degree of ionization of the adsorbate during the reaction. When the pH of the solution is higher than that of the pH_{pzc} of the adsorbent, the negative charge (-) on the surface provides electrostatic interactions which are favorable for adsorbing cationic species. The decrease of the pH leads to neutralization of the charge on the surface, and as pH value decreases less than the pH_{pzc} of the adsorbing materials, the positive charge density increases and adsorption capacity of anions increases.

According to figure 34, pH_{pzc} of raw CNT and CNT-Oxidized are 6.6 and 3.1 respectively. So, the adsorption of bromate will increase as much as the pH of the

solution decreases less than 6.6 for raw CNT sample. On the other hand, the removal of BrO_3^- will be higher in case of raw CNT than the CNT-Oxidized because the pH_{pzc} is lower in the second one and the negative charge is prominent when the pH > 3.1. This finding is demonstrated from by Figure 35. However, the maximum adsorption capacities for raw CNT and CNT-Oxidized at pH 3.0 were 0.283 and 0.352 mg/g respectively, and at a pH of 7.0 were 0.091 and 0.046 mg/g respectively when HCl is used for the pH adjustment.

The effect of acid used in the pH adjustment was also studied. Figure 36 shows the removal of BrO_3^- by raw CNT when two acids used for the pH adjustment (HCl and HNO_3) of the same concentration 0.1N. The lower adsorption capacity of BrO_3^- in the presence of NO_3^- can be attributed to the competitive adsorption behavior between BrO_3^- and NO_3^- on CNT surface due to better NO_3^- affinity toward adsorption than BrO_3^-, and could be attributed also to the smaller size of NO_3^- compared to BrO_3^- ion which makes it better adsorbed anion at CNT surface. Also it was noticed that on using HNO_3 for the adjustment of the pH, very small concentrations of nitrite anions (NO_2^-) were produced as can be seen from IC results. This is due to the reduction of NO_3^- on the few reducing cites of CNT. However, the maximum adsorption capacities of raw CNT (Modified by HCl) and raw CNT (modified by HNO_3) at pH 3.0 were 0.283 and 0.102 mg/g respectively, and at pH 7.0 were 0.091 and 0.010 mg/g respectively.

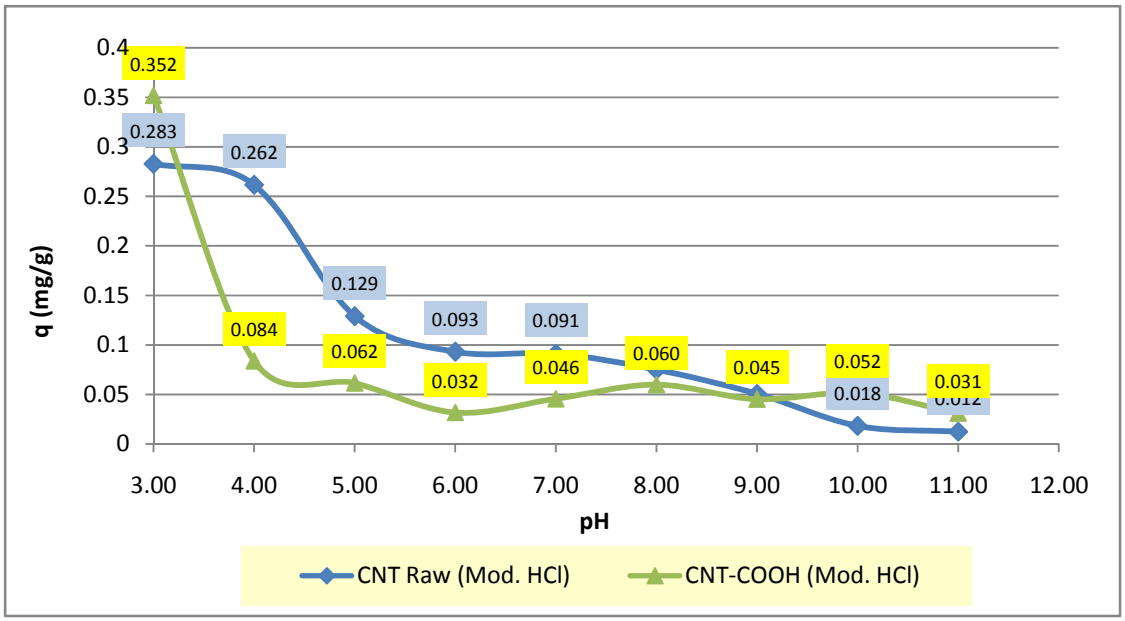

Figure 35: Bromate removal by raw CNT and CNT-Oxidized Vs. pH.

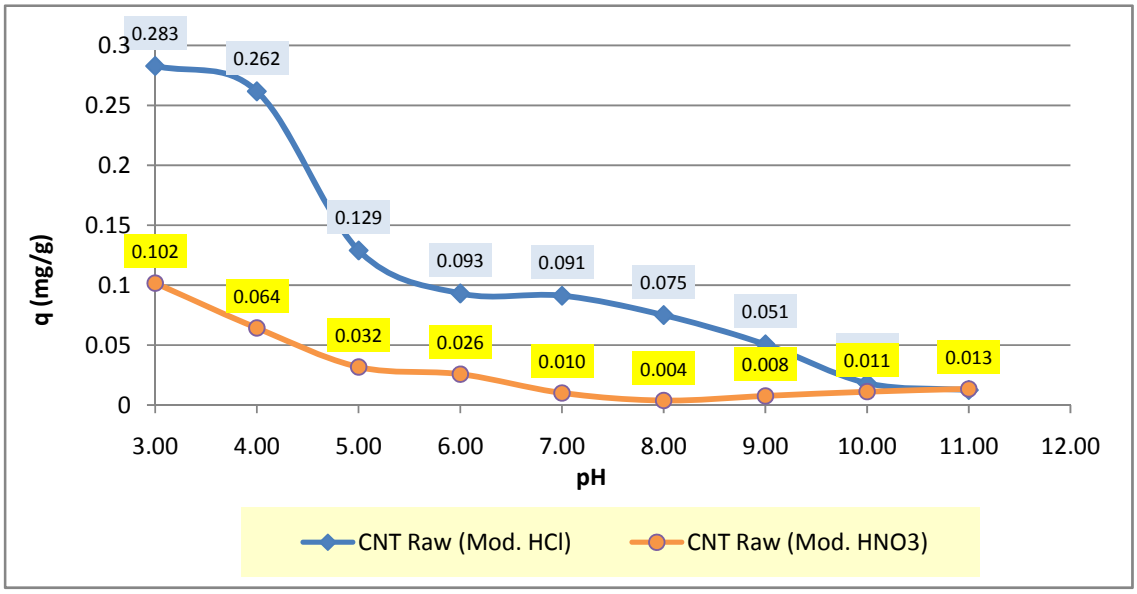

Figure 36: Bromate removal by raw CNT modified by different acids Vs. pH.

The adsorption of CNT with metals impregnated was also investigated in this study. Many samples of metal impregnated CNT investigated, but the advanced studies were carried out for CNT impregnated with iron shows better adsorption capacity than the others. The results of CNT-Fe 1% were better than all other CNT samples at pH 3.0 with adsorption capacity higher than 0.5 mg/g. The adsorption capacity at pH 7.0 is 0.0377 mg/g which is lower than that for raw CNT. Figure 37 shows the adsorption capacities for all of the CNT types studied.

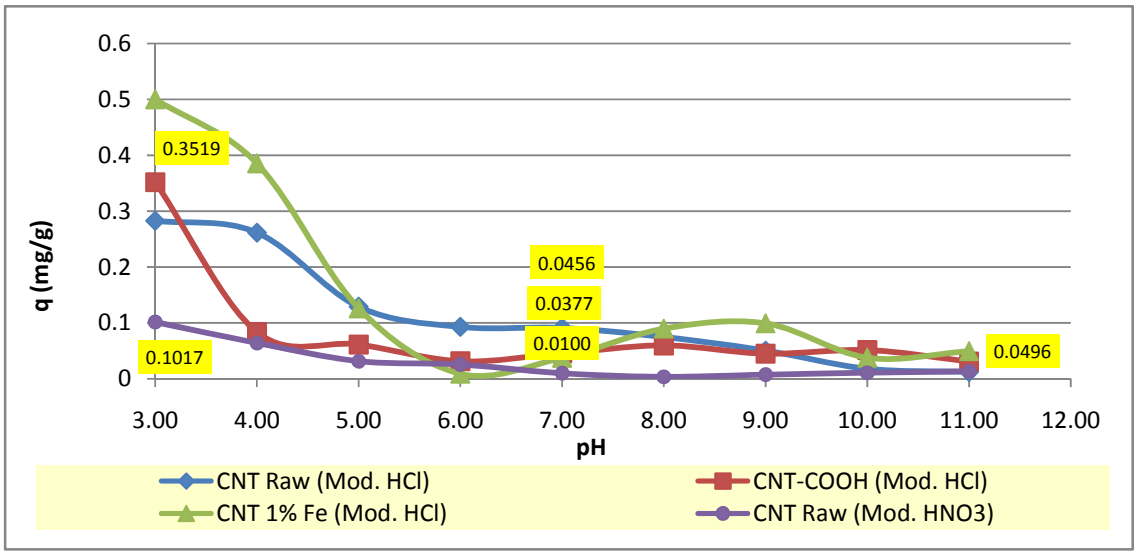

Figure 37: Bromate removal by different CNT types versus pH

4.1.2.2 Effect of Contact Time

By keeping the values of CNT dosage, agitation speed, pH and initial bromate concentration constant, it was observed that BrO_3^- adsorption has positive results in terms of time. The amount of bromate adsorbed for both raw CNT and CNT 1% Fe was investigated. Bromate adsorption increases in the first case, then desorption

effect starts to be effective, as a result the adsorption capacity (q) decreases until reaching the equilibrium state.

Figure 38 shows the adsorption capacity of raw CNT at different contact time when all of the other variables are constant. The maximum adsorption capacity was 0.2656 mg/g reached after 5 hours of contact with raw CNT. The equilibrium adsorption capacity is 0.0713 mg/g which resulted after a period of 48 hours. The phenomenon behavior of BrO_3^- adsorption by CNT 1% Fe resembled the adsorption of raw CNT. Figure 39 shows the adsorption capacity of CNT 1% Fe at different contact times. The equilibrium adsorption capacity was 0.08 mg/g resulted after a period of 12 contact hours. Therefore, the adsorption capacity by CNT 1% Fe is better than that obtained using raw CNT.

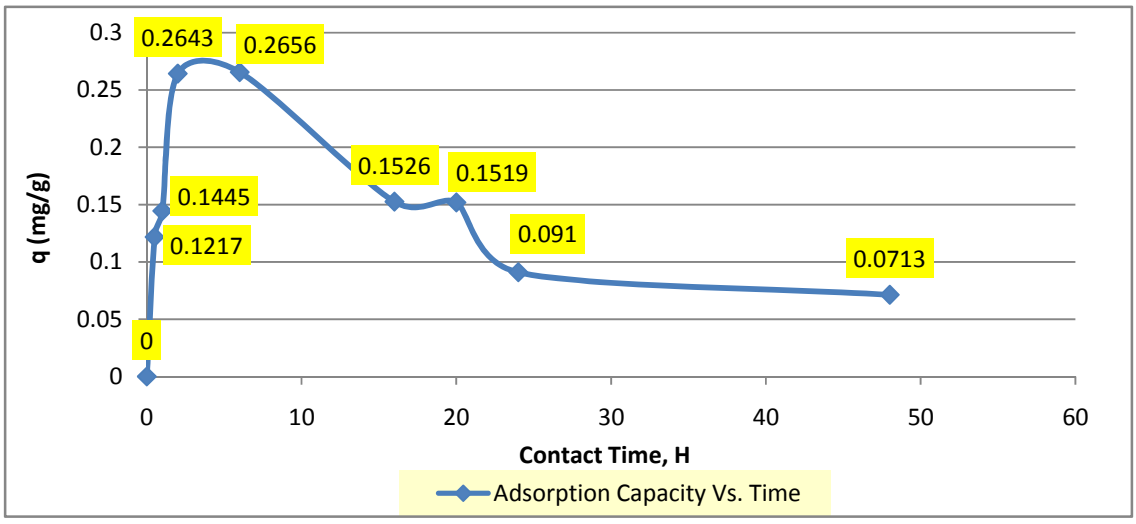

Figure 38: The effect of contact time for raw CNT on Bromate Adsorption, Speed 150 rpm, Dose 50 mg, pH 7.5

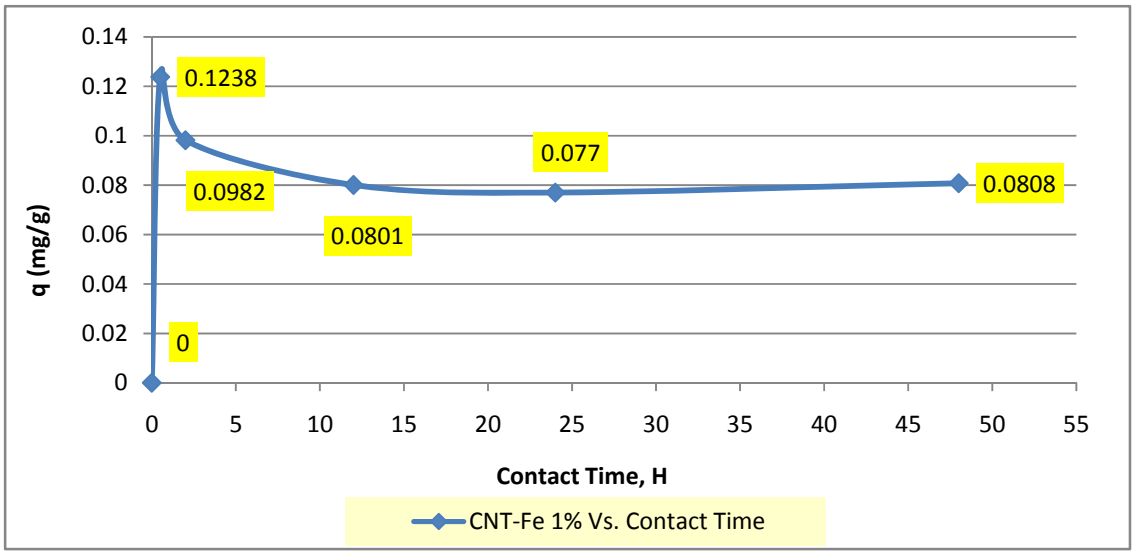

Figure 39: The effect of contact time for CNT raw on Bromate Adsorption, Speed 150 rpm, Dose 50 mg, pH 7.5

4.1.2.3 Effect of CNT Dosage

The batch adsorption experiments were carried out by using various amounts of raw CNT, CNT-Oxidized and CNT-1% Fe. These amounts range from 5 to 125 mg while the pH, agitation speed and contact time were fixed at 7.5, 150 rpm and 24 h respectively. It has been noted that even on increasing the amount of CNTs in the solution, the removal percentage of BrO_3^- remains almost constant (± 5%). However, the overall adsorption capacity decreases since the BrO_3^- concentration was constant but the CNTs dosage has increased. The behavior is different from that of ACs as in case of AC where an increase in the dosage increases the removal percentage of BrO_3^- . This could be attributed to the bundling feature of CNTs in solutions which decrease the open surface for adsorption when more CNT we are introduced into the solution.

Figure 40 shows the adsorption capacity and the percentage removal of bromate by using raw CNT. A maximum adsorption capacity of 0.322 mg/g was achieved by decreasing the amount of CNT which will open the surface of the latter to adsorb BrO_3^-. The percentage removal was found to be less than 20% when the initial concentration of BrO_3^- was 0.5 mg/l (ppm).

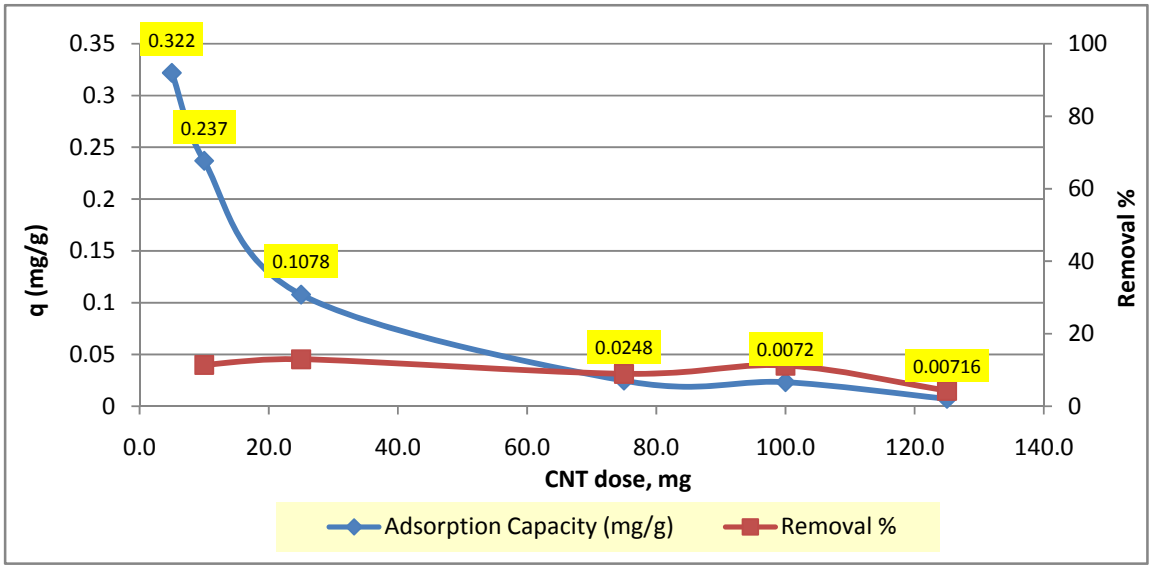

Figure 40: Bromate removal by CNT raw at different dosages. pH 7.5, BrO_3^- 0.5 mg/l, contact time 24h, agitation speed 150 rpm.

Figure 41 shows the adsorption capacity and the percentage removal of BrO_3^- when the CNT-oxidized was used. The maximum adsorption capacity obtained when CNT-oxidized used was 0.290 mg/g. On decreasing the amount of CNT-oxidized to 5 mg more BrO_3^- get adsorbed because of more surface was accessible. The percentage removal was found to be less than 20% when the initial concentration of BrO_3^- was about 0.5 mg/l (ppm).

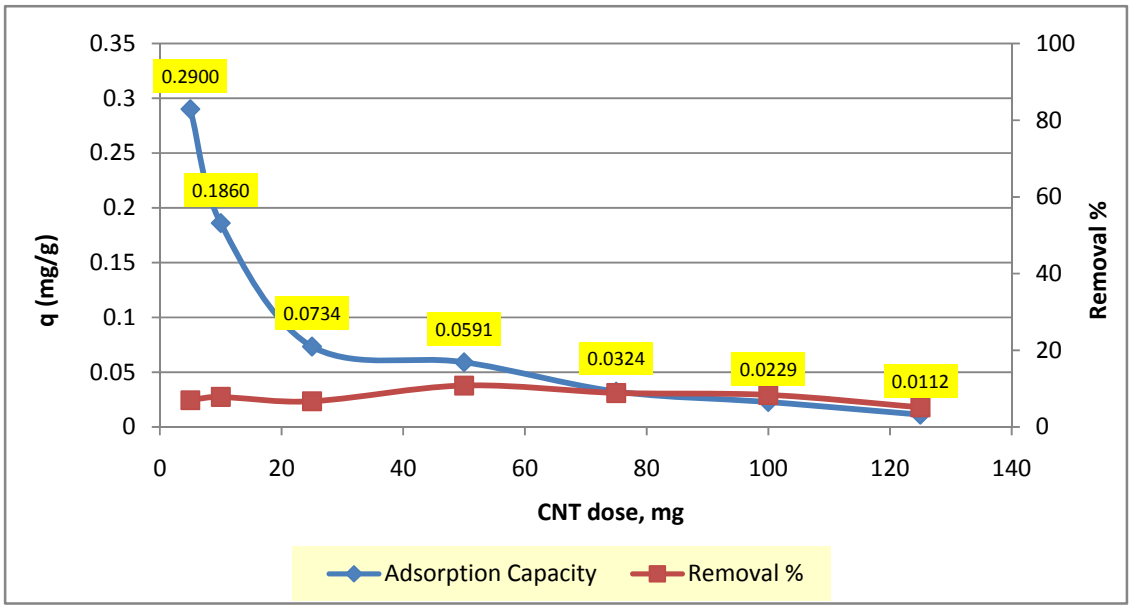

Figure 41: Bromate removal using CNT-Oxidized at different dosages. pH 7.5, BrO_3^- 0.5 mg/l, contact time 24h, agitation speed 150 rpm.

Figure 42 shows the adsorption capacity when CNT 1% Fe sample was used. The maximum adsorption capacity was 0.3460 mg/g when the CNT 1% Fe dosage was 5 mg. The adsorption capacity for CNT 1% Fe is higher than other types of CNTs, thus this type has potential applications. Finally, Figure 43 shows the adsorption capacities for all types of CNTs used for the removal of BrO_3^- at different dosages. The highest adsorption capacity and best performance was obtained for CNT 1% Fe and then for raw CNT with adsorption capacities of 0.346 mg/g and 0.320 mg/g respectively.

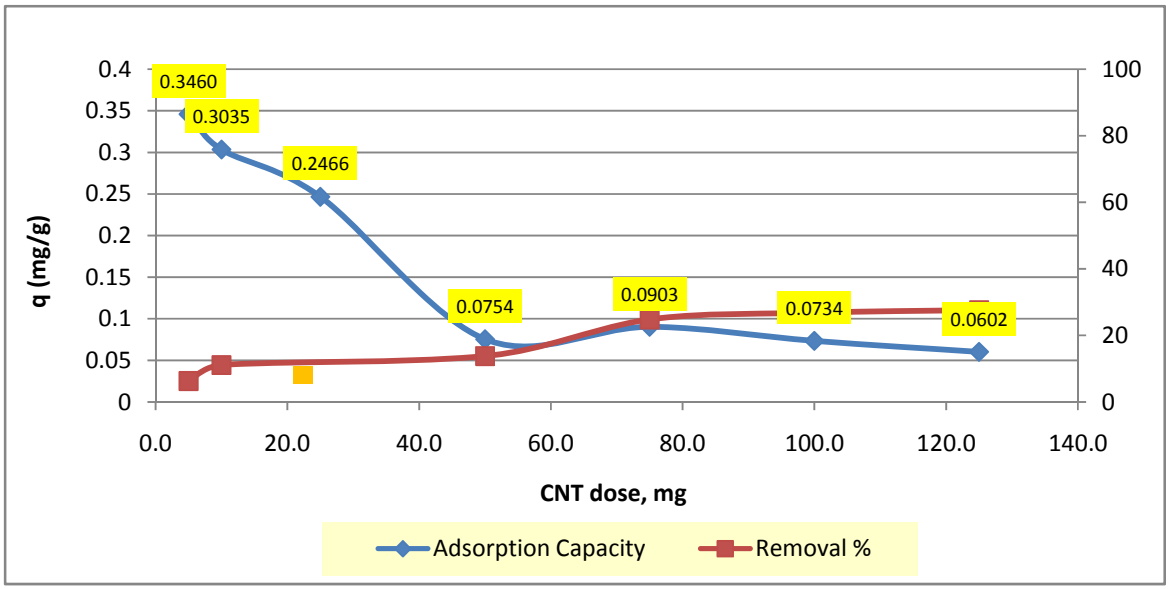

Figure 42: Bromate removal using CNT 1% Fe at different dosages. pH 7.5, BrO_3^- 0.5 mg/l, contact time 24h, agitation speed 150 rpm.

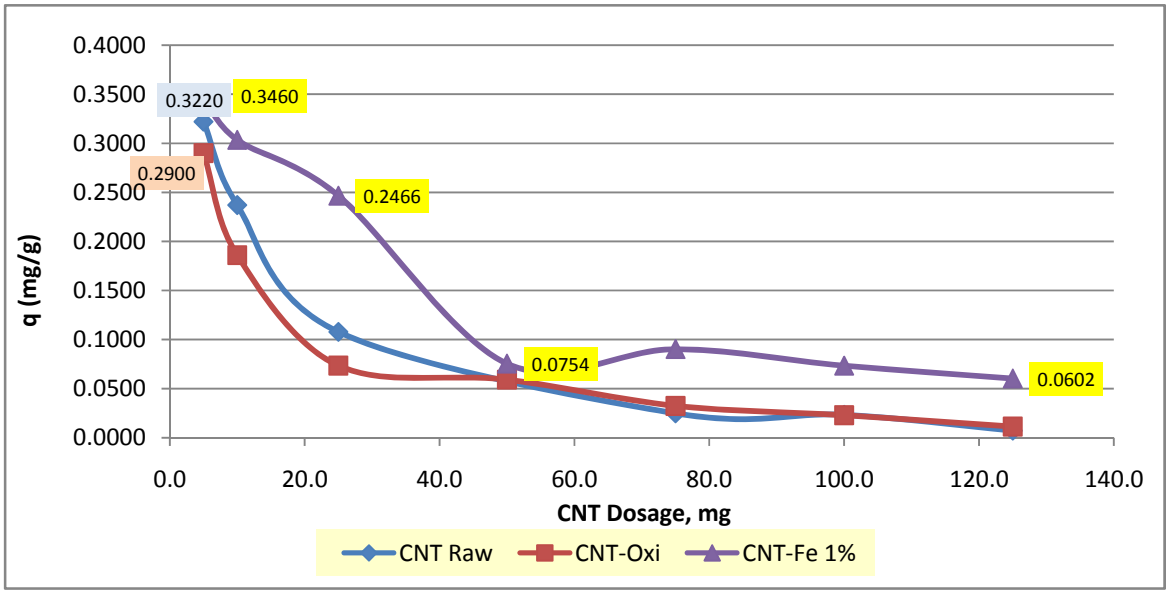

Figure 43: Bromate removal using different CNTs versus dosages. pH 7.5, BrO_3^- 0.5 mg/l, contact time 24h, agitation speed 150 rpm.

4.1.2.4 Effect of Initial Bromate Concentration

The effect of the initial concentration of BrO_3^- on the adsorption capacity by CNT was also investigated. The adsorption capacity has increased as the BrO_3^- concentration was increased in the solution when all other variables were kept constant, pH 6.0, agitation speed 150 rpm and CNT dosage of 50 mg. This can be explained easily since BrO_3^- introduced more to CNT surface and enhance the adsorption process. Figure 44 shows the relationship between BrO_3^- adsorption capacity of raw CNT and initial BrO_3^- concentration.

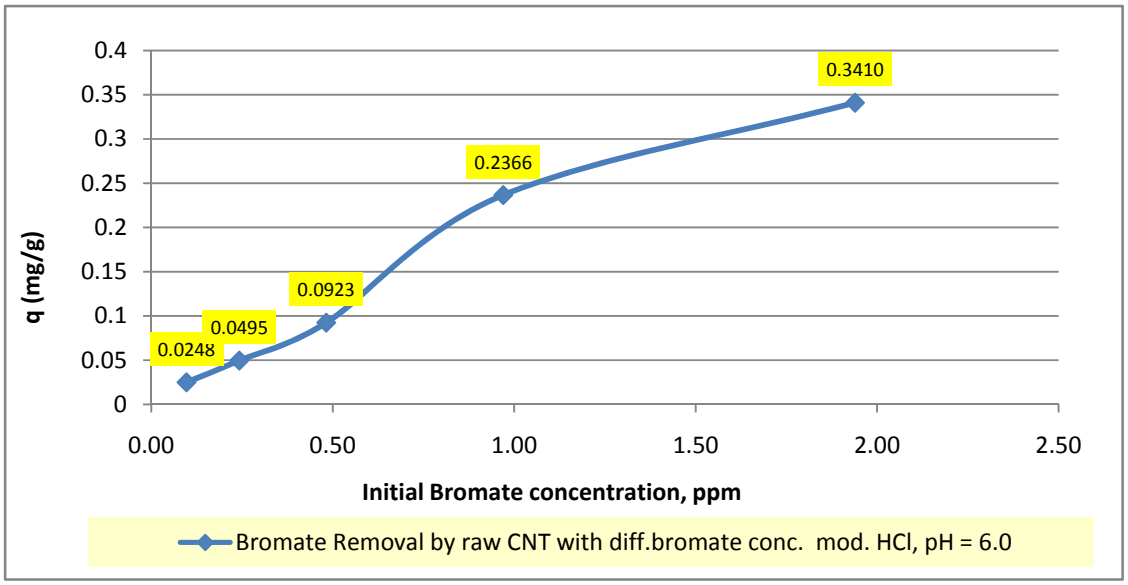

Figure 44: Adsorption capacity at different BrO_3^- concentrations. pH 6.0, Dosage 50 mg, contact time 24h, agitation speed 150 rpm.

4.2 ADSORBENTS CHARACTERIZATION

4.2.1 Activated Carbons

Three commercial samples of AC were ordered from the local market, however the oxidized form of AC was prepared. The physical & chemical properties of those types are listed below in Table 14. Full characterization was made for these samples with FE-SEM, FTIR, XRD and TGA-DSC to differentiate between them.

Property	Raw AC	AC 0.2% Ag
Manufacturer	Calgon	Tangshan Tianhe
Type	Filtrasorb 400	JX-126
Surface Area, S_{N2} (m^2/g)	1075	> 800
Volume of Pores, V_2 (cm^3/g)	0.37	~ 0.38
pH_{pzc}	7.91	7-8
Acid Groups (μeq/g)	234	NA
Basic Groups (μeq/g)	570	NA
Ash (%)	6.6	4.0 max

Table 14: AC types and their basic physical & chemical properties from the manufacturers.

4.2.1.1 Thermogravimetric Analysis (TGA)

Thermogravimetric analysis (TGA) is a type of testing performed on samples to determine the changes in their weights on changing the temperature. Such analysis relies on a high degree of precision in three measurements: weight, temperature, and temperature change. As many weight loss curves look similar, the weight loss curve may require transformation before results may be interpreted. A derivative weight

loss curve can identify the point where weight loss is most apparent. The TGA nalysis was done for all of the AC samples by using SDT Q600 instrument. The furnace type is Horizontal, Bifilar Wound and in the presence of air flow. The applied temperature is between 1000-1400^{o}C.

It is obvious from Figures 45, 46 and 47 that the raw AC decomposition starts at 501.8^{o}C while the decomposition of AC-Oxidized starts at about 413.5^{o}C which can be attributed to the surface modification of AC-Oxidized and the appearance of carboxyl, carbonyl and hydroxyl functional groups and the weakening of the AC structure. The decomposition of functional groups is easier than the raw AC.

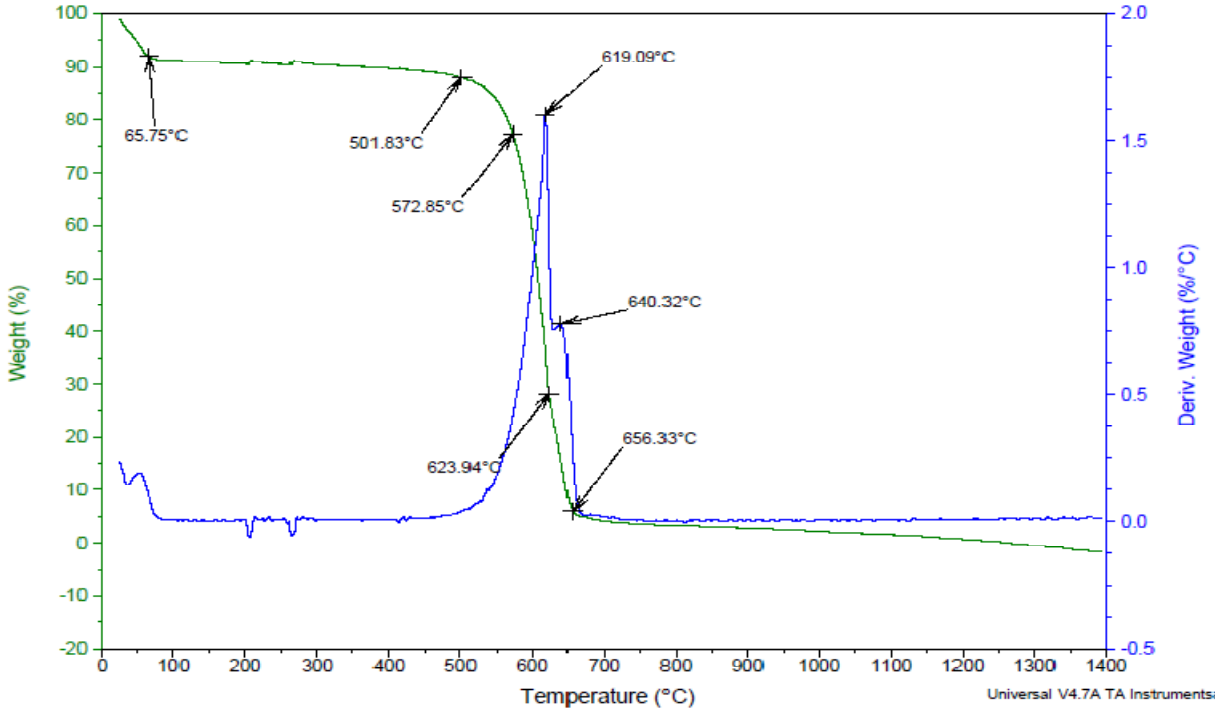

Figure 45: TGA for raw AC sample used in the research.

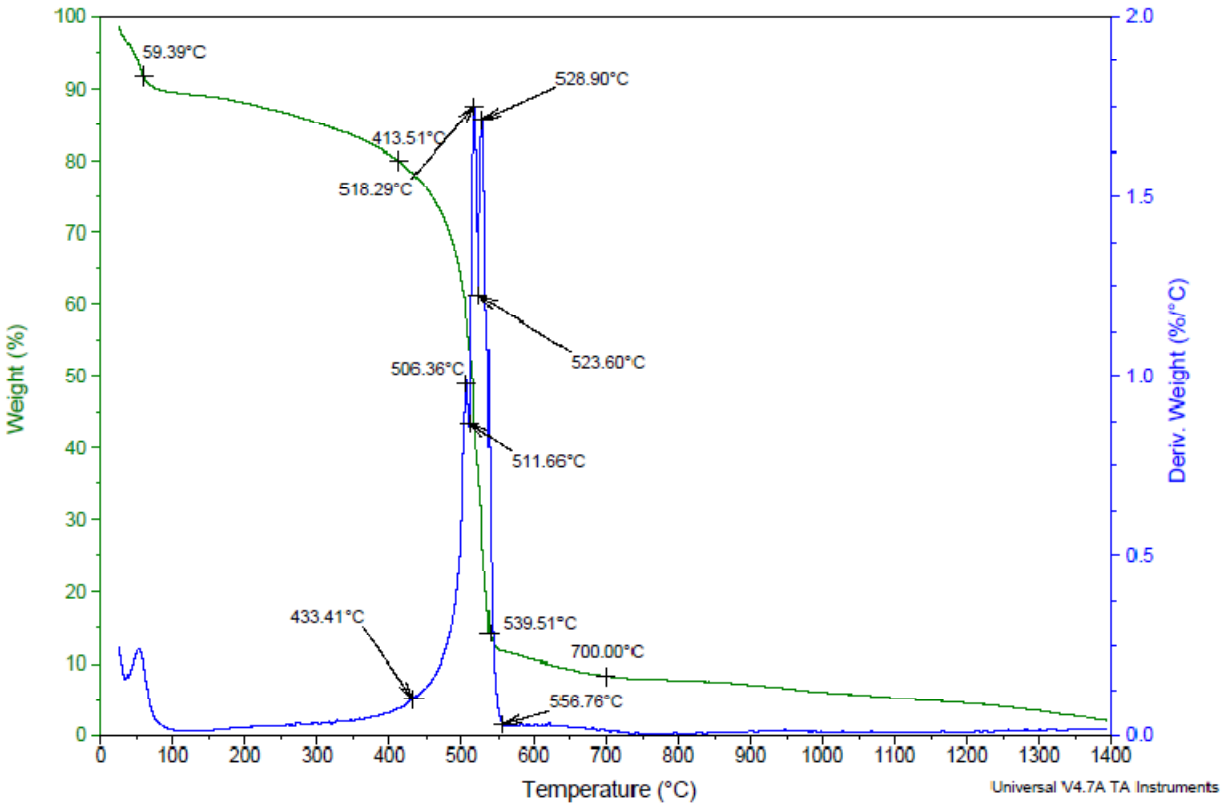

Figure 46: TGA for AC-Oxi sample used in the research.

The first weight losses before 100°C is probably caused by thermodesorption of physically adsorbed materials such as water, hydrocarbons or other volatile materials. The starting decomposition temperature of AC 0.2% Ag is in the middle between the two above AC types. This is due to the more solid structure of silver impregnated AC than the oxidized one because the impregnation process doesn't include oxidation or intensive conditions may destroy the structure of AC.

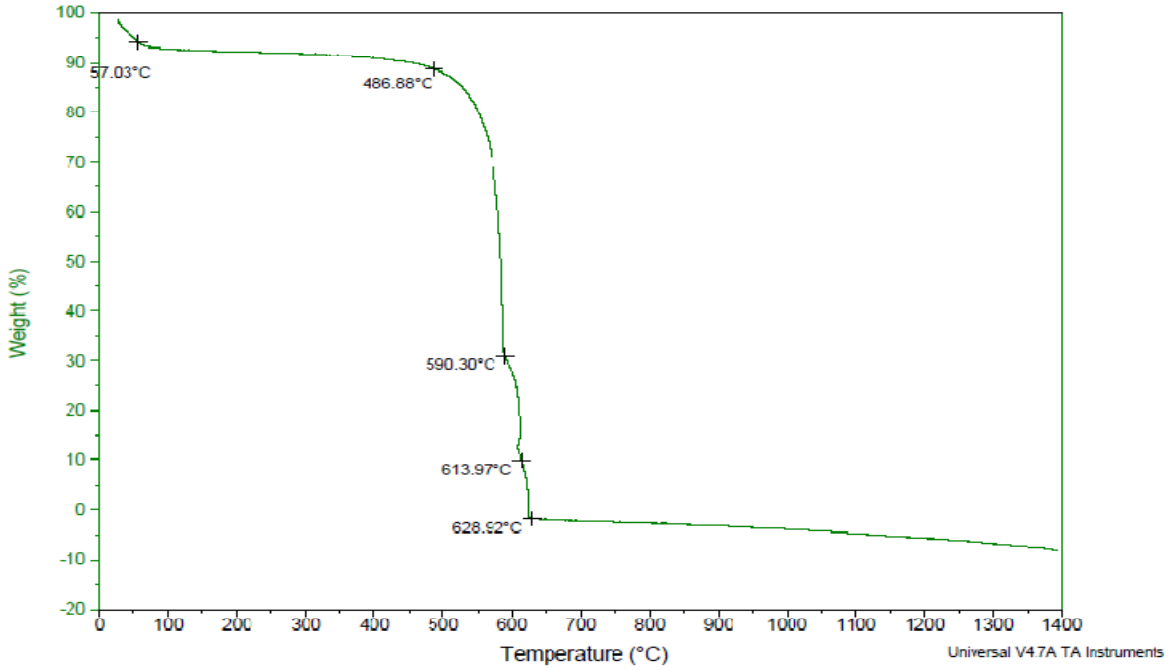

Figure 47: TGA for AC-Ag 0.2% sample used in the research.

4.2.1.2 Scanning Electron Microscope

Scanning electron microscope (SEM) is a type of electron microscope that images a sample by scanning it with a high-energy beam of electrons in a raster scan pattern. The electrons interact with the atoms that make up the sample producing signals that contain information about the sample's surface topography, composition, and other properties such as electrical conductivity. SEM images of three AC samples were done with different resolutions and without gold coating. Figure 48 shows the raw AC images used in this research and it is noticeable in high magnification images the pores in the surface and the amorphous nature of AC. The pores are relatively less than other types of activated carbon and that is related to many factors such as carbon source, activation process and activation period. Figure 49 shows the SEM

images of AC-Oxidized used in this work. There are no special features could be observed in the images rather than the raw AC.

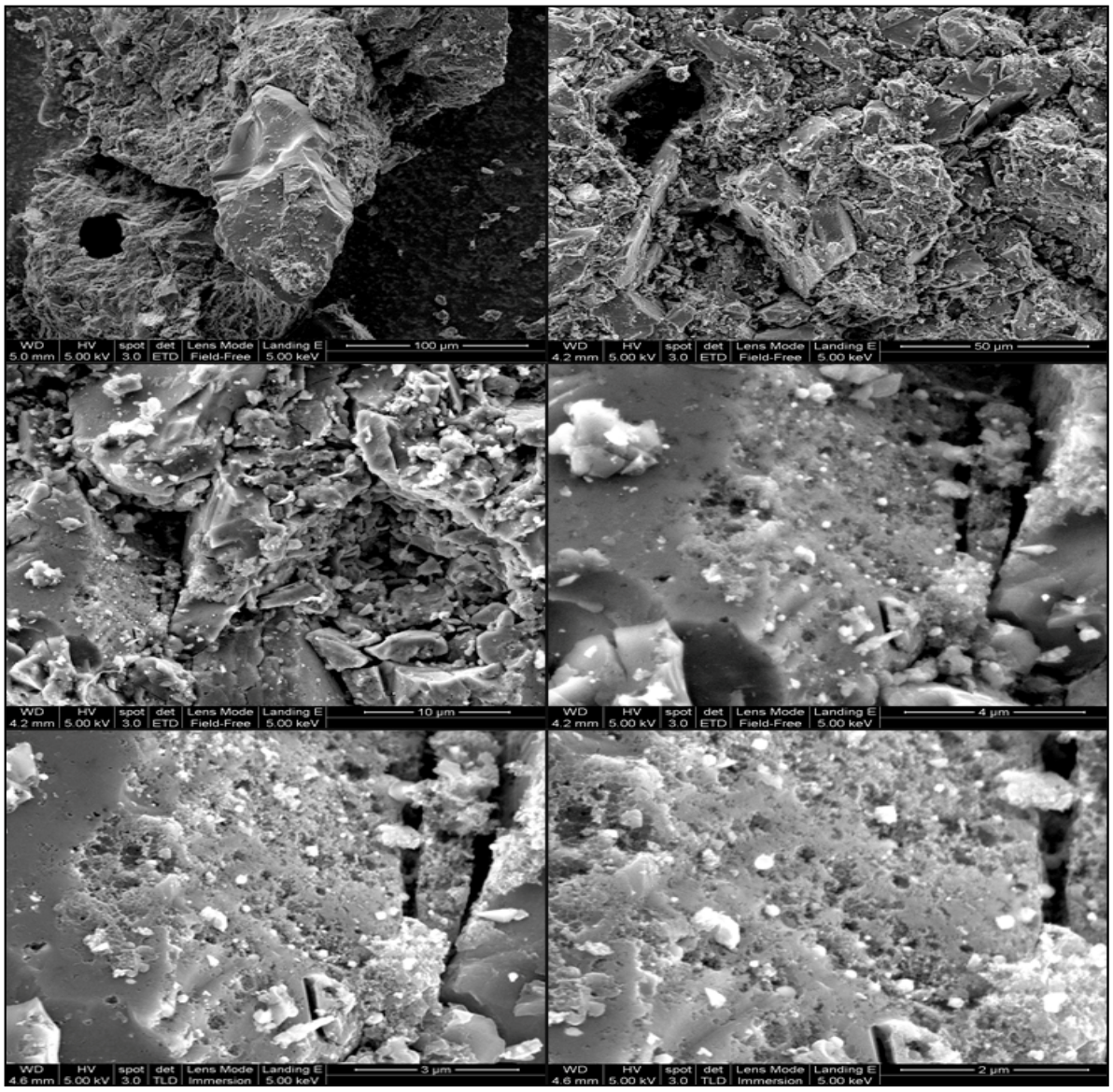

Figure 48: SEM images of raw AC used in this research

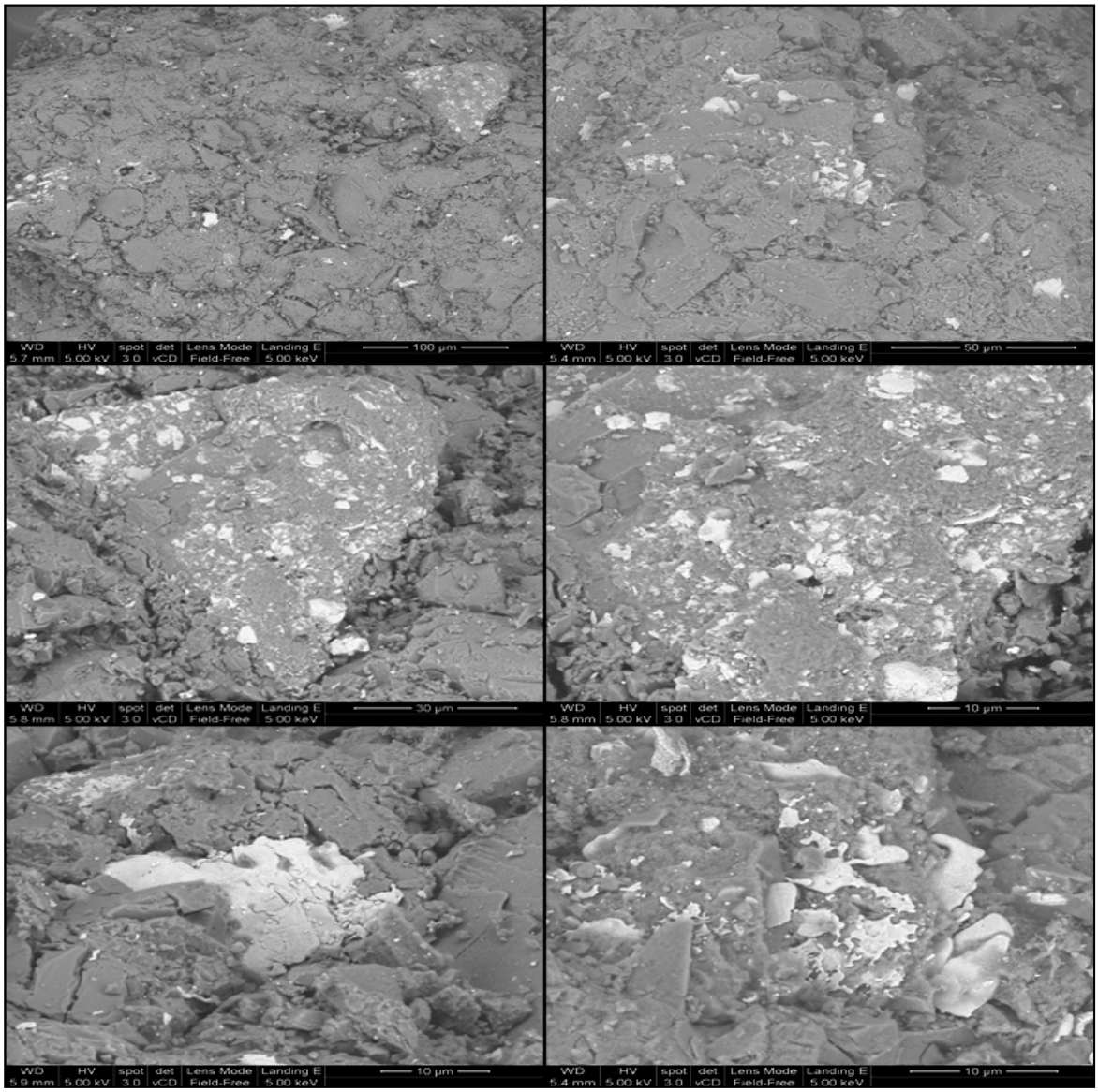

Figure 49: SEM images of AC-Oxidized used in this research

The effects of oxidation or functionalization of AC on the porosity and other physical properties were not considered here in this work since it is for bromate removal and the efficiency of raw AC was better than the oxidized one. Figure 50 shows the SEM images of AC-Ag 0.2% where white spots in the image refers to metal substances which are mainly silver clusters according to EDS findings. The yellow boxes in the images are examples of such silver clusters on the surface. This

type of layer does not exist in raw AC or oxidized one which can be attributed to silver impregnation to AC.

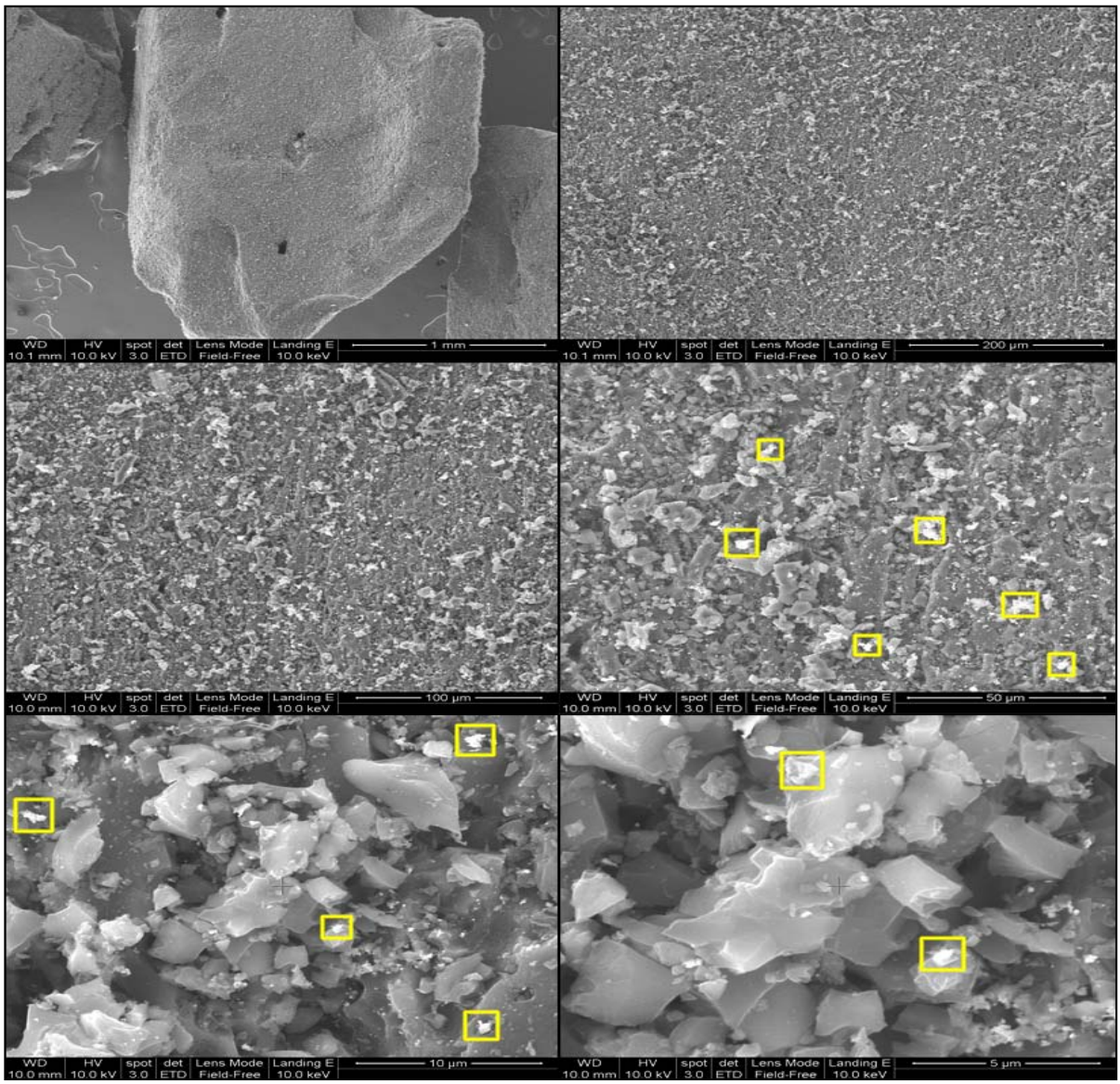

Figure 50: SEM images of AC-Ag 0.2% used in this research

4.2.1.3 Energy Dispersive Spectroscopy (EDS)

Energy-dispersive X-ray spectroscopy (EDS or EDX) is an analytical technique used for the elemental analysis or chemical characterization of a sample. It relies on the investigation of an interaction of some source of X-ray excitation and a sample. Its characterization capabilities are due in large part to the fundamental principle that each element has a unique atomic structure allowing X-rays that are characteristic of an element's atomic structure to be identified uniquely from one another. EDS analysis was done for all adsorbents used in this research. AC three samples have been analyzed and the results are presented in figures 51, 52, 53.

AC Raw

Element	Weight%	Atomic%
C	76.90	84.62
O	14.00	11.56
Al	2.45	1.20
Si	3.07	1.44
S	1.30	0.54
K	0.23	0.08
Ca	0.73	0.24
Fe	1.33	0.31
Totals	100.00	

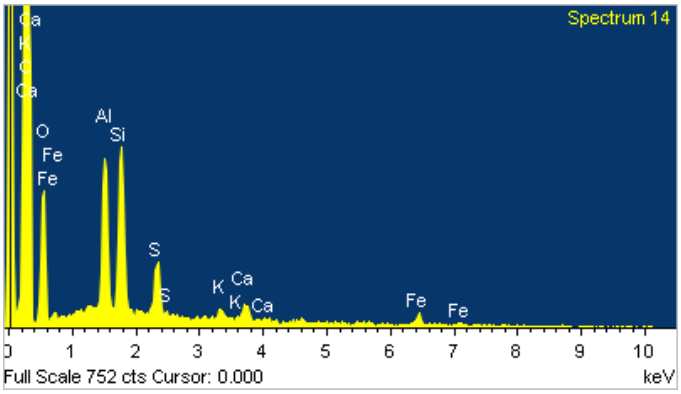

Figure 51: EDS Analysis for raw AC sample used in the research.

Figure 51 shows the EDS results for raw AC sample. The carbon content and oxygen content are 76.9%, 14.0% respectively. There are other impurities in the sample which are out of our interest. In comparing results between Figures 51 and 52, it is noticeable that the oxygen content in AC-Oxidized sample is higher than that for the raw AC which is attributed to the formation of carboxylic (-COOH), hydroxyl (-

OH) and carbonyl (-CHO) groups on the surface of activated carbon during oxidation process by sulfuric acid.

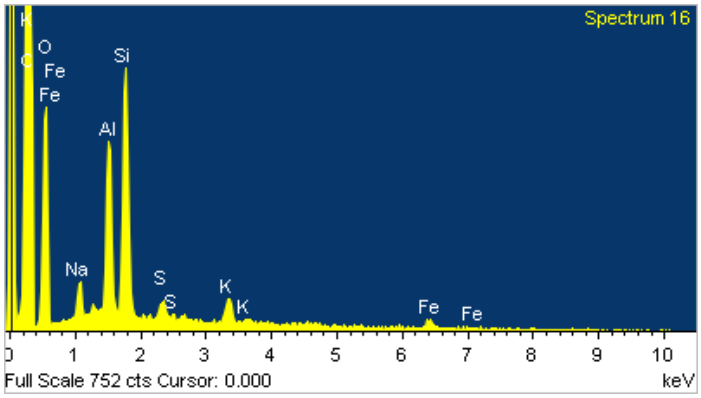

Figure 52: EDS Analysis for AC-Oxidized sample used in the research.

Figure 53 shows the EDS analysis of the commercial sample AC-Ag 0.2% used in this work. The resulting silver content was 5.68 % which is higher than the actual impregnated concentration 0.2%. This could be attributed to the localized superficial analysis by EDS instrument, and also silver clusters will accumulate on the surface of activated carbon granules. The main objective for EDS analysis in this sample was to ensure the presence of silver on the activated carbon surface as presented in SEM and EDS findings.

AC Ag 0.2%

Element	Weight%	Atomic%
C	92.75	98.70
S	1.56	0.62
Ag	5.68	0.67
Totals	100.00	

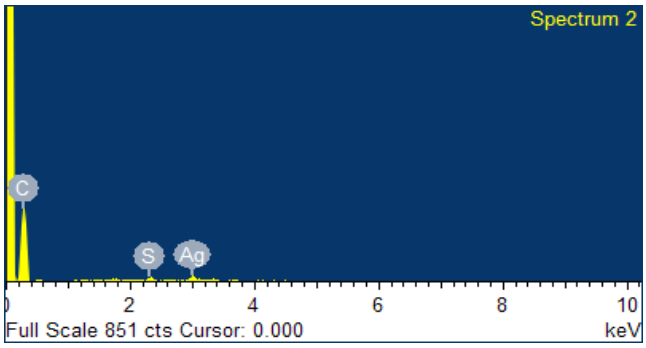

Figure 53: EDS Analysis for AC-Ag 0.2% sample used in the research.

4.2.1.4 Fourier Transform infrared spectrometer (FTIR)

Infrared spectroscopy (IR spectroscopy) is the spectroscopy that deals with the infrared region of the electromagnetic spectrum that is light with a longer wavelength and lower frequency than visible light. It covers a range of techniques, mostly based on absorption spectroscopy. As with all spectroscopic techniques, it can be used to identify the chemicals. A common laboratory instrument that uses this technique is a Fourier transform infrared (FTIR) spectrometer.

FTIR spectra were produced for two activated carbon samples: raw AC and AC-Oxidized to confirm - along with the confirmation done by EDS – the presence of carbonyl, carboxyl and hydroxyl due to oxidation process. Figure 54 shows FTIR spectra for both mentioned samples used in this research. It is noticeable that high peak appears on 1355 cm^{-1} at AC-Oxidized sample which is attributed to the carboxylic groups and exactly (C-O) stretching mode. This peak of carboxylic group is accompanied with peaks at (1700-1725 cm^{-1}) & (2500-3300 cm^{-1}) specific for (C=O) stretching and (O-H) stretching modes respectively.

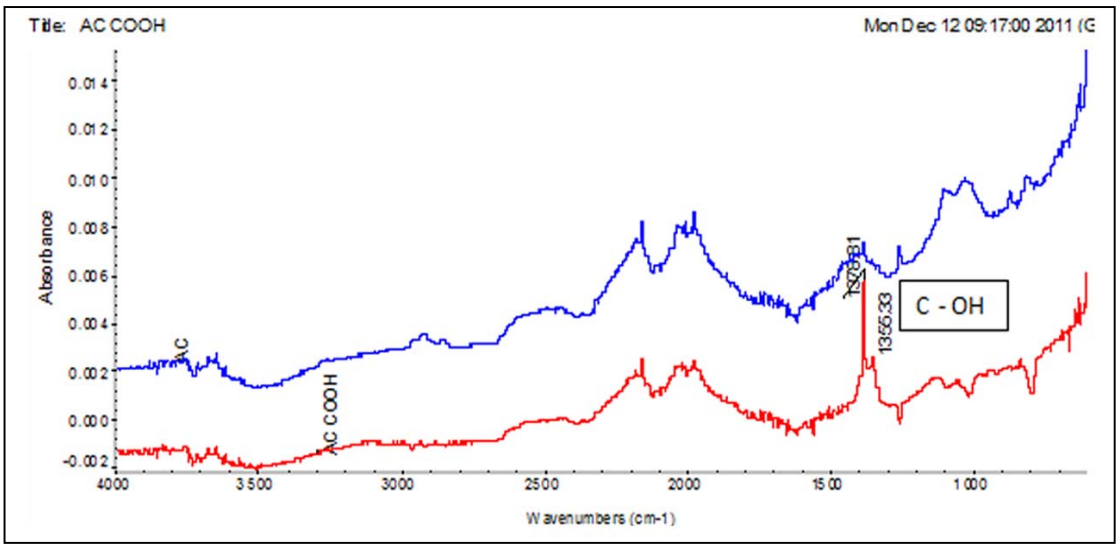

Figure 54: FTIR Spectra for raw AC and AC-Oxidized

4.2.1.5 X-Ray Diffraction

X-ray diffraction (XRD) is a technique used to characterize the crystallographic structure, crystallite size (grain size), and preferred orientation in polycrystalline or powdered solid samples. Powder diffraction is commonly used to identify unknown substances, by comparing diffraction data against a database maintained by the International Centre for Diffraction Data. It may also be used to characterize heterogeneous solid mixtures to determine relative abundance of crystalline compounds and, when coupled with lattice refinement techniques, such as Rietveld refinement, can provide structural information on unknown materials. XRD is also a common method for determining strains in crystalline materials. An effect of the finite crystallite sizes is seen as a broadening of the peaks in an X-ray diffraction as is explained by the Scherrer Equation.

XRD analysis was done for activated carbon samples (raw AC and AC-Oxi.) and the results are presented in Figures 55 and 56. Figure 55 shows the spectrum of raw AC and peaks numbers 1, 7, 8 are characterized to graphite phases 2H(0,0,2), 2H(1,0,0) and 2H(1,0,2) respectively. Also, Figure 56 shows the spectrum of AC-oxidized sample and peaks numbers 1, 8, 11, 12, 14 are characterized to graphite phases 2H(0,0,2), 2H(1,0,0), 2H(1,0,2), 2H(1,0,3) and 2H(1,1,0) respectively. Therefore, the main structure for activated carbon samples is graphite with little difference in phases.

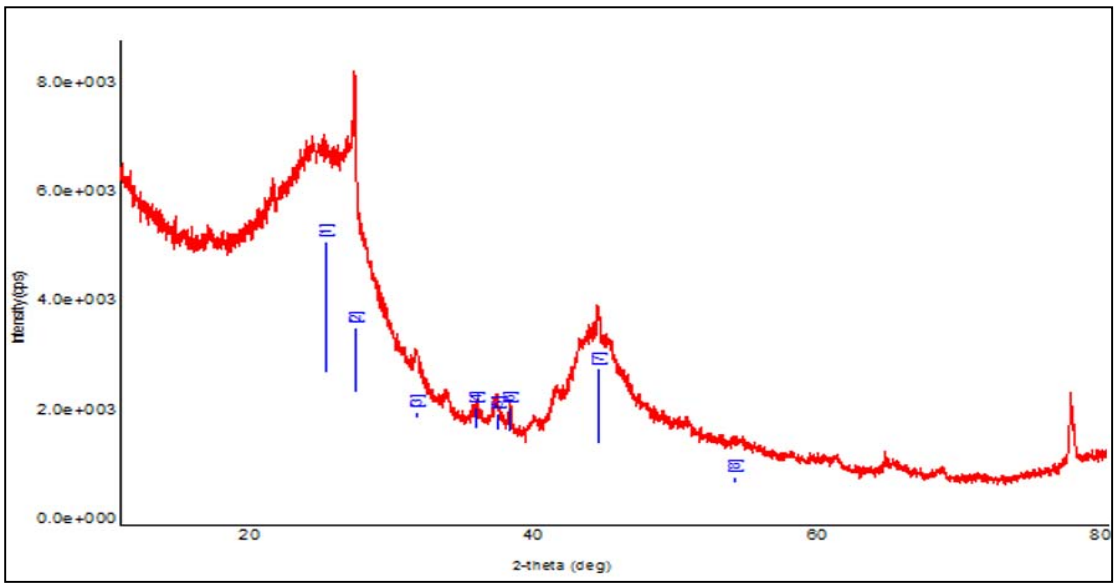

Figure 55: XRD spectrum for raw AC sample.

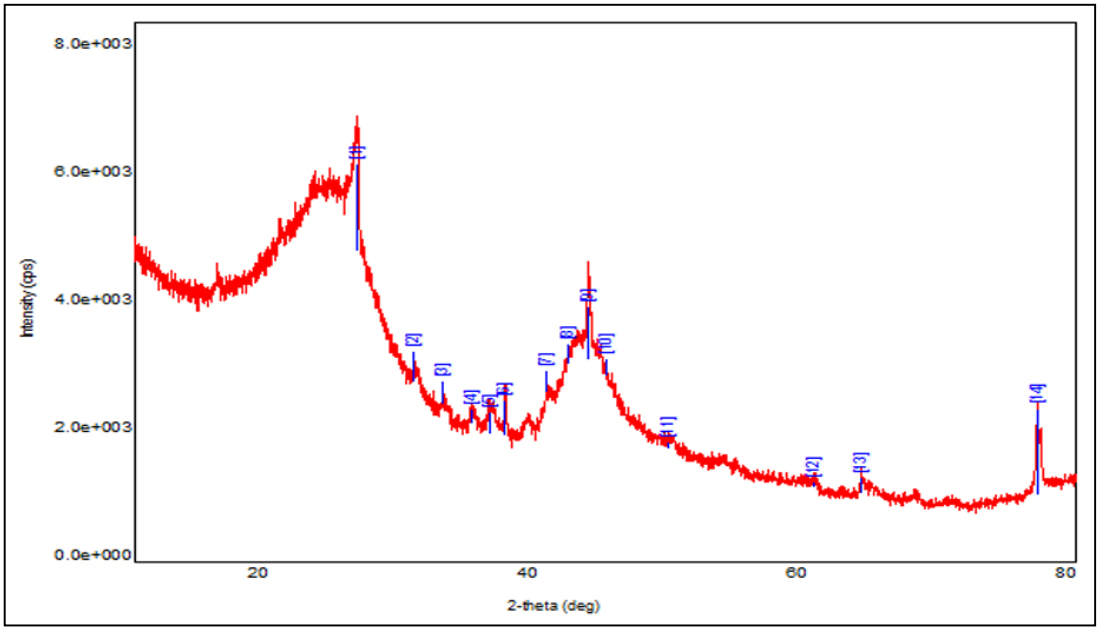

Figure 56: XRD spectrum for AC-Oxidized sample.

4.2.2 Carbon Nanotubes (CNT)

Three samples of CNTs were prepared and used in this work. Table 15 shows the basic chemical & physical characteristics of the CNT samples. Full characterization was made for the three samples and the results are presented. Figure 57 shows FE-SEM images of raw CNT used in this experiment for measuring its outside diameter.

Property	CNT Raw	CNT Oxidized	CNT 1% Fe
Manufacturer	KFUPM	KFUPM	KFUPM
Purity (%)	> 95	> 95	> 95
Surface Area, (m^2/g)	233	NA	NA

pH_{pzc}	6.6	3.1	NA
Outer Diameter (nm)	20-30	20-30	20-30
Inside Diameter (nm)	3-5	3-5	3-5
Length (μm)	10-30	10-30	10-30

Table 15: CNT types and their basic physical & chemical

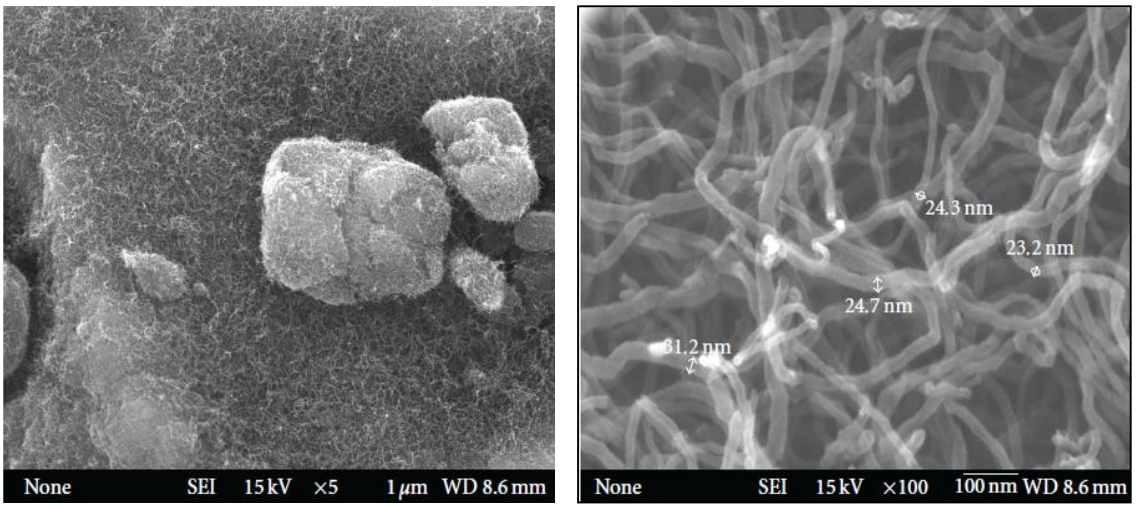

Figure 57: FE-SEM of raw CNT with tubes diameters

4.2.2.1 Thermogravimetric Analysis (TGA)

TGA analysis for three samples of CNTs was done by using SDT Q600 instrument. The furnace type is Horizontal, Bifilar Wound and in the presence of air flow. The applied temperature was between 1000-1400^{o}C. Looking to Figures 58, 59 and 60, it is noticeable that the decomposition of the raw CNT starts at 445.3^{o}C and the CNT-Oxidized starts decomposition at around 306.2^{o}C which can be attributed to the surface modification of CNT-Oxidized and the formation of carboxyl, carbonyl and hydroxyl functional groups which in turn act to weaken the CNTs structure. The

decomposition of oxidized CNT is easier than the raw CNT. The first weight losses before 100^{o}C is probably caused by thermodesorption of physically adsorbed materials such as water, hydrocarbons or other volatile materials. The starting decomposition temperature of CNT 1% Fe is in the middle between the two above CNT types which is 367.3^{o}C. Figure 60 shows TGA spectra of CNT 1% Fe.

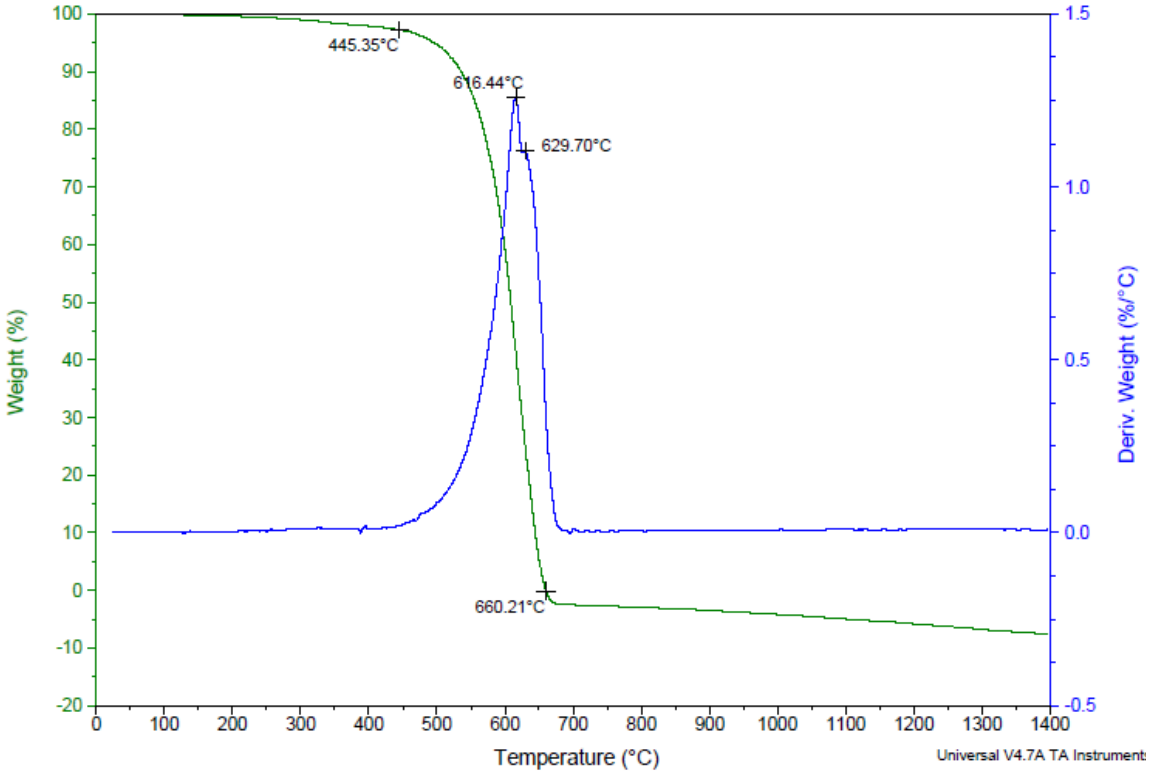

Figure 58: TGA for raw CNT sample used in the research.

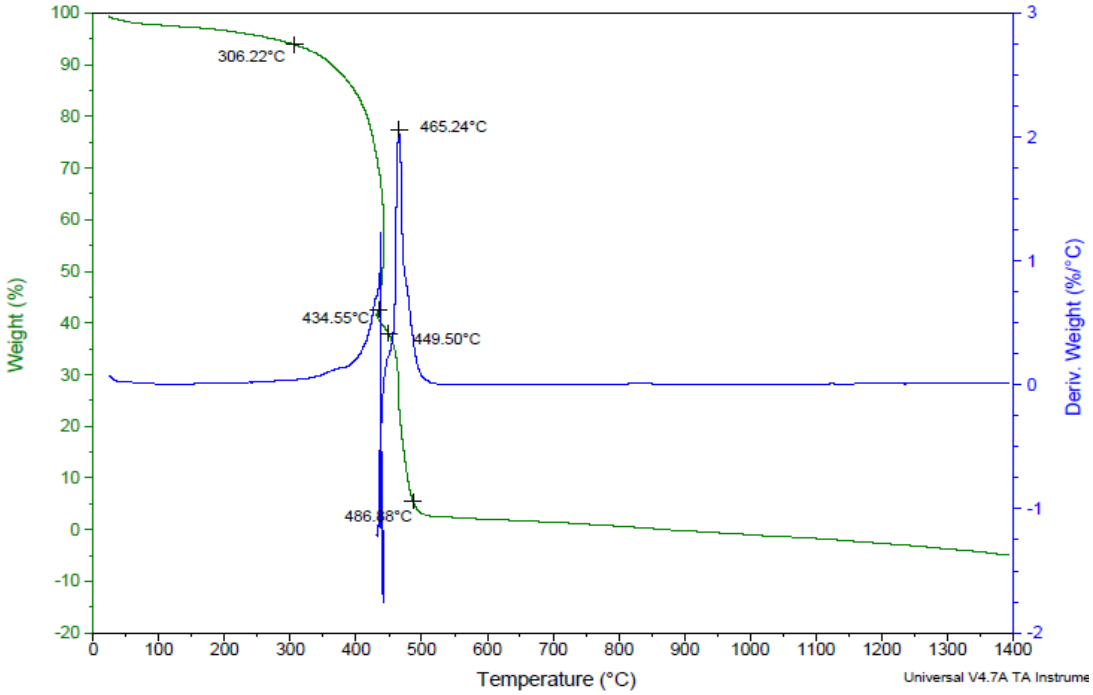

Figure 59: TGA for CNT-Oxidized sample used in this research.

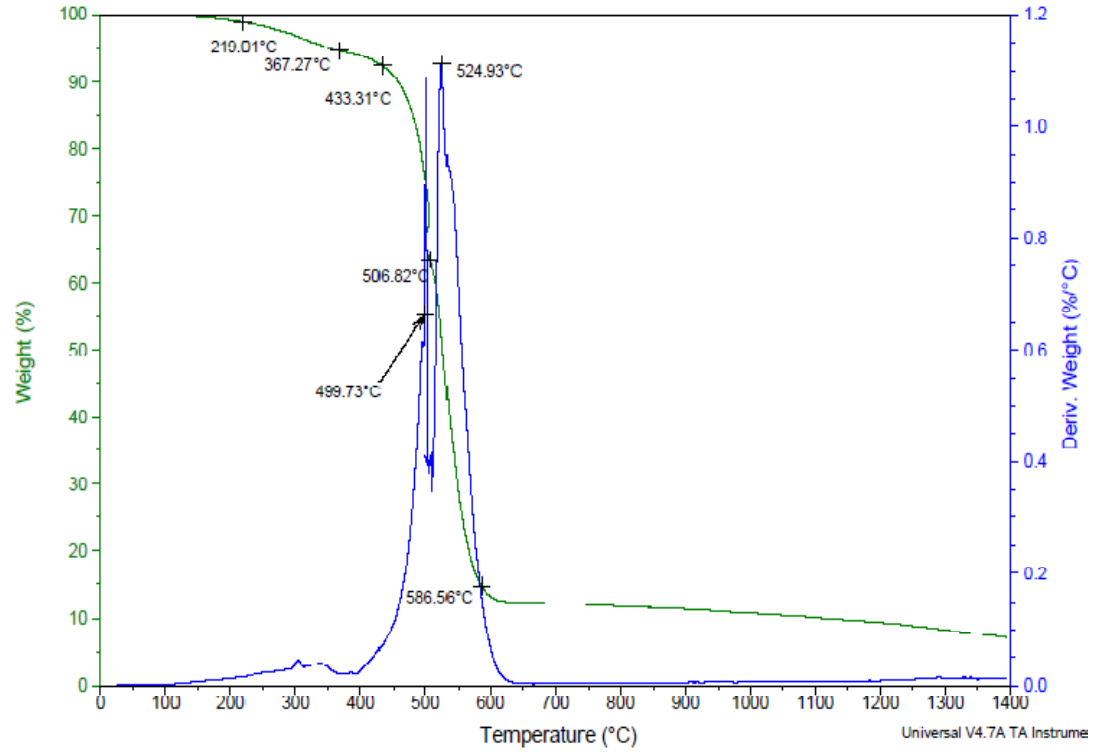

Figure 60: TGA for CNT 1% Fe sample used in the research.

4.2.2.2 Scanning Electron Microscope (SEM)

SEM images have been taken for the three CNT samples which were used in this work at different resolutions and without gold coating. Figure 61 shows raw CNT images used in this work and it is noticeable in high magnification the bundles of tubes. The alignment of CNTs is related to many factors which can be described in other sources. Figure 62 shows the SEM images of CNT-Oxidized used in this work. There are no special features that could be observed in the images rather than the raw CNT. Figure 63 shows SEM images of CNT 1% Fe. Iron metal clusters on the surface of the CNTs are shaded by the yellow color.

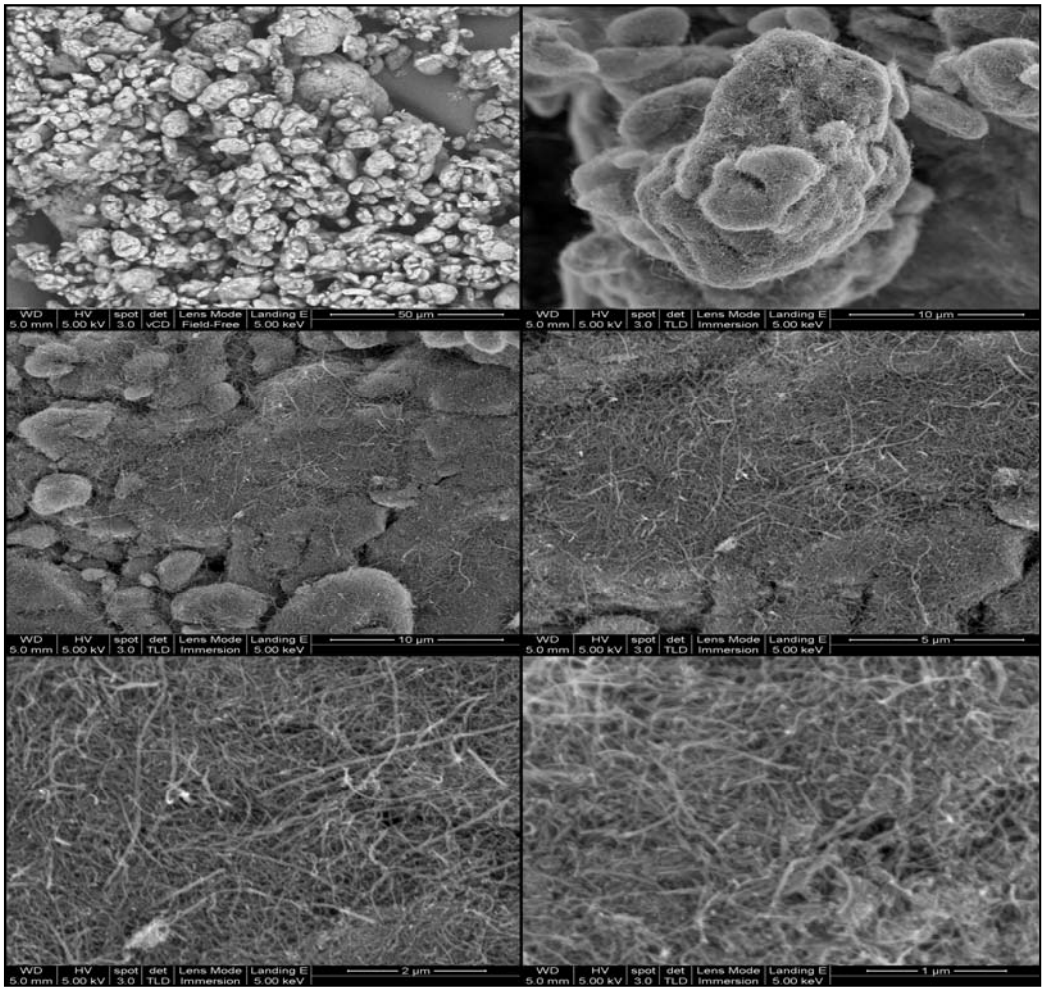

Figure 61: SEM images of raw CNT

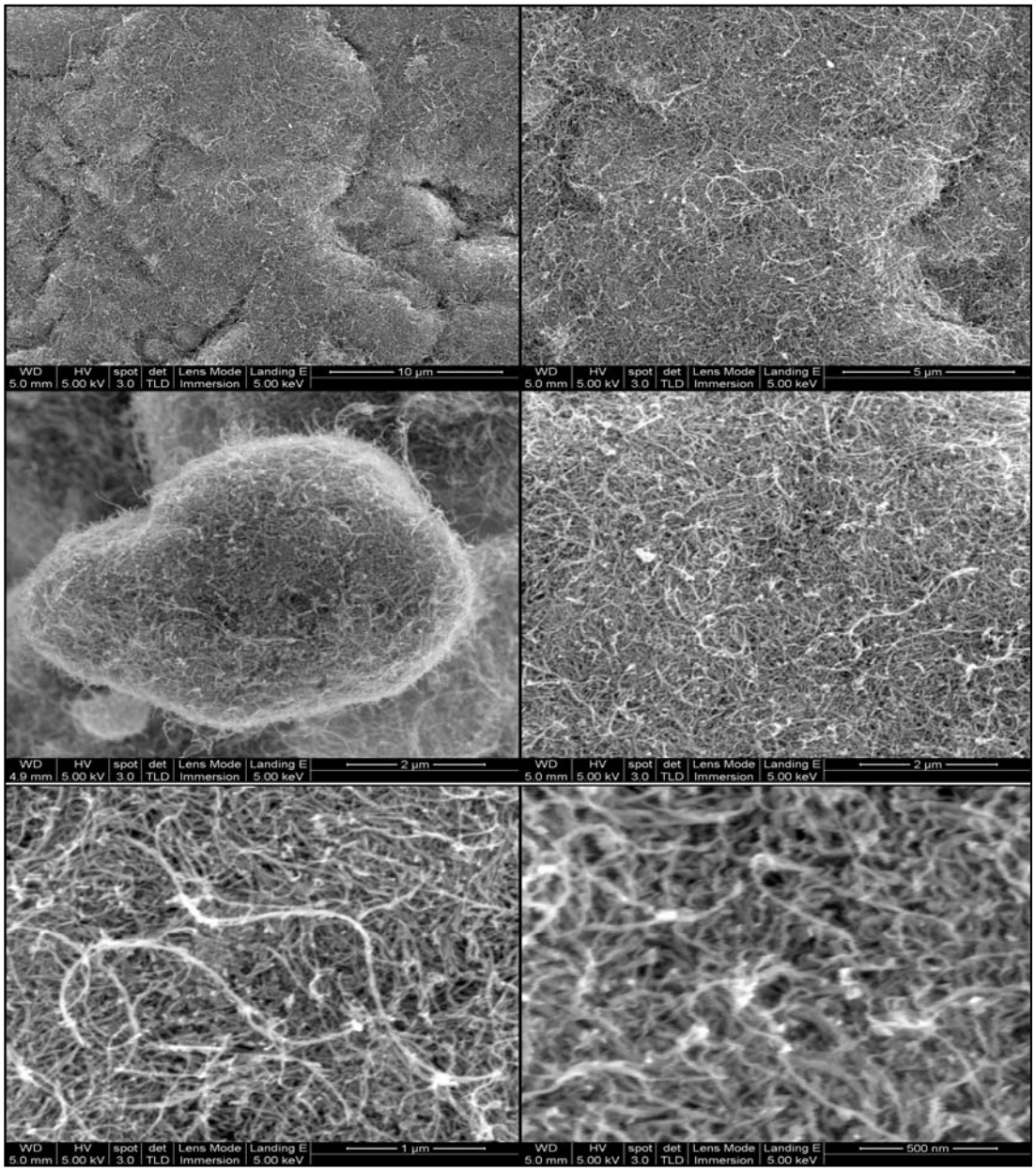

Figure 62: SEM images of CNT-Oxidized

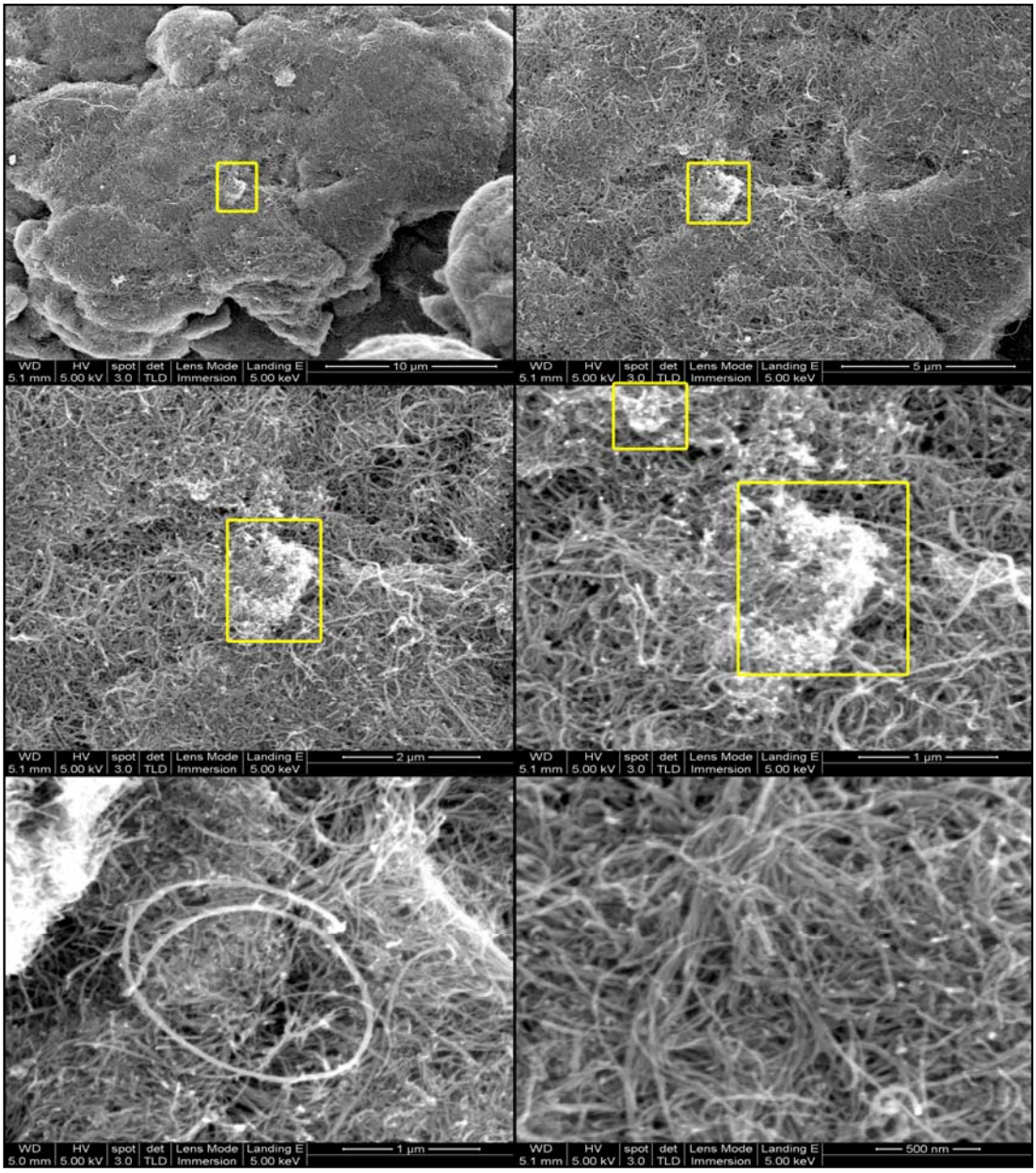

Figure 63: SEM images of CNT 1% Fe

4.2.2.3 Energy Dispersive Spectroscopy (EDS)

EDS analysis was done for all of the adsorbents used in this work. Three samples of CNTs have been analyzed and the results are presented in figures 64, 65 and 66.

CNT Raw

Element	Weight%	Atomic%
C	94.42	96.99
O	3.28	2.53
Ni	2.31	0.48
Totals	100.00	

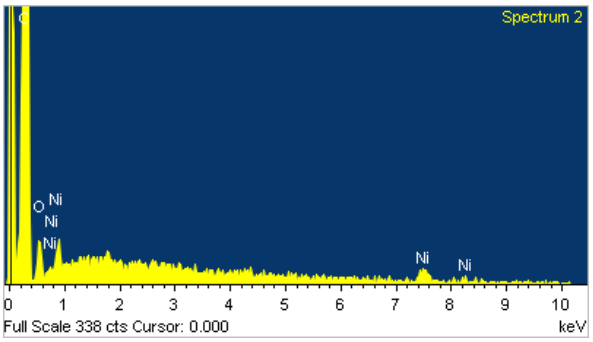

Figure 64: EDS Analysis for CNT Raw sample used in the research.

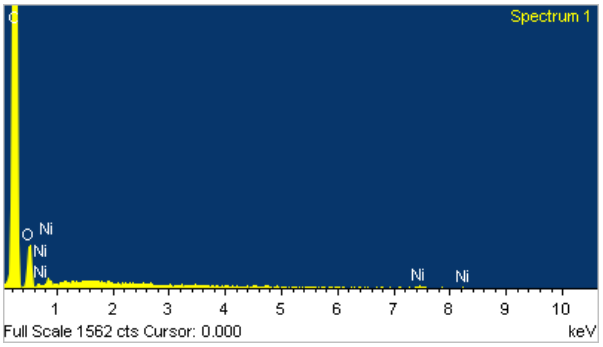

Figure 65: EDS Analysis for CNT Oxidized sample used in the research.

Figure 64 shows the EDS results for the raw CNT sample. The carbon content and oxygen content are 94.4%, 3.3% respectively. The presence of nickel in the sample is as catalyst during the CNTs synthesis. Comparing the results between Figures 64 and 65, it is evident that the oxygen content in CNT-Oxidized sample is higher than that of the raw CNT which is attributed to the formation of carboxylic (-

COOH), hydroxyl (-OH) and carbonyl (-CHO) groups on the surface of activation carbon during the oxidation process by sulfuric acid.

Figure 66 shows the EDS analysis of the sample CNT Fe 1% used in this work. The results of the iron content was found to be 2.2 % which is higher than the actual impregnated concentration 1%. This could be attributed to the localized superficial analysis by EDS instrument. Furthermore, iron clusters will accumulate on the surface of carbon nanotubes. The main objective for EDS analysis was to ensure the presence of iron metal on the CNT surface as presented in SEM and EDS findings.

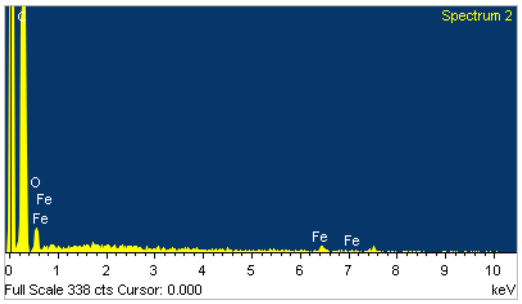

Figure 66: EDS Analysis for CNT Fe 1% sample used in the research.

4.2.2.4 Fourier Transform infrared spectrometer (FTIR)

FTIR spectra were produced for two carbon nanotubes samples: raw CNT and CNT-oxidized to confirm - along with the confirmation made by EDS – the presence of carbonyl, carboxyl and hydroxyl groups (some) after the modification/oxidation process. Figure 67 shows FTIR spectra for the aforementioned samples used in this work. It is noticeable that high peak appears on 1460 cm^{-1} at CNT-Oxidized sample which is attributed to the carboxylic groups and exactly (C-O) stretching mode. This

peak for the carboxylic is accompanied with peaks at 1634 cm^{-1} & 3300-3500 cm^{-1} specified for (C=O) stretching and (O-H) stretching modes respectively.

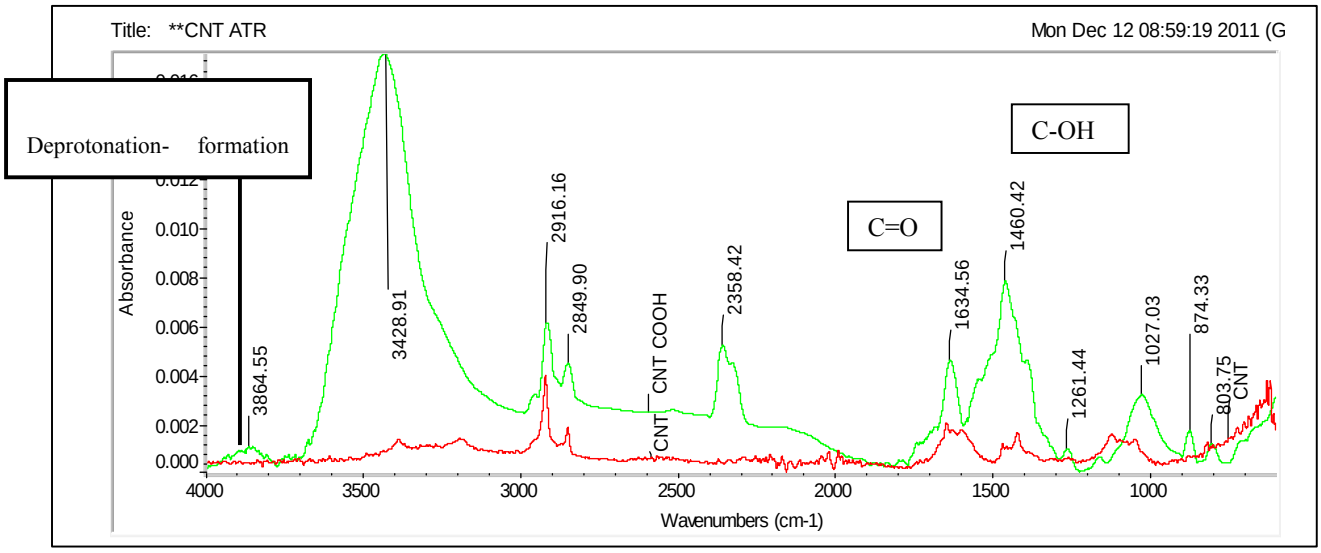

Figure 67: FTIR Spectra for CNT raw and CNT-Oxidized

4.3 COMPARING THE RESULTS OF BROMATE REMOVAL BY AC AND CNT

The results of bromate removal by the three samples of AC and the other three samples of CNTs, are statistically compared in order to find out the highest adsorption capacity for each type. The oxidized samples of AC and CNT were both excluded because they have shown the lowest adsorption capacities. Figure 68 shows a comparison between four types of adsorbents at different pH values when all other factors were kept constant.

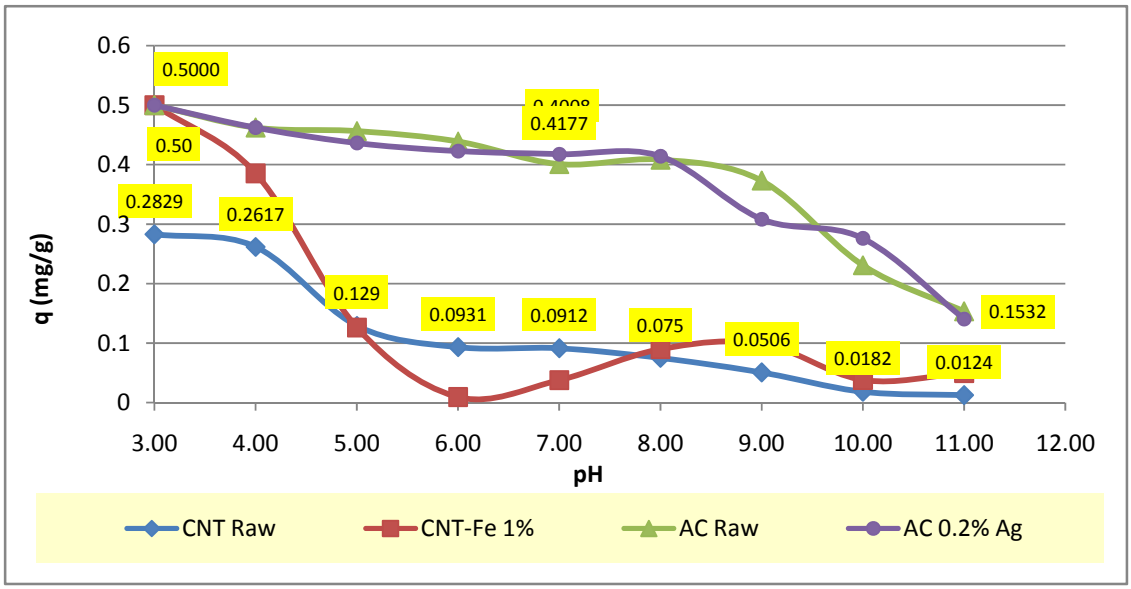

Figure 68: The effect of pH and adsorbent type on Bromate Removal, Contact time 24h, Speed, 150 rpm, Dose 50 mg, BrO_3^- concentration 0.5 ppm.

From Figure 68 we found that the best adsorbents were raw AC and AC 0.2% Ag with adsorption capacity at pH = 3.0 was > 0.5 mg BrO_3^-/g AC. The maximum adsorption capacity for CNT-Fe 1% is > 0.5 mg/g when pH = 3.0. At the normal water pH value ~ 7.0, the highest adsorption capacities were for activated carbon samples since they have strong reducing properties in comparison with carbon nanotubes. The highest value of the adsorption capacity was 0.4177 mg/g for the raw AC when all other factors were kept constant. The highest adsorption capacity for raw CNT at pH = 7.0 was 0.0912 mg/g.

Figure 96 shows the adsorption capacity of AC & CNT types at different dosages when all other factors were kept constant and the solution pH was 7.5. It is clear that the highest adsorption capacity of BrO_3^- was for AC-0.2% Ag when only 5

mg of AC used for adsorption. However, the adsorption capacities were as follow: 1.19 mg/g for AC-0.2% Ag, 0.486 mg/g for Raw AC, 0.3460 mg/g for CNT-Fe 1% and finally 0.3220 mg/g for Raw CNT.

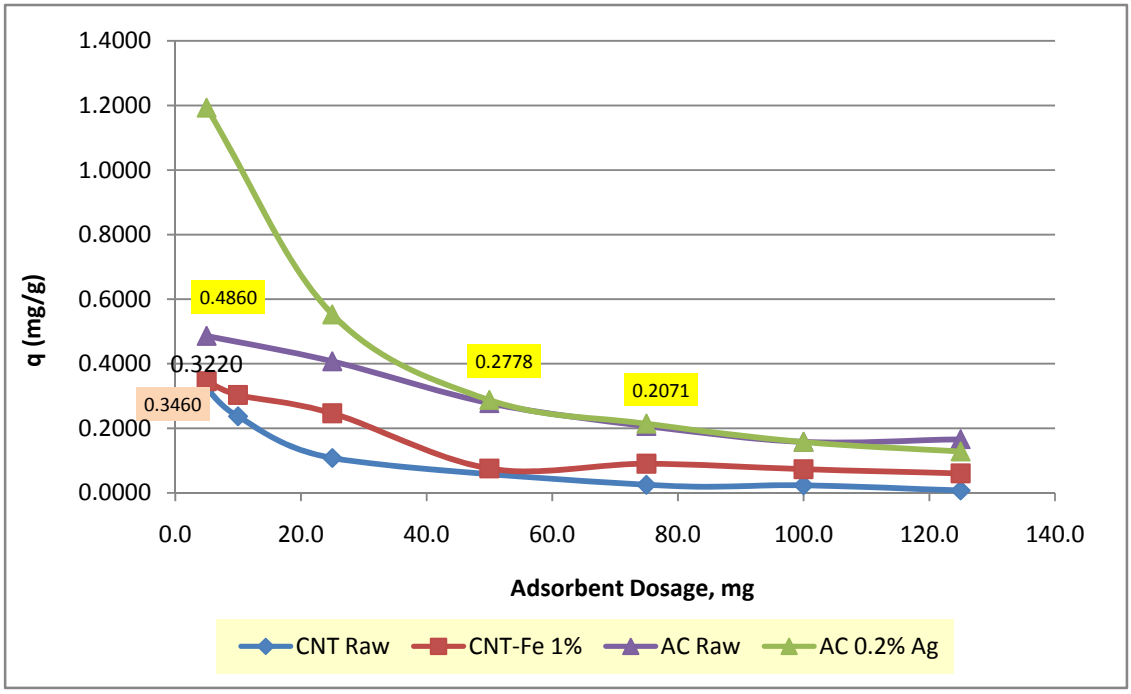

Figure 69: The effect of adsorbent type and dosage on Bromate Removal, Contact time 24h, Speed, 150 rpm, pH 7.5 , BrO_3^- concentration 0.5 ppm.

CHAPTER 5

CONCLUSION

5.1 CONCLUSIONS

After studying the applicabilities of six types of adsorbing materials for the removal of bromate, the below points are the concluded points out of this research:

- Raw AC and raw CNT adsorption capacities were better than the oxidized types of each one.
- As the pH value of the solution decreases, the adsorption capacities of all the adsorbents increase. This is also dependent on pH_{pzc} of the adsorbent.
- The adsorption capacity of bromate increases as the pH_{pzc} of the adsorbent increases.
- The overall adsorption capacities of Activated Carbons (AC) are better than that for the raw, oxidized and iron impregnated Carbon nanotubes (CNTs).
- Co-anions will decrease the adsorption/reduction capacity for both AC & CNT.
- AC is removing bromate through mainly via a reduction of BrO_3^- to Br^-.
- The best removal of BrO_3^- by using Activated carbon was with AC-0.2% Ag.
- CNT removes bromate mainly via an adsorption mechanism.
- The best removal of BrO_3^- by using CNT was with CNT-1% Fe

Table 16 summarizes the above mentioned points.

Variable/Adsorbent	AC		MWCNT	
The best Samples	AC-0.2% Ag	Raw AC	CNT-Fe 1%	Raw CNT
Maximum q (mg/g) @ pH 7.5	1.1930	0.4860	0.346	0.322
q (mg/g) @ pH 3.0 (HCl)	> 0.5	> 0.5	> 0.5	0.283
q (mg/g) @ pH 3.0 (HNO_3)	-	0.334	-	0.102
q (mg/g) @ pH 7.0 (HCl)	0.4177	0.4000	0.0377	0.091
q (mg/g) @ pH 7.0 (HNO_3)	-	0.1878	-	0.046
Previous studies (review)	New Study	> 8.0 mg/g	New Study	New Study
Main Removal Mechanism	Reduction	Reduction	Adsorption	Adsorption
pH effect (Decreasing)	Increasing	Increasing	Increasing	Increasing
Increasing adsorbent on Removal %	Increasing	Increasing	No effect due to bundling	No effect due to bundling
Co-anions effect (increasing)	Decreasing	Decreasing	Decreasing	Decreasing

Table 16: The Summarized results from all above experiments

APPENDIX A: Adsorbents Preparation

Raw CNT

CNTs prepared by the floating catalyst chemical vapor deposition (FC-CVD) reactor. The production of CNTs in the present work has been conducted in a horizontal tubular reactor. The horizontal reactor is a quartz tube of 50 mm in diameter and 900 mm in length and heat by silicon carbide heating element. In this study benzene (C6H6 99.5% purity) was used as a hydrocarbon source and ferrocene (Fe C_{10} H_{10} 98% purity) and Hydrogen as carrier gas and argon for flushing the air from the system. Several experiments were performed at the reaction temperature ranging from 500◦C to 1200◦C. Other conditions like the reaction time (45 minutes) and hydrogen flow rate (300 mL/min) were fixed.

Oxidized CNT

Three hundred milliliters of a concentrated nitric acid of Analar (69%) were added to 2 g of as-received MWCNT. The mixture was refluxed for 48 h at 120◦C. After cooling at room temperature, the reaction mixture was diluted with 500 ml of deionized water and then vacuum-filtered through a filter paper (3 μm porosity). This washing operation was repeated until the pH became the same as that of the deionized water and is followed by drying in a vacuum oven at 100◦C.

Impregnated CNT by 1% Fe

The iron precursor used is ferric nitrate extra pure, $Fe(NO_3)_3.9H_2O$ (MW: 404.0, min. assay 98%). The weight taken was 0.03 g (as Fe 1%) and 0.2164 g (as precursor). The amount used of CNT-COOH was 2.97 g (3.0 - 0.03). Ferric nitrate was dissolved in ethanol without water. The sample after mixing was kept in the bath sonicator for a period of 1 hour without heating. After that, the sample was kept for drying under the fume hood on the hot plate with stirring until it becomes like a dry paste. Finally, calcination of the sample was made in the oven for 3 h of a temperature of 350^{o} C. The sample has crushed into small particles and became ready to be used.

APPENDIX B: Nomenclature

CNT	Carbon Nanotubes
MWCNT	Multi-walled Carbon nanotubes
AC	Activated Carbon
MBR	Membranes Bio-reactor
USEPA	United States Environmental Protection Agency
WHO	World Health Organization
FDA	Food & Drug Administration
SWCNT	Single-Walled Carbon Nanotubes
CVD	Chemical Vapor Deposition
GAC	Granular Activated Carbon
DBP	Disinfection by-products
MCL	Maximum Contaminant Level
THM	Trihalomethanes
AWWA	American Water Works Association
DDW	Distilled Deionized Water
EDS	Energy Dispersive Spectroscopy

REFERENCES

[1] Balkis, N., Water Pollution book, InTech, 2012.

[2] Iijima, S., Nature, 1991, 354, pp. 56-58.

[3] Wang, X., *et al. Nano Letters*, 2009, **9** (9).

[4] Renetal, X., Chemical Engineering Journal, 2011, 395-410.

[5] Harry M., Francisco R. R. Activated Carbon Book, ELSEVIER, 2005.

[6] Marhaba, T. F.; Bengraı¨ne, K. *Clean Technol. Environ. Policy* 2003, *5*, 101–112.

[7] European Union. Council directive of 15 July 1980 relating to the quality of water intended for human consumption *Official J. Eur. Communities* 1980, 11, *23* L229.

[8] U. S. EPA National primary drinking water standards.

[9] World Health Organization. Guidelines from Drinking Water Quality, 2nd ed.; Chemical Aspects: Geneva, 1996.

[10] Rakness, K. L., Ozone in Drinking Water Treatment: Process Design, Operation and Optimization, American Water Works Association, Denver, Co.2005.

[11] California Public Health Goal, Public Health Goals for Chemicals in Drinking Water, December, 2009.

[12] Weinberg, et al., Environ. Sci. Technol., 2003, 37, 3104–3110.

[13] Budavari, S.; O'Neil, M.; Smith, A.; et al., the Merck index: an encyclopedia of chemicals, drugs and biologicals.1989, 11th ed., NJ: Merck and Company, Inc.

[14] Hazardous Substance Data Bank. (HSDB) Bethesda, MD: National Library of Medicine, National Toxicology Information Program. April 1991.

[15] International Agency for Research on Cancer (IARC), Potassium Bromate, Lyon, France: World Health Organization, International Agency for Research on Cancer, 1986, 207-220.

[16] Marhaba, T. F.; Bengraı¨ne, K. *Clean Technol. Environ. Policy* 2003, *5*, 101–112.

[17] Singer, P. C., Obolensky, A., Greiner, A., J. Am. Water Works Assoc.1995, 87 (10), 83–92.

[18] USEPA, Stage 2 Disinfectants and Disinfection Byproducts Rule.2006 EPA-HQ-OW-2002-0043.

[19] Guanghui H., David A. R., WATER RESEARCH, 2007, 41, 1667–1678.

[20] Finch G., BIaclc E., Gyürék L. Ozone Disinfection of Giardia and Cryptosponaiurn, AWWA Research Foundation and AWWA, USA.1994 .

[21] Langlais B., Reckhow D., Brink, D., AWWARF and Lewis Publis hers Inc, Denver, Colorado and Chlesea, Michigan. 1991.

[22] Taha F.; Marhaba K. B., Clean Techn Environ Policy, 2003, 5 101–112

[23] Urs V. G., Jurg, H., *Environ. Sci. Technol. 1994,* 7904, *28,* 1234-1242.

[24] Mary J. K., et. al, AWWA research foundation, Removal of Bromate & Perchlorate in conventional Ozone/GAC systems.

[25] Kurokawa Y., Aoki S., Matsushina Y., Takamura N., Imazawa T., Hayashi Y., *J.* National Cancer Institute, 1986, 77:977.

[26] DeAngeIo A., George M., Kilburn S.R., Moore T. M., Wolfe D. C., Toxicology Pathology, 1998, 26:5.

[27] Von G. U., Hoignb J., Aqua, 1992, vol. 41, 299-304.

[28] Singer P. C., Hickey T. Weinberg S., Proceedings WQTC Conference, Denver, Colorado,1997 November, 9-1 2.

[29] Von G. U., Pinkernell U., Water Science and Technology, 2000, vol. 41, 53-59.

[30] Fabian I., Progress in Nuclear Energy, 1995, 29, 167-174

[31] Langlais B., Reckhow D. A., Brink D.R., Ozone in Water Treatment: Application and Engineering, LEWIS, 1991.

[32] Song R., Minear R., Westerhoff P., Amy G., Environmental Technology, 1996, 17, 861-868.

[33] Jianping Z., Dissertation, An Integrated Design Approach for Improving Drinking Water Ozone Disinfection Treatment Based on Computational Fluid Dynamics Waterloo, Ontario, Canada, 2006.

[34] IARC. Potassium Bromate (Summary of Data Reported and Evaluation). Lyon. 1999.

[35] Melnick R., Regulatory Toxicology and Pharmacology, 1992, 16(3), 111-125.

[36] U.S. Environmental Protection Agency, Toxicological review of bromate, EPA/635/R-01/002, Environmental Protection Agency, Washington, DC, 2001.

[37] World Health Organization. Guidelines for drinking-water quality, Geneva, 2006.

[38] European Union. Official J. Eur. Communities, 1980, 23 (L229), 11.

[39] Gerz R., Schneider W., 11th Inter. ozone Assoc. Proceedings, San Francisco, CA. 1993.

[40] Miller J., Snoeyink V. L., Harrell S., Environmental Chemistry Division, 1993, 206th ACS National Meeting, 237-240.

[41] Yamada H., 11th Proceedings, 1993, San Francisco, CA.

[42] Siddiqui M., Amy S., Ozekin K., Zhai W., Westerhoff P., J. Amer. Water Works. Assoc., 1994, 10, 86.

[43] Mills, A., Belghazi, A., Rodman D., Hitchins P., J. Institution of Water and Environmental Management, 1996, 10(3), 215±217.

[44] Asami M., Aizawa T., Morioka, T., Nishijima, W., Tabata A., Magara Y., Water Research, 1999, 33(12), 2797±2804.

[45] Bao M. L., Grini O., Santianni D., Barbieri K., Burrini D., Pantani F., Water Research, 1999, 33(13), 2959±2970.

[46] Miller J. A., The reduction of bromate in drinking water by activated carbon, PhD Thesis, University of Illinois at Urbana-Champaign, 1996

[47] Siddiqui M., Zhai W., Amy G., Mysore C., Water Research, 1996, 30(7), 1651±1660.

[48] Huang C. P., Chemical Interactions between Inorganic and Activated Carbon. In **Carbon Adsorption Handbook** (Eds. P.N. Cheresiminoff and F. Ellerbush), Ann Arbor Science Publisher, pp 281-329 (1978).

[49] Graham D., J. Physical Chemistry, 1955, 59(8), 896±900.

[50] Razvigorova M., Budinova T., Petrov N., Minkova V., Water Research, 1998, 32(7), 2135±2139.

[51] Butler R., Godley A., Lytton L., Cartmell E., Environ. Sci. Technol. 2005, 35, 193–217.

[52] W.-J. Huang, Y.-L. Cheng, Separation and Purification Technology, 2008, 59, 101–107.

[53] Barton, S. S., Evans, M.J.B., Halliop, E., MacDonald J.A.F., Carbon, 1997, 35, 1361–1366.

[54] Mary J. K. et al., Reduction of bromate by GAC, Wat. Res. 2000, Vol. 34, No. 17, pp. 4250±4260, 2000

[55] Cookson Jr J. T. (1978) Adsorption mechanisms: the chemistry of organic adsorption on activated carbon. In Carbon Adsorption Handbook, eds P. N. Cheremisinoff and F. Ellerbusch, pp. 241±279. Ann Arbor Science Publishers, Inc, Ann Arbor, MI.

[56] Bautista, T. I., Rivera-U. J., Ferro-G. M. A., Moreno, C. C., Carbon, 1994, 32(1), 93±100.

[57] Kim B. R., Snoeyink V. L., J. American Water Works Association, 1980, 72(8), 488±490.

[58] Wen-yi D., Zi-jun D., Rong-shu Z., Yang D., Feng O., Hong D., Removal of Bromate from Water by Silver-supported Activated Carbon, 2009 International Conference on Energy and Environment Technology.

[59] Naoyuki K.; Nobuaki M., Environ. Sci. Technol. 2009, 43, 2054–2059.

[60] Cristina T.; Matos S. V., Maria A. M., Reis J. G. C., Environ. Sci. Technol., 2008, 42, 7702–7708.

[61] Leon S. D., Robert N., AWWA Inorganic Contaminants Conference 2006.

[62] Daenen M., De Fouw, R.D., Hamers B., Janssen P.G.A., Schouteden K., M.A.J. Veld., Eindhoven University of Technology, 2003.

[63] Iijima, S.; Ichihashi, T.; Nature, 1993, 363, 603-605.

[64] Bethune, D. S.; Klang, C. H.; de Vries, M. S.; Gorman, G.; Savoy, R.; Vazquez, J.; Beyers, R., Nature, 1993, 363, 605 - 607.

[65] Thess, A.; Lee, R.; Nikolaev, P.; Dai, H.; Petit, P.; Robert, J.; Xu, C.; Lee, Y.H.; Kim, S.G.; Rinzler, A.G.; Colbert, D.T.; Scuseria, G.E.; Tománek, D. J.; Fischer, E.; Smalley, R.E., Science, 1996, **273**, 483-487.

[66] Meyappan, M.; Carbon Nanotubes Science and Applications, CRC Press, USA. 2005

[67] Zheng, L. X et al., Nature Materials, 2004, 10, 673-676.

[68] Tang Z. K.; Sun, H. D.; Wang, J.; Chen, J.; Li, G., Applied Physics Letters, 1998, 16: 2287-2289.

[69] Satio, R.; Fujita, M.; Dresselhaus, G.; Dresselhaus, M. S., Applied Physics Letters, 1992 18:2204-2206.

[70] Thostenson et al. Composites Science and Technology, 2001, 61, 1899–1912.

[71] Nicole, G., Carbon nanotubes becoming clean. 2007, Vol. 10.

[72] Lambert, J. M.; Ajayan, P. M.; Bernier, P.; Planeix, J. M.; Brotons, V.; Coq, B.; Castaing, J., Chemical Physics Letters ,1994 Issues 3-4:364-371.

[73] Ando, Y.; Zhao, X.; Sugai, T.; Kumar, M., Materials Today, 2004, 22-29.

[74] Guo, T.; Nikolaev, P.; Thess, A.; Colbert, D.T.; Smalley, R.E. Chemical Physics Letters, 1995, Issues 1-2:49-54.

[75] José-Yacamán, M., Miki-Yoshida, M., and Rendón, L., Applied Physics Letters, 1993, 62: 657.

[76] Endo, M. et al.; Journal of Physics and Chemistry of Solids, 1993, 54 (12), 1841-1848.

[77] José-Yacamán, M.; Miki-Yoshida, M.; Rendón, L., Applied Physics Letters, 1993 62: 657.

[78] Dai, H.; Rinzler, A. G.; Nikolaev, P.; Thess, A.; Colbert, D. T.; Smalley, R. E.; Chemical Physics Letters 1996 Issues 3-4, Pages 471-475.

[79] Paradise, M.; Goswami, T.; Materials and Design, 2007, 28:1477–1489

[80] Li, Y-H.; Wang, S.; Luan, Z.; Ding, J.; Xu, C.; Wu, D., Carbon, 2003, 41, 1057-1062.

[81] Li, Yan-Hui; Yanqiu, Z.; Yimin, Z.; Dehai W.; Zhaokun, L., Diamond & Related Materials, 2006, 15, 90 – 94.

[82] Li, Y-H.; Wang, S.; Luan, Z.; Ding, J.; Xu, C.; Wu, D., Carbon, 2003, 41, 1057-1062.

[83] Li, Yan-Hui, Shuguang, W.; Anyuan, C.; Dan, Z.; Xianfeng, Z.; Cailu, X.; Zhaokun, L.; Dianbo, R.; Ji, Liang.; Dehai, Wu.; Bingqing, Wei., Chemical Physics Letters, 2001, 350:412–416.

[84] Peng, X.; Luan, Z.; Di, Z.; Zhang, Z.; Zhu, C.; Carbon, 2005, 43:855–894.

[85] Wang, H.J.; Zhou, A.L.; Peng, F.; Yu, H.; Chen, L.F.; Materials Science and Engineering, 2007, 466:201–206.

[86] Hsieh, S.; Horng, J.; Journal of University of Science and Technology Beging, 2007, Vol. 1, Page 77.

[87] Meijers, R. T.; Kruithof J. C.; Pre-prints of Atelier International workshop-Bromate and Water Treatment, 1993 pp. 199±206, Paris, France.

[88] Muataz, A. A.; Omer, Y. B.; Bassam Al-T.; Alaadin, A. B.; Faraj, Ahmad .A.; Mohamed B. F.; Bioinorganic Chemistry and Applications, 2010, Article ID 603978, 9 pages

VITAE

NAME: Aasem Mohammed Nour Zeino

NATIONALITY: Syrian

DATE OF BIRTH: 7th November 1984

E-MAIL: Aasem.zeino@gmail.com

MOBILE: 00966503491797

EDUCATION:

B.Sc. Applied Chemistry

Damascus University

Damascus – Syria

2006

M.Sc. Chemistry

King Fahd University of Petroleum and Minerals (KFUPM)

Dhahran – Kingdom of Saudi Arabia

2012

EXPERIENCE:

Senior Research Analyst

Veolia Water Solutions & Technologies

Khobar – Saudi Arabia

2007 - 2012